



1 Improved parameterization of the weathering kinetics module in 2 the PROFILE and ForSAFE models 3

4 Harald Ulrik Sverdrup^{1,*}, Eric H. Oelkers^{2,3} Martin Erlandsson Lampa⁴,
5 Salim Belyazid⁵, Daniel Kurz⁶, Cecilia Akselsson⁷
6

7 1- System Dynamics, Department of Gamification, Inland Norway University of Applied Sciences, NO- 2318,
8 Hamar, Norway, 2-Earth Sciences, University College London, WC1E 6BT, London, UK, 3-CNRS, UMR-
9 5563, Toulouse, France, 4-Institute of Hydrology, University of Uppsala, SE-751 05 Uppsala, Sweden, 5-
10 Physical Geography, Stockholm University, SE-106 91 Stockholm, Sweden, 6-EKG Geoscience, CH-3012
11 Bern, Switzerland, 7-Earth Sciences, University of Lund, SE-221 00 Lund, Sweden. 8-Industrial Engineering,
12 University of Iceland, IS-107 Reykjavik, Iceland. *corresponding author (harald.sverdrup@inn.no)
13

14 Abstract

15 Although the PROFILE and ForSAFE model can accurately reproduce the chemical and
16 mineralogical evolution of the soil unsaturated zone, it overestimates weathering rates in deeper
17 soil layers and in groundwater systems. This overestimation has been corrected by improving the
18 kinetic expression describing mineral dissolution by adding or upgrading ‘braking functions’. The
19 base cation and aluminium brakes have been strengthened, and an additional silicate brake has
20 been developed, improving the ability to describe mineral-water reactions in deeper soils. These
21 brakes are developed from a molecular-level model of the dissolution mechanisms. Equations,
22 parameters and constants describing mineral dissolution kinetics have now been obtained for 113
23 minerals from 12 major structural groups, comprising all types of minerals encountered in most
24 soils. The PROFILE and ForSAFE weathering sub-model was extended to cover two-dimensional
25 catchments, both in the vertical and the horizontal direction, including the hydrology.
26 Comparisons between this improved model and field observations are available in Erlandsson
27 Lampa et al. (2019, This special issue). The results showed that the incorporation of a braking
28 effect of silica concentrations was necessary and helps obtain more accurate descriptions of soil
29 evolution rates at greater depths and within the saturated zone.
30

31 1. Introduction

32 This manuscript reviews the chemical weathering approach adopted by the PROFILE and ForSAFE
33 models and describes continuing efforts to upgrade the kinetic databases of these models for improved model
34 calculations. The application of mineral dissolution kinetics to natural systems requires a large amount of field
35 input including information on mineral surface areas, mineral abundances over time and their spatial
36 distribution, fluid flow and biotic activity. As such this manuscript will by design describe both the weathering
37 models and the evaluation of laboratory mineral dissolution rate used in the development of the upgraded
38 kinetic database.

39 Chemical weathering of silicate minerals, and notably the dissolution rates of these minerals are one
40 of the most important factors shaping soil chemistry. The quality of the kinetic database in most cases
41 determines the quality of its simulations of soil evolution. In the 1980’s, the need arose to mitigate acid
42 deposition, to set critical loads for acid deposition, and to set limits for sustainable forest growth and nitrogen
43 critical loads. This need led to a re-evaluation of the weathering observations available in scientific
44 publications and books (Sverdrup 1990, Sverdrup and Warfvinge 1992, 1993, 1995, Drever et al., 1994, Drever
45 and Clow 1995, Ganor et al., 2005, Svoboda-Colberg and Drever 1993, Crundwell 2013). These observations
46 led to a model that accurately reproduced weathering rates under field conditions. The early history of these
47 efforts was reported by Sverdrup and Warfvinge (1988a,b, 1992, 1993, 1995) and Sverdrup (1990). By 1990,
48 we had a set of equations that described the dissolution rates of 14 minerals (K-feldspar, albite, plagioclase,
49 pyroxene, hornblende, garnet, epidote, chlorite, biotite, muscovite, vermiculite, apatite, kaolinite, and calcite).
50 Later more silicate minerals were added, including illite, smectite, montmorillonite, sericite and volcanic glass.
51 Eventually we amassed kinetic data for 45 additional silicate minerals and 25 different carbonates¹ at the time.

¹ **Calcite** (The calcites are all slightly different; CaCO₃ with 0-3% MgCO₃ and 0.05%-0.5% apatite, from Sweden, Norway, Denmark, and the United States. In addition, kinetics on **aragonite** (CaCO₃), **slavsonite** (SrCO₃), **dolomite** (CaMg(CO₃)₂), **magnesite** (MgCO₃), **brucite** (MgOH), **siderite** (FeCO₃), **witherite** (BaCO₃), and **rhodochrosite** (MnCO₃) is available.



52 By the middle of the 1980's, it became clear that we did not have a standard procedure for building a
53 weathering rate model based on molecular level mechanisms. There are many reasons for this, the most
54 important was the lack of a mechanistically oriented approach for guiding experimental studies. The lack of a
55 mechanistic understanding resulted in important factors being overlooked. Many essential variables required
56 for a weathering model were missing in the older experimental studies, sample preparation was often
57 inadequate or not done, and/or the material was inadequately characterized (Sverdrup et al., 1981, 1984,
58 Sverdrup, 1990). Often the experimental design had significant flaws and many experiments ran for too short
59 a time; see Sverdrup (1990) for a full description. As such there needed to be a sorting of the data, to avoid the
60 confusion brought by misleading data. This effort led to the creation of the original PROFILE mineral kinetic
61 weathering model (Sverdrup, 1990) to estimate the rate at which mineral dissolution provided essential cations
62 to soil waters. Although this model provides accurate estimates for shallow soils, it became less accurate for
63 deeper soils (e.g. > 1.5 meter soil depth).

64 This report outlines our efforts to update these early mineral weathering kinetics models for accurate
65 predictions of watershed water and deeper groundwater chemistry. This effort builds upon the weathering book
66 by Sverdrup (1990) and the articles Sverdrup and Warfvinge (1988a,b, 1992, 1995) and Warfvinge and
67 Sverdrup (1993). There is an advisory chapter on how to estimate weathering rates in soils on a regional scale
68 in Europe in the United Nations Economic Commission for Europe, Long Range Transboundary Convention
69 Mapping Manual for Critical loads (Sverdrup, 1996). The weathering rate mapping methodology based on
70 PROFILE model predictions was tested and used throughout 26 different European countries, and peer
71 reviewed at annual workshops from 1988 to 2017.

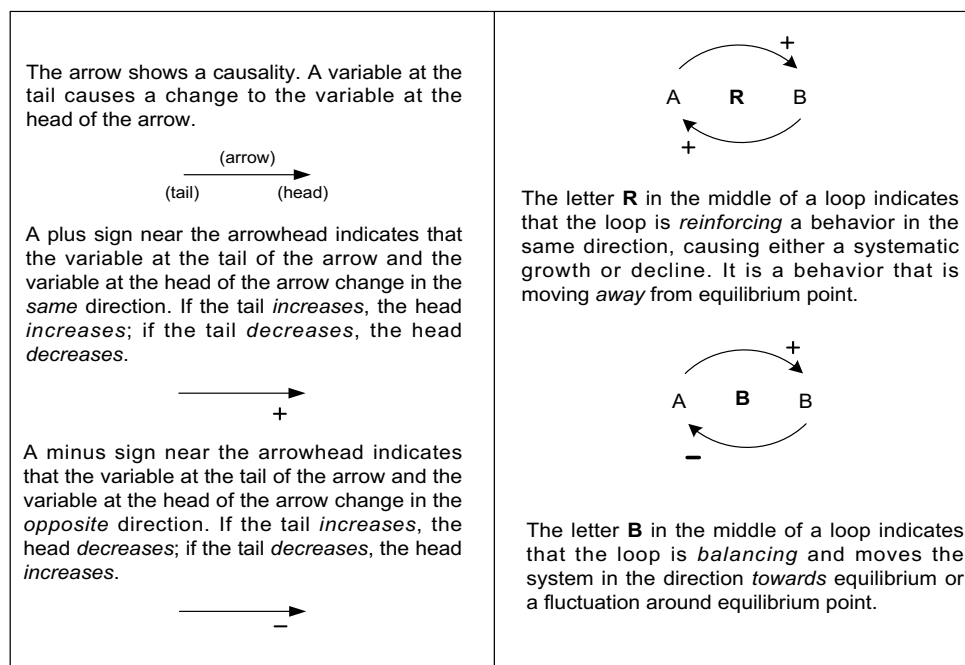
72 The revision of the original PROFILE weathering rate models described in this report was motivated
73 by several observations:

- 74
- 75 1. The PROFILE model was found to work satisfactorily in the unsaturated zone (0-1 meter), on thin
76 soils, on rock surfaces, and in low concentration systems (Sverdrup and Warfvinge 1988a,b, 1991,
77 1992, 1993, 1995, 1998, Sverdrup 1990, Sverdrup et al., 1998, Hettelingh et al., 1992, Alveteg et al.,
78 1996, 1998, 2000, Alveteg and Sverdrup 2000).
 - 79 2. However, the chemical weathering rate for minerals is overestimated by this model in deeper soils,
80 and at depths of more than 1.5 meters. The original PROFILE model was used down to this depth
81 (Sverdrup et al., 1988a,b, 1992, 1996, Sverdrup 1990, Janicki et al., 1993, Holmqvist et al., 2003) for
82 critical loads for streams (Sverdrup et al., 1996) and groundwater (Warfvinge et al., 1987), and may
83 have possibly resulted in overestimates of the critical load.
 - 84 3. The weathering rate is overestimated in the deeper soils and in ground water (Sverdrup 1990,
85 Warfvinge and Sverdrup 1987, 1992a,b,c, Sverdrup et al., 1996).
 - 86 4. New experimental data published in the literature after 1995 is of far better quality and consistency,
87 with better experimental designs, better characterized materials and more complete observations than
88 previous studies. For example, the reader is encouraged to read two studies published by Holmqvist
89 et al., (2002, 2003) on the weathering rates of clay minerals under soil conditions and the concept of
90 mineral alteration sequences (Holmqvist 2004, PhD thesis from Chemical Engineering, Lund
91 University). The minerals used in the weathering rate experiments in those studies were extracted and
92 separated from in-situ soils at experimental field sites near Uppsala, Sweden.

93

94 This study describes the updated mineral kinetics database used in the PROFILE and ForSAFE
95 models. Notably this update includes revised 'brake functions' in the kinetic rate equations to better fit the
96 observed field data down to the groundwater table and below. This was necessitated when the ForSAFE model
97 (thus also the PROFILE model) was reconfigured for a sloping catchment, expanding the model structure from
98 a 1-dimensional to a 2-dimensional model accounting for vertical and horizontal solute transport in a
99 catchment, including the ecosystem. In total 102 minerals are considered in the updated and expanded kinetics
100 parameter databases. An exhaustive description of the parameterization of the rate equations for all of the 102
101 minerals will require a text far beyond what is possible in this manuscript, so that only a summary and several
102 examples are provided here.

103



104
105
106
107
108
109
110
111
112
113
114
115
116
117
118
119
120
121
122
123
124
125
126
127
128
129
130
131
132
133
134
135
136
137

Figure 1. Weathering processes were mapped using systems analysis and by drawing causal loop diagrams (CLD) for the process and the whole system of the weathering process. This is a standard procedure in model building (Sverdrup and Stiernquist 2002, Sverdrup et al., 2018). B is a balancing loop (sometimes referred to as a negative feedback) and R is a reinforcing loop (sometimes referred to as a positive feedback) as explained in the figure.

2. Methodology

The methods used in this study have their basis in terrestrial ecosystems system analysis and ecosystems system dynamics as described by Sverdrup and Stiernquist (2002) and Sverdrup et al. (2018). The main tools employed are the standard methods of system analysis and integrated system dynamics modelling (Forrester 1961, 1969, 1971, Meadows et al., 1972, 1974, 1992, 2005, Roberts et al., 1982, Senge 1990, Bossel 1998, Haraldsson and Sverdrup 2005, Haraldsson et al., 2006, Sverdrup and Stiernquist 2002, Sverdrup et al., 2018). The overall system is analysed using stock-and-flow charts and causal loop diagrams (Sverdrup et al., 2002). The learning loop was used as the adaptive learning procedure in past studies (Senge 1990, Kim 1992, Senge et al., 2008, Sverdrup et al., 2018). The conceptual model must be clearly defined and constructed before any computational work can be undertaken. It is fundamental to understand that the causal understanding is the model. Systems analysis produces a causal loop diagram (CLD) linking causes, effects, and feedbacks among the processes in terms of causalities and flows (Albin 1997, Sverdrup et al., 2018, Kim 1992). These CLD need to be internally consistent. A summary of this approach is provided in Figure 1. A causal loop diagram is thus a map of the differential equations describing the evolution of the system. Mass- or energy flow charts and the causal loop diagram uniquely define the system. The ForSAFE model is not calibrated on large amounts of system output data (Sverdrup and Warfvinge 1992, Sverdrup et al., 2018). Instead, the system's causal linkages and the mass balances lead to equations that are parameterized using independent system properties, initial states and boundary conditions (Sverdrup et al., 2018).

2.1 Earlier development work and background

Critical to developing a database describing mineral dissolution rates is that it is coupled into a comprehensive model that can account for the large number of processes that affect rates in the field. From the beginning, weathering kinetics was developed and incorporated into the PROFILE model. The kinetics were parameterized using laboratory measurements and applied to field conditions on a plot scale and on a regional scale for Sweden (Sverdrup 1990, Sverdrup and Wafvinge 1988a,b, 1992, 1995, Warfvinge and Sverdrup 1992, 1993). The resulting kinetics sub-model was subsequently coupled into a biogeochemical ecosystem model, linking solute transport, soil chemistry, weathering, ion exchange, hydrology and biological



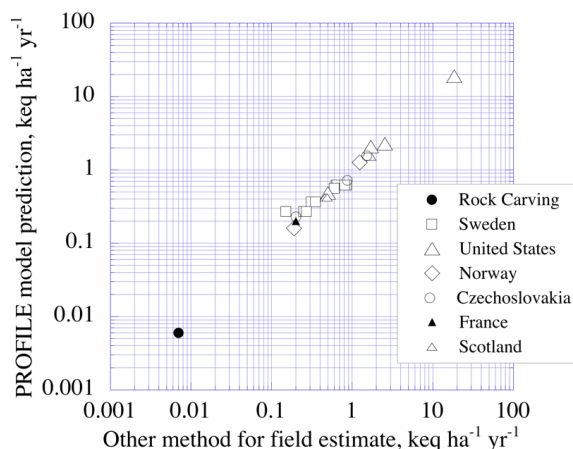
138 interactions with microbiology and forest plants, called the SAFE model (Sverdrup et al, 1995). The steady-
139 state model PROFILE and its dynamic variant SAFE, was further developed into other models as described in
140 the Appendix.

141 142 **2.2. Weathering under field conditions**

143 The dissolution of primary minerals at ambient temperature and pressure is irreversible with the
144 exceptions of a few simple chloride and sulphate salts and a few carbonates (Sverdrup 1990). Such irreversible
145 reactions do not attain equilibrium in near to ambient temperate systems as the chemical species released to
146 natural waters combine to form secondary solid phases far before the waters attain close to equilibrium
147 conditions with respect to primary minerals. Nevertheless, the dissolution rates of the primary minerals have
148 been observed to slow at far from equilibrium conditions in response to the increased concentration of
149 dissolved metals including Al and Si. A formulation based on transition state theory for the formation of
150 activated surface complexes that decay irreversibly was developed by (Sverdrup 1985, Sverdrup and
151 Warfvinge 1987, 1988a,b, 1992, Sverdrup 1990) to describe the effect of dissolved metals on primary mineral
152 dissolution at far from equilibrium conditions. Taking account of this approach as well as their coupling to
153 solute transport, ion exchange, plant nutrient uptake, organic matter decomposition and nitrogen
154 transformations detailed modelling of chemical weathering rates have been made (Sverdrup and Warfvinge
155 1988a,b, Sverdrup 1990, Akselsson et al., 2006, 2005, 2004, Sverdrup et al., 1990, 1995, 2017). A comparison
156 of calculated and observed weathering rates shown in Figure 2, demonstrates this approach can reproduce the
157 observed rates within $\pm 5\%$ across 4 orders of magnitude for the upper unsaturated parts of a soil (Sverdrup
158 and Warfvinge 1992, Barkman et al., 1999, Jönsson et al., 1995, Belyazid 2005, Kurz et al., 1998a,b). Further
159 comparisons of computed and calculated rates made with these models for field tests at Gårdsjön, Sweden and
160 at various sites were published by Sverdrup et al. (1988a,b, 1993, 1995, 1996, 1998, 2010), Sverdrup (1990,
161 2009), Sverdrup and Alveteg (1998), Rietz (1995) and Warfvinge et al., (1996), and Holmqvist et al., (2003,
162 2002). In addition, several other authors tested this approach independently (In the United States; Kolka et al
163 1996, Phelan et al., 2014, in Scotland; Langan et al. 2006b, in Germany; Becker 2002, in New Zealand;
164 Zabowski et al., 2007; tests on controlled experiments with granite slabs in the Swedish nuclear waste storage
165 assessment research programme at Göteborg by Claesson-Nyström and Andersson 1996, in Swedish soil
166 profiles; Lång 1998). Gunnar Jacks in KTH, Stockholm put these models to several blind test of the alteration
167 of blank granite surfaces used for ancient rock carvings and controlled mini-catchments (Jacks, unpublished
168 1990). In each case a close correspondence was observed in calculated as compared to the field weathering
169 rates. The current manuscript reports on our efforts to extend these accurate calculations to deeper in the soil
170 column.

171 172 **3. Theory**

173 The kinetic weathering model presented in this manuscript originates from that of Sverdrup and
174 Warfvinge (1987a,b, 1988a,b, 1992a, 1995) and Sverdrup (1990), but numerous features have been added
175 since. Some of the updates have been described in later studies (Akselsson et al., 2005, 2005, 2006, 2007,
176 Alveteg et al., 2000, Kurz et al., 1998a,b, Sverdrup et al., 1997, 2002, 2008). Further updates are described in
177 this study. New weathering rate data published over the past 25 years have been regressed and new temperature
178 dependencies and modifications of some rate coefficients has resulted (Sverdrup 2010, Sverdrup et al., 1998,
179 Rizzetto et al., 2016, Holmqvist et al., 2002, 2003). The mineralogy and surface area inputs to the models are
180 based on site measurements, and in general are not adjustable parameters. Some of parameters can be
181 challenging to measure, such as some primary minerals with low soil content (apatite, epidote, pyroxene,
182 amphiboles, garnets accurate to 0.1%), or mineral surface area. However, getting accurate field estimates of
183 the weathering rates is also challenging, as it requires making many assumptions, so may be of limited
184 accuracy. Thus, we are comparing uncertain model estimates with equally or more uncertain field estimates at
185 the best (Sverdrup et al., 1998). Nevertheless such comparisons are essential to validate model results. Of all
186 the parameters needed for calculating mineral dissolution rates in natural systems using laboratory measured
187 rates among the most challenging are mineral surface areas. Whereas in laboratory studies of the dissolution
188 rates of individual minerals it is possible to measure directly the areas of cleaned mineral surfaces using gas
189 adsorption techniques, field samples are more complex as they many contain the surfaces of several minerals
190 and these surfaces can be covered by both organic substances or secondary minerals. Assuming that the surface
191 area of each mineral in a soil is proportional to its mass or volume fraction may not be appropriate due to the
192 differing typical shapes of distinct minerals. The protocols used to estimate the surface areas of natural
193 minerals in soils within the PROFILE and the ForSAFE models have been reviewed in detail by Sverdrup
194 (1990).

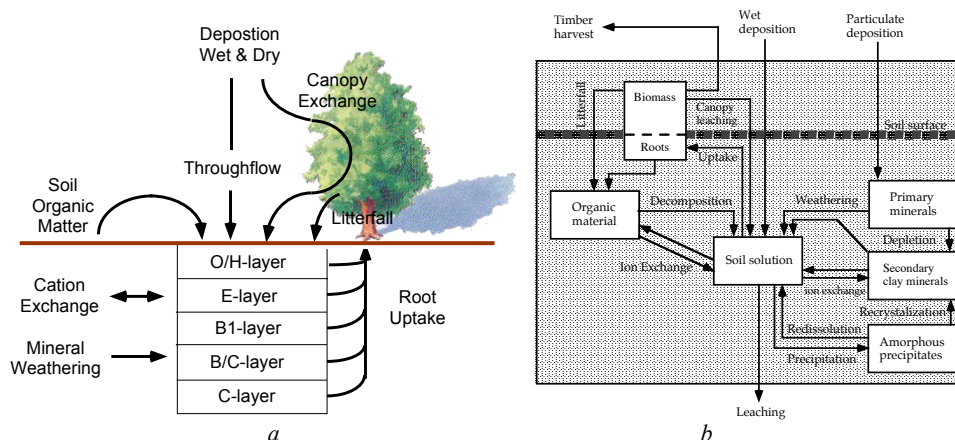


195
 196 *Figure 2. Comparison of weathering rates calculated using the original PROFILE model with corresponding*
 197 *rates obtained from field observations of the upper undersaturated parts of soils. Rates shown were reported*
 198 *or compiled by Sverdrup and Warfvinge (1988a,b, 1991, 1992, 1993, 1995, 1998), Sverdrup (1990), Sverdrup*
 199 *et al. (1990, 1998), Hettelingh et al. (1992), Barkmann et al. (1999), Holmqvist et al. (2003). The model test*
 200 *was performed on shallow soil profiles, no deeper than 0.6 meter.*

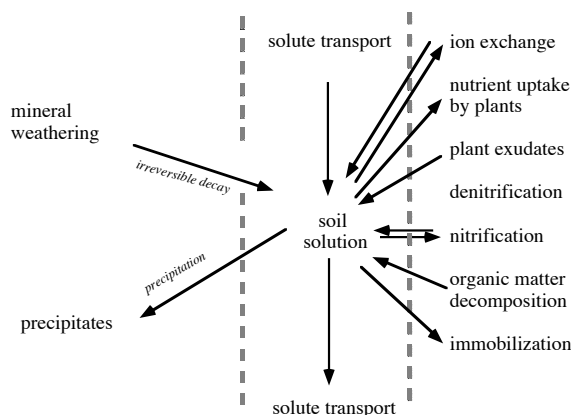
201 202 3.1. Defining chemical weathering

203 Weathering neutralizes acids (neutralizing all or part of acid rain) and provides nutrients for vegetation
 204 (e.g. Ca^{2+} , Mg^{2+} , K^+ , PO_4) (Sverdrup 1990, Sverdrup and Warfvinge 1995, Sverdrup et al., 2002). Thus
 205 weathering rates are defined as “the base cation release rates from the chemical weathering of minerals”, “plant
 206 nutrient base cation release rates from the chemical weathering of minerals” or “the rate of acid neutralization
 207 by chemical weathering of soil minerals”. Only secondarily are we interested in loss of minerals and soil profile
 208 development (Rietz 1995, Warfvinge et al., 1996, Sverdrup et al., 1996, 2002). Thus, the weathering rates in
 209 this study have been expressed as the sum of the release rates of base cations (Ca^{2+} , Mg^{2+} , K^+ , Na^+) from the
 210 process. This is linked to the destruction of minerals, though results are generally expressed in these terms.

211
 212



213
 214 *Figure 3. Overview of the PROFILE model. The original PROFILE model operates with a number of layers,*
 215 *and a vertical percolation of water. A set of processes take place in every layer. (b) A look inside PROFILE,*
 216 *showing how weathering is connected with other ecosystem processes (Sverdrup and Warfvinge 1995).*
 217



218
 219 *Figure 4. Different soil processes communicate with the weathering processes via the soil solution. (Sverdrup*
 220 *et al., 2002).*
 221

222 3.2. Mineral weathering rates

223 The weathering rate of a mineral, r , defined here as its dissolution rate, is assumed to stem from the
 224 sum of 5 simultaneous chemical reactions, involving the mineral surface and either aqueous H^+ , H_2O , OH^- ,
 225 organic acid ligands, or CO_2 . Assuming that the reactions occur at distinct active mineral surface sites, they
 226 can be summed linearly in accord with (Sverdrup 1990, Sverdrup and Warfvinge 1995):

$$227 \quad R_W = \sum_{j=1}^{\text{Minerals}} A_j * \sum_{i=1}^{\text{Dissolution reactions}} r_i \quad (1a)$$

228 where R_W stands for the soil weathering rate in a single soil layer. A_j refers to the soil mineral surface available
 229 for dissolution for each mineral j considered, r_i designates the rate of the individual chemical reactions i . If
 230 some reactions occupy the same active mineral surface sites, the expression given above would change to a
 231 quadratic sum. Note that the results of the two equations are quite similar, so that the importance of knowing
 232 if several reactions operate of the same surface site is relatively small. For the whole soil profile the rates are
 233 summed over the different soil layers with depth and we get:
 234

$$235 \quad R_{\text{Soil}} = \sum_{s=1}^{\text{Layers}} R_{W,s} \quad (2)$$

236 where R_{Soil} denotes the weathering rate in the whole soil profile, and s represents the layer number. Evidence
 237 that the H^+ , H_2O and OH^- reactions take place at distinct surface sites has been reviewed by Sverdrup (1990)
 238 and again by Holmqvist et al., (2003). The H_2O , the organic reaction and the CO_2 reactions may occur at the
 239 same sites, but considering the available data, we have assumed that they occur at distinct sites and thus favour
 240 a linear sum of rates. More on these assumptions have been reported by Sverdrup (1990), Sverdrup and
 241 Warfvinge (1995), and Holmqvist et al. (2002, 2003).
 242

243 3.3. Field weathering rates

244 To estimate field weathering rates using laboratory determined kinetic coefficients, an ecosystem
 245 model is required to scale the process to field conditions. This ecosystem model includes effects of climate,
 246 soil morphology, plants, trees, microbiology in the soil and fungi (Lin et al., 2017, Smits and Wallander 2016,
 247 Smits et al., 2014). An ecosystem model is incorporated within PROFILE and ForSAFE (Sverdrup and
 248 Warfvinge 1988a,b, 1991, 1992, 1993, 1995, 1998, Sverdrup 1990, Sverdrup et al., 1998, Hettelingh et al.,
 249 1992, Barkmann et al., 1999, Holmqvist et al., 2003, Barkman et al., 1999). Figure 3 shows how the steady-
 250 state PROFILE model was configured (Sverdrup and Warfvinge 1988a,b, 1992, 1993, Sverdrup and Alveteg
 251 1998). In the dynamic integrated terrestrial ecosystem assessment model ForSAFE-VEG, the system evolution
 252 takes account of interactions with a living biosphere, organic matter turnover and ion exchange (c.f. Figure 4).
 253 Further details of these models can be found in the appendix and the literature (Sverdrup et al., 1987, 1995,
 254
 255



256 1996a,b, 1998, 2007, 2014, 2016, 2017, 2019, Wallman et al., 2002, 2003, Zancchi et al., 2014, 2016a,b,
257 Belyazid et al., 2017, 2018).

258 To estimate field weathering rates, each reaction i for every mineral j is corrected for the field site
259 temperature and for the partial wetting of the soil (Sverdrup 1990, Sverdrup and Warfvinge 1995, Sverdrup
260 and Alveteg 1998) in accord with:

261

$$262 \quad R_W = h(\theta) * \sum_{j=1}^{\text{Minerals}} A_j * \sum_{i=1}^{\text{Dissolution reactions}} (r_i * g_{i,j}(T)) \quad (3)$$

263

264 where θ stands for the fraction of the soil mineral surfaces wetted, A_j designates the surface area of the mineral
265 j , $h(\theta)$ refers to a wetting function for the mineral material and T signifies the soil temperature in centigrade.
266 $g_{ij}(T)$ corresponds to the temperature adjustment function for reaction i of mineral j . r_i denotes the reaction rate
267 of dissolution reaction i . This adjustment is based on the Arrhenius equation and takes account of the
268 difference in rates between the temperature of the field site and that of the parameter database, which was set
269 at 8°C (Sverdrup 1990). Figure 6 shows the reaction causal loop diagram for silicate minerals in the soil
270 (Sverdrup 1990, Sverdrup and Warfvinge 1995). This diagram shows how the mineral weathering process
271 communicates with other biogeochemical processes in a terrestrial ecosystem. The causal loop diagram is a
272 graphical display of the differential balances in the system. Together with the flow charts, they define the
273 system. The process has several intermediate equilibrium steps, but pass an irreversible dissolution threshold
274 (Figure 7). The single irreversible step makes the whole process irreversible. The reaction products exert a
275 negative effect on the amount of activated complex that can decay, thus they slow the dissolution reaction. But
276 once the activated complex has formed, it has a constant decay rate, set by quantum mechanics (Sverdrup
277 1990, Sverdrup and Warfvinge 1995). The full derivation of the rate equations, starting from the elementary
278 chemical reactions and the decay of the surface complexes according to transition state theory has been
279 reviewed by Sverdrup (1990) and Sverdrup and Warfvinge (1995).

280

281 3.4 Mineral reaction kinetics

282 As stated above, five reactions are assumed to contribute to the total chemical weathering rate of a silicate
283 mineral in soils (Sverdrup 1990, 2009, Sverdrup and Warfvinge 1995):

284

- 285 1. The reaction between the mineral surface and the aqueous hydrogen ion
- 286 2. The reaction between the mineral surface and the water molecule
- 287 3. The reaction between the mineral surface and aqueous carbon dioxide
- 288 4. The reaction between the mineral surface and aqueous organic acid ligands
- 289 5. The reaction between the mineral surface and the aqueous hydroxy ion

290

291 Reactions 1-4 in the list above were included in earlier versions of the PROFILE and ForSAFE mineral
292 dissolution rate equations (Sverdrup 1990, Sverdrup and Warfvinge 1995). This original model has been
293 enlarged to include reaction 5.

294

295 The reaction of the mineral surface with the aqueous H^+ ion, reaction 1, is considered part of the
296 reaction with the H^+ reaction regardless of the source of H^+ (Figures 5 and 7). Both CO_2 and organic acids can
297 change the fluid pH, and this is accounted for in the H^+ reaction. Figure 5 shows the reaction pathway through
298 the H^+ reaction, adapted after Sverdrup (1990). Some of the reaction products form secondary minerals.
299 Amorphous phases may also precipitate from solution. These can slowly recrystallize to secondary minerals.
This has been generalized in Figure 6.

300

301 Reaction number 4 between organic acid ligands and the mineral surface contains at least two distinct
302 contributions: one from fast and one from slower reacting organic acid ligands (Sverdrup 1990). We have
303 simplified this to one generic rate equation that could be parameterized for some minerals (feldspar, olivine,
304 pyroxenes, hornblende, apatite; Sverdrup et al., 1990, later literature has extended the list somewhat). The
305 importance of organic acids for weathering has been frequently over estimated in the literature, and several
306 claims of strong effects of organic acids have been made (For a review see Smits and Wallander 2016, Smits
307 et al., 2014, Sverdrup 1990, 2009 but also Keegan and Laskow-Lehey 2014 on why these claims have been so
308 persistent). The highest concentration of organic acids occur in the upper soil layers, where the mineral content
309 is relatively low. As the mineral contents increase with depth, the concentrations of organic acids are lower
and have only a marginal effect on the overall weathering rate (Sverdrup 2009).



310 Organic acids in soils are mostly sourced from soil organic matter decomposition. Trees, soil fungi
 311 and mycorrhiza do not have the ability to increase the weathering rate significantly (See Sverdrup 1990, 2009,
 312 Sverdrup and Warfvinge 1992, Warfvinge and Sverdrup 1993 for details, kinetic expressions and data
 313 underpinning this, see Smits and Wallander 2016 and Smits et al., 2014 on the subject concerning apatite).
 314 Trees and vegetation can indirectly affect weathering rates when they take up Ca, Mg, K as nutrients, and
 315 thereby removing weathering rate products that can slow mineral dissolution. Decomposition of plant debris
 316 and soil organic matter produce organic acids that may react with the minerals. This effect is passive, and does
 317 not occur not by design of the plants (See Smits and Wallander 2016 and Smits et al., 2014 for measurements,
 318 Keegan and Laskow-Lehey 2014 for some social aspects and Sverdrup 2009 for a further analysis from a
 319 systemic perspective).

320
 321
 322
 323
 324
 325
 326

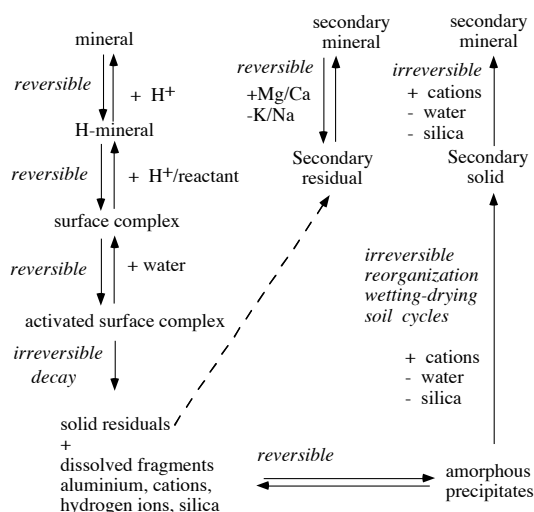
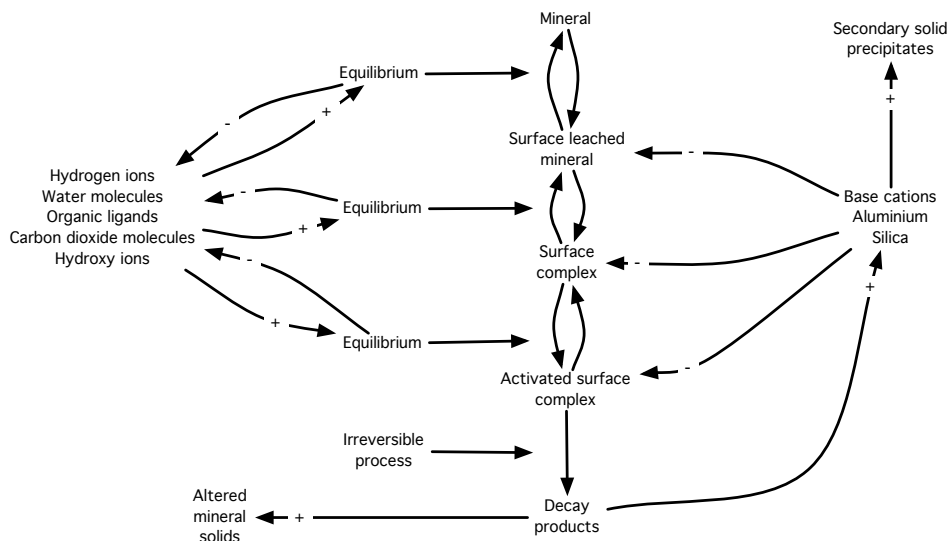
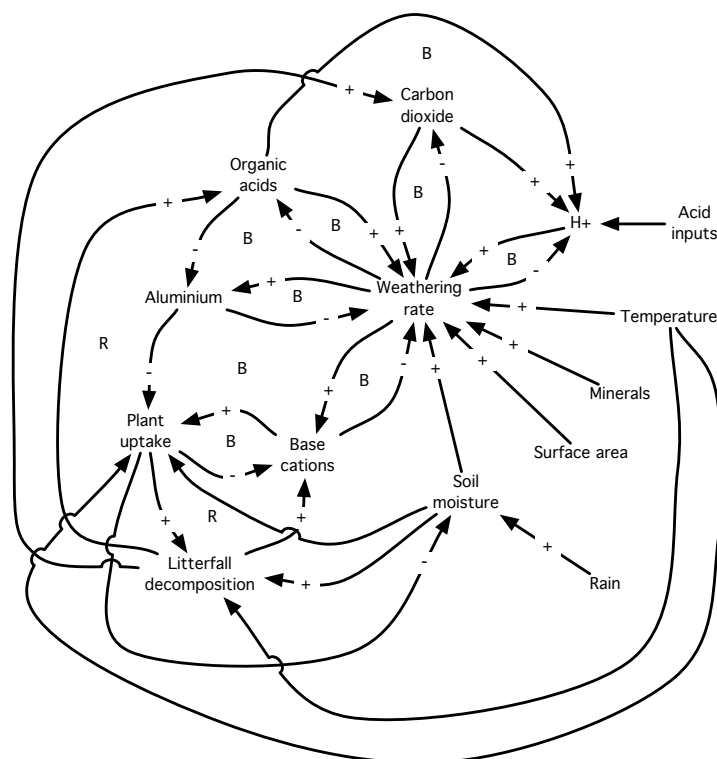


Figure 5. The reaction pathway through the H^+ reaction passes over several reversible steps that change the surface sites and create an unstable surface complex; the Transition State Surface Complex that will decay irreversibly. Note that the process is irreversible, and thus cannot go backwards. The mineral may dissolve completely, be altered to a secondary mineral or form precipitates that slowly recrystallize to secondary solid phases.



327
 328
 329

Figure 6. Reaction pathway for silicate minerals in soils according to Transition State Theory as implemented by the authors (See Sverdrup 1990, Sverdrup and Warfvinge 1995 for a full explanation).



330 Figure 7. The partial causal loop diagram for the weathering of a soil. See Sverdrup et al. (2018) for a full
 331 explanation of causal loop diagrams and their use in modelling.
 332
 333

334 Fluorides form soluble complexes in water with aluminium and silicates. The reaction of the mineral
 335 surface with fluoride anions forms a strong reactions, but this occurs very rarely as the fluoride concentrations
 336 are very low. The fluoride reaction has been ignored in this approach for most soils in natural terrestrial
 337 ecosystems, as this would cause an unnecessary complication of the aluminium and silicate chemistry. The
 338 dissolution rate per surface area of a mineral considering the first of the four above reactions is thus consistent
 339 with (Sverdrup and Warfvinge 1988, 1992):

340
 341
$$r_{\text{Total}} = r_{\text{H}^+} + r_{\text{H}_2\text{O}} + r_{\text{CO}_2} + r_{\text{R}} \quad (4)$$

 342

343 The mineral dissolution kinetic equation for the 4 individual reactions applied in the original PROFILE
 344 model was the simplified version of the full kinetic expression based on the Transition State Theory applied
 345 to silicate chemical weathering (see Sverdrup 1990, Sverdrup and Warfvinge 1995):
 346

347
$$r = k_{\text{H}} * \frac{[\text{H}^+]^{n_{\text{H}}}}{f_{\text{H}}} + \frac{k_{\text{H}_2\text{O}}}{f_{\text{H}_2\text{O}}} + k_{\text{CO}_2} * P_{\text{CO}_2}^{n_{\text{CO}_2}} * \frac{1}{f_{\text{CO}_2}} + k_{\text{R}} * \frac{[\text{R}]^{n_{\text{R}}}}{1 + K_{\text{Org}} * [\text{R}]^{n_{\text{R}}}} * \frac{1}{f_{\text{R}}} \quad (5)$$

 348

349 where the different n designate reaction orders. The different k_{H} , $k_{\text{H}_2\text{O}}$, k_{CO_2} , k_{R} stand for rate coefficients.
 350 Constituents within brackets [c] are concentrations, and R refers to organic ligands. The different f_{H^+} , $f_{\text{H}_2\text{O}}$,
 351 f_{CO_2} , f_{R} , f_{OH} signify retarding or ‘brake’ functions defined by (Sverdrup 1990, Sverdrup and Warfvinge 1992,
 352 Warfvinge and Sverdrup 1993, Sverdrup and Warfvinge 1995):
 353

354
$$f_{\text{H}^+} = \left(1 + \frac{[\text{BC}]}{C_{\text{BC,H}}}\right)^{x_{\text{H}}} * \left(1 + \frac{[\text{Al}^{3+}]}{C_{\text{Al,H}}}\right)^{y_{\text{H}}} \quad (6)$$

 355



$$f_{\text{H}_2\text{O}} = \left(1 + \frac{[\text{BC}]}{C_{\text{BC,H}_2\text{O}}}\right)^{x_{\text{H}_2\text{O}}} * \left(1 + \frac{[\text{Al}^{3+}]}{C_{\text{Al,H}_2\text{O}}}\right)^{y_{\text{H}_2\text{O}}} \quad (7)$$

$$f_{\text{CO}_2} = \left(1 + \frac{[\text{BC}]}{C_{\text{BC,CO}_2}}\right)^{x_{\text{CO}_2}} * \left(1 + \frac{[\text{Al}^{3+}]}{C_{\text{Al,CO}_2}}\right)^{y_{\text{CO}_2}} \quad (8)$$

$$f_{\text{R}} = \left(1 + \frac{[\text{BC}]}{C_{\text{BC,R}}}\right)^{x_{\text{R}}} * \left(1 + \frac{[\text{Al}^{3+}]}{C_{\text{Al,R}}}\right)^{y_{\text{R}}} \quad (9)$$

$$f_{\text{OH}^-} = \left(1 + \frac{[\text{BC}]}{C_{\text{BC,OH}}}\right)^{x_{\text{OH}}} * \left(1 + \frac{[\text{Al}^{3+}]}{C_{\text{Al,OH}}}\right)^{y_{\text{OH}}} \quad (10)$$

Note that the retardation or ‘braking’ functions represent molecular mechanisms that slow the reaction by forming fewer active surface complexes (Sverdrup 1990, Sverdrup and Warfvinge 1995). Al^{3+} is the concentration of positive aluminium species in the aqueous solution, and not necessarily equal to the total aluminium concentration (Sverdrup 1990 – see also section 4.8); this concentration can be calculated using aqueous speciation estimates as described below. The subscript BC,OH represents a term related to base cations (BC) in the OH⁻ reaction, Note this slowing of the rates with increasing fluid concentration is not due to the approach to a mineral-water equilibrium state. The dissolution of many primary silicate minerals is not reversible under normal soil conditions as the fluids do not attain close to equilibrium conditions. Instead, there will be a steady-state between the reaction at the surface and the removal of ions by solute transport and precipitation into secondary phases. This may look like an equilibrium condition, but does not behave like one. A few minerals are exceptions such as calcite, a few other carbonates, hydroxides and quartz. Even with these the attainment of equilibrium is kinetically limited. For calcite in soils we have observed this to take several days or weeks (Warfvinge et al., 1987). All other minerals (feldspars, pyroxenes, amphiboles, etc.) do not precipitate from solution, some amorphous aluminosilicate clay precursors only precipitate very slowly.

3.5. The updated kinetics equation

The original 4 mineral dissolution reactions have been enlarged to include OH⁻-reaction in the present study. The complete equation is consistent with

$$r_{\text{Total}} = r_{\text{H}^+} + r_{\text{H}_2\text{O}} + r_{\text{CO}_2} + r_{\text{R}^+} + r_{\text{OH}^-} \quad (11)$$

The full kinetic equation for all 5 reactions is (Sverdrup 1990, Sverdrup and Warfvinge 1995):

$$r = k_{\text{H}} * \frac{[\text{H}^+]^{n_{\text{H}}}}{f_{\text{H}}} + \frac{k_{\text{H}_2\text{O}}}{f_{\text{H}_2\text{O}}} + k_{\text{CO}_2} * \frac{P_{\text{CO}_2}^{n_{\text{CO}_2}}}{1 + K_{\text{CO}_2} * P_{\text{CO}_2}^{n_{\text{CO}_2}}} * \frac{1}{f_{\text{CO}_2}} + k_{\text{R}} * \frac{[\text{R}]^{n_{\text{R}}}}{1 + K_{\text{Org}} * [\text{R}]^{n_{\text{R}}}} * \frac{1}{f_{\text{R}}} + k_{\text{OH}} * \frac{[\text{OH}^-]^{n_{\text{OH}}}}{f_{\text{OH}}} \quad (12)$$

For most minerals, the strongest effect of the brake functions is that of aluminium at pH < 7, followed by silica and base cations. At pH > 8, the strongest effect is from silica and base cations, and less pronounced for aluminium (Sverdrup 1990). Before applying Equation (12) a number of new adaptations have been carried out as described below.

3.6. Retardation of mineral dissolution rates by organic ligands

The original formula for the slowing of mineral dissolution rates with increasing organic ligand concentration was (Sverdrup 1990, Sverdrup and Warfvinge 1995):

$$r_{\text{Org}} = k_{\text{R}} * \frac{[\text{R}]^{n_{\text{R}}}}{1 + [\text{R}]^{n_{\text{R}}}} * \frac{1}{f_{\text{R}}} \quad (13)$$

this has been reformulated to:



402

403

$$r_{org} = k_R * \left(\frac{[R]}{1 + [R] + [R]_{limit}} \right)^{n_R} * \frac{1}{f_R} \quad (14)$$

404

405

406

407

408

409

The difference in these equations is that the latter contains one additional parameter $[R]_{Limit}$ in f_R that has the effect to set a lower concentration, below which the organic acids have no effect. This equation has been parameterized and used in the final expression provided below. This limit was incorporated into the organic acid ligand retardation function f_R (Smits and Wallander 2016, Smits et al., 2014, Sverdrup 1990, 2009).

410

3.7. Retardation of mineral dissolution rates by aqueous CO₂

411

412

413

414

415

416

417

418

419

420

The main effect of the presence of CO₂ on mineral dissolution rates is to change the pH of the solution. This effect is accounted for by the chemical solution equilibria, and dealt with in the H⁺ reaction. The dedicated CO₂ term takes into account the effect of a reaction between the CO₂ and the mineral surface. The effect of the presence of aqueous organic species decreases at higher concentrations of organic acids as the surface sites have become saturated with organic acid ligands. We hypothesize that CO₂ exhibits the same behaviour. Some data show that CO₂ also reacts with mineral surface sites as some type of carbonate ligand (a bicarbonate coordinated towards a cation in the lattice) adsorbed to the surface, setting up a transitional surface complex may decay. The mechanism by which CO₂ effects silicate dissolution rates appears to follow the sequence (Sverdrup 1990, Sverdrup and Warfvinge 1995, Brady and Carrol 1994, Golubev et al., 2005, Navarre-Sitchler and Thyne 2007, Berg and Banwart 2000):

421

422

423

424

425

426

427

428

1. The CO₂ molecule attaches to the mineral surface
2. The CO₂ molecule forms a bicarbonate-water-metal complex with the mineral surface on singly coordinated metal cations. Indications are that it may be the CO₃²⁻ ligand that is forming a surface complex.
3. A cation is lifted into the complex (K, Na, Mg, Ca, Fe, etc..)
4. A small fraction of the surface complexes detach from the surface and the mineral dissolves.

429

430

431

432

433

434

435

436

437

438

Thus there should potentially be an upper concentration limit where additional aqueous CO₂ will have no further effect on mineral dissolution rates. This seems to occur between 10 and 50 atmospheres of CO₂ partial pressure for mica and chlorites (Drever et al., 1996, Mast and Drever 1987, Hausrath et al., 2009). Observations on some other minerals indicate of a similar behaviour, but this limit remains elusive due to lack of data. In addition the dissolution rates of some minerals exhibit no detectable effect of the presence of aqueous CO₂, and some are only slightly inhibited by this species. Lagache (1965, 1976), Busenberg and Clemency (1976), Berg and Banwart (2000) and Golubev et al., (2005) reported experiments performed at different CO₂ partial pressures between 0 and 26.3 CO₂ atmospheres and temperatures between 0 °C and 200 °C. The original equation used by Sverdrup (1990) and Sverdrup and Warfvinge (1995) to describe these data was

439

$$r_{CO_2} = k_{CO_2} * \frac{P_{CO_2}^{n_{CO_2}}}{1 + K_{CO_2} * P_{CO_2}^{n_{CO_2}}} * \frac{1}{f_{CO_2}} \quad (15)$$

440

441

442

In this study we use a variation of this equation of the form:

443

$$r_{CO_2} = k_{CO_2} * \left(\frac{P_{CO_2}}{1 + K_{CO_2} * (P_{CO_2} + P_{CO_2 Limit})} \right)^{n_{CO_2}} * \frac{1}{f_{CO_2}} \quad (16)$$

444

445

446

447

448

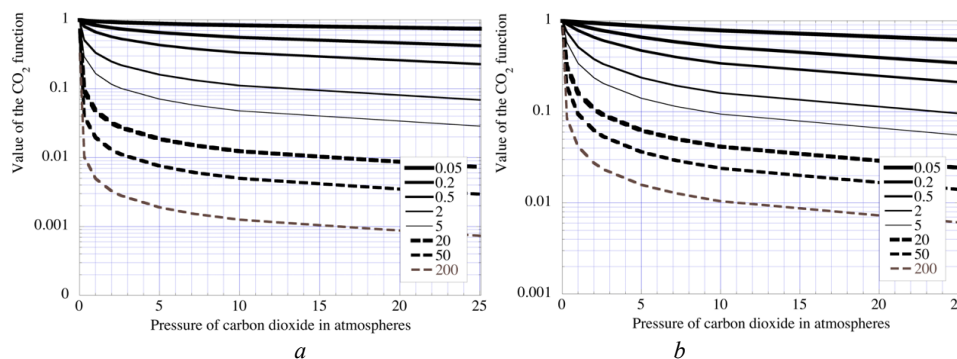
449

450

451

452

Evidence suggests that the value of $P_{Limit CO_2}$ is in the range of 5 to 10 atmospheres and $K_{CO_2}=0.05$ and $n_{CO_2}=0.6$ for albite (Sverdrup 1990). Navarre-Sitchler and Thyne (2007) suggest $n_{CO_2}=0.45$, which is for practical purposes the same. Berg and Banwart (2000) suggested $n_{CO_2}=0.25$ at low pressures of CO₂. As mentioned above, a similar behaviour was observed for mica, biotite and chlorites. Indications are that something similar takes place on the surface of montmorillonite, diaspore, gibbsite, goethite and lepidocrite. There almost no experimental data available allowing the retrieval of the parameters in Equation (16) for other minerals. The effect of increasing aqueous CO₂ has been overlooked in most experimental studies.



453
 454
 455
 456
 457

Figure 8. The calculated effect of aqueous carbon dioxide on mineral dissolution reactions using Equation 15 in (a) and Equation 16 in (b). See Table 2 for values for different minerals.

Table 1. Retrieved values of the parameter z in the silica brake function describing the dissolution rates of various silicate minerals (see equations 24-28).

#	Silica brake response group	z-values suggested by the mineral reactions				
		H ⁺	H ₂ O	CO ₂	Organic acids	OH ⁻
1	K-Feldspar and sericite	6	2	2	2	1
	Muscovite group and illites	7	3	3	3	2
2	Albite	8	4	4	4	3
	Na-rich Plagioclase	7	4	4	4	3
	Ca-rich Plagioclase	10	6	6	6	4
3	Biotite group	16	6	6	6	4
	Chlorite group					
	Serpentinite					
	Aluminum-nesosilicates					
	Aluminium pyroxenes					
Tourmaline group						
4	Amphibole group	20	16	16	16	8
	Pyroxene group	32				
	Epidote group	32				
	Nesosilicate	32				
5	All other silicates	32	16	16	16	8
6	Carbonates	n.a	n.a	n.a	n.a	n.a

458
 459
 460
 461
 462
 463
 464
 465
 466
 467
 468
 469
 470
 471

Values calculated of the effect of aqueous CO₂ on silicate dissolution rates are illustrated in Figure 8. These calculations suggests that there is a significant saturation of the surface with CO₂ at approximately 5 to 10 atmospheres partial pressure of CO₂. See Table 1 for the z-values suggested for different minerals. Note that the values of this parameter are based on minimal supporting experimental data - the available experimental data are few and somewhat incomplete (See Golubev et al., 2005 for a limited but useful assessment). Overall, the effect of CO₂ at normal soil conditions is limited. Nevertheless, these results provide a range for model parameter adjustment. The effect of dissolved CO₂ on rates may become significant for deep aquifers, subsurface CO₂ storage and in industrial high-pressure situations (Sverdrup 1990).

3.8 The silica retarding or 'brake' function

An illustrative plot of the effect of aqueous silica on silicate mineral dissolution rates is provided in Figure 9. The equation used to describe the retardation effect of dissolved Si on mineral dissolution rates was:

472

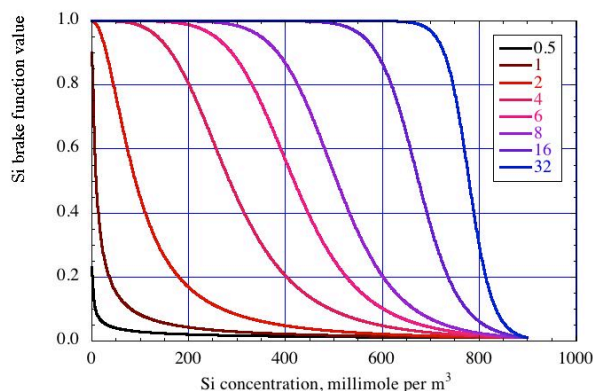
$$\frac{1}{f_{\text{Si}}} = \frac{1}{1 + K_{\text{Si},i} * \left(\frac{[\text{Si}]}{C_{\text{Si}}}\right)^{z_{\text{Si}}}} \quad (17)$$

473
 474
 475
 476

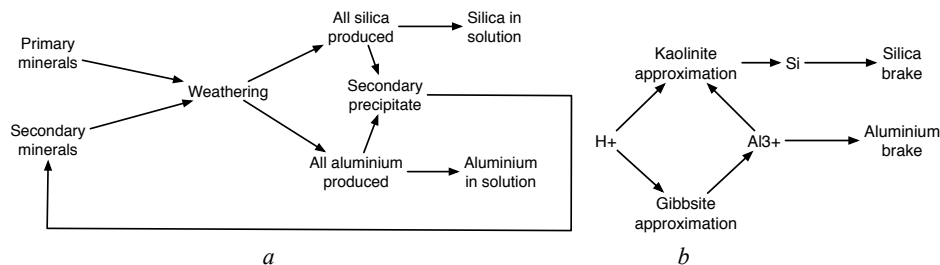
The value for the silica brake coefficient $K_{\text{Si},i}=100$ was chosen, and causes a gradual reduction in the dissolution rate of minerals down to a minimum of approximately 0.9% of the rate unaffected by silica at very high silica concentrations (see Table 1). Figure 9 shows values of the silica brake function calculated using



477 Equation 17, using the surface constant value, $K_{Si}=100$, and the saturation concentration $C_{Si}=900$ mmol per m^3
 478 in Equation 17 together with the coefficients in Table 3. Exponents from $z_{Si} = 0.5$ to 32 in Equation (17) of the
 479 silica rate brake are shown in Figure 9.
 480



481
 482 *Figure 9. Calculated effect of dissolved Si on silicate dissolution rates generated using Equation (17) together*
 483 *with $K_{Si}=100$, and the saturation concentration, $C_{Si}=900$ mmol per m^3 and the coefficients in listed in Table*
 484 *1.*



485
 486
 487 *Figure 10. a) Plot illustrating the fate of silica during the mineral dissolution process. b) Diagram showing*
 488 *how the aluminium and silica concentrations are estimated in the model. The H^+ concentration is used with*
 489 *the equation called the “Gibbsite” equation (Eq. 19) to estimate the Al^{3+} concentration in the soil solution.*
 490 *These H^+ and Al^{3+} concentrations are used in Equation 21 to estimate the silica concentration that is used to*
 491 *quantify the silica ‘brake’ on the mineral weathering reactions.*
 492

493 Figure 10a shows a plot illustrating the fate of silica in the dissolution process. Only a small part of the aqueous
 494 aluminium and aqueous silica produced by the dissolution of minerals remain in solution. Most precipitates
 495 out as secondary phases. Figure 10b shows how the aluminium and silica concentrations are estimated in the
 496 model. To estimate $[Al^{3+}]$ and $[SiO_2]$ in the above equations we assume the systems are close to equilibrium
 497 with a gibbsite-like and a kaolinite-like phase. Thus we assume that aluminium precipitates out from the
 498 solution, controlled by something that appears to be gibbsite-like; it is likely something amorphous of unknown
 499 composition, see Alveteg et al. (1995). The “Gibbsite” reaction is:



503 Leading to the “Gibbsite” expression:

$$[Al^{3+}] = K_G * [H^+]^Y \quad (19)$$

507 where the exponent Y has a value of 2.4 to 3. K_G is the Gibbsite coefficient and defined in the critical loads
 508 mapping manual (Sverdrup et al., 1990). An expression analogous to the Gibbsite approximation is used to
 509 calculate the SiO_2 concentration (Equation 22b, below). We assume that the Si will be present as $H_4Si(OH)_4$
 510 in the fluid phase, not upsetting any charge balance constraints. We assume that silica precipitates out,
 511 controlled by what that appears to be kaolinite. As such, there is a similar expression can be used for
 512 approximating the silica concentration:



515
 516 which gives the apparent equilibrium expressions:

517
 518
$$[\text{Al}^{3+}]^2 * [\text{OH}^-]^6 * [\text{SiO}_2]^2 = K_{\text{Kaolinite}} \quad (21)$$

519
 520 And this can be re-arranged to:

521
 522
$$[\text{SiO}_2]^2 = K_{\text{Kaolinite}}^2 * \frac{[\text{H}^+]^6}{[\text{Al}^{3+}]^2} \quad (22a)$$

523
 524 which leads to the “kaolinite” expression:

525
 526
$$[\text{SiO}_2] = K_{\text{Kaolinite}} * \frac{[\text{H}^+]^3}{[\text{Al}^{3+}]} \quad (22b)$$

527 where $K_{\text{Kaolinite}}$ is the equilibrium coefficient being used. Note that the “equilibrium” equations assumed above,
 528 are not true equilibrium, and that kaolinite and gibbsite minerals dissolve very slowly under normal conditions.
 529 Both the “gibbsite” and “kaolinite” mentioned above are crude simplifications, possibly representing an
 530 amorphous precipitate combined with precipitation kinetics and ion exchange (see Alveteg et al., 1995, Rietz
 531 1995, Warfvinge et al., 1996 for more information).

534 3.9. The full kinetic expression

535 The equations and approximations summarized above leads to the full revised mineral dissolution rate
 536 equations given by

537
 538
$$r = k_H * \frac{[\text{H}^+]^{n_H}}{f_H} + \frac{k_{\text{H}_2\text{O}}}{f_{\text{H}_2\text{O}}} + k_{\text{CO}_2} * P_{\text{CO}_2}^{n_{\text{CO}_2}} * \frac{1}{f_{\text{CO}_2}} + k_R * [\text{R}]^{n_R} * \frac{1}{f_R} + k_{\text{OH}} * \frac{[\text{OH}^-]^{n_{\text{OH}}}}{f_{\text{OH}}} \quad (23)$$

539 where the retarding or ‘brake’ functions are given by:

540
 541
 542
$$f_{\text{H}^+} = \left(1 + \frac{[\text{BC}]}{C_{\text{BC,H}}}\right)^{x_H} * \left(1 + \frac{[\text{Al}^{3+}]}{C_{\text{Al,H}}}\right)^{y_H} * \left(1 + K_{\text{Si,H}} * \left(\frac{[\text{Si}]}{C_{\text{Si,H}^+}}\right)^{z_H}\right) \quad (24)$$

543
 544
$$f_{\text{H}_2\text{O}} = \left(1 + \frac{[\text{BC}]}{C_{\text{BC,H}_2\text{O}}}\right)^{x_{\text{H}_2\text{O}}} * \left(1 + \frac{[\text{Al}^{3+}]}{C_{\text{Al,H}_2\text{O}}}\right)^{y_{\text{H}_2\text{O}}} * \left(1 + K_{\text{Si,H}_2\text{O}} * \left(\frac{[\text{Si}]}{C_{\text{Si,H}_2\text{O}}}\right)^{z_{\text{H}_2\text{O}}}\right) \quad (25)$$

545
 546
$$f_{\text{CO}_2} = \left(1 + K_{\text{CO}_2} * \frac{P_{\text{CO}_2}}{P_{\text{CO}_2\text{Limit}}}\right)^{n_{\text{CO}_2}} * \left(1 + \frac{[\text{BC}]}{C_{\text{BC,CO}_2}}\right)^{x_{\text{CO}_2}} * \left(1 + \frac{[\text{Al}^{3+}]}{C_{\text{Al,CO}_2}}\right)^{y_{\text{CO}_2}} * \left(1 + K_{\text{Si,CO}_2} * \left(\frac{[\text{Si}]}{C_{\text{Si,CO}_2}}\right)^{z_{\text{CO}_2}}\right) \quad (26)$$

547
 548
 549
$$f_R = \left(1 + \frac{[\text{R}]}{[\text{R}]_{\text{Limit}}}\right)^{n_R} * \left(1 + \frac{[\text{BC}]}{C_{\text{BC,R}}}\right)^{x_R} * \left(1 + \frac{[\text{Al}^{3+}]}{C_{\text{Al,R}}}\right)^{y_R} * \left(1 + K_{\text{Si,R}} * \left(\frac{[\text{Si}]}{C_{\text{Si,R}}}\right)^{z_R}\right) \quad (27)$$

550
 551
$$f_{\text{OH}^-} = \left(1 + \frac{[\text{BC}]}{C_{\text{BC,OH}}}\right)^{x_{\text{OH}}} * \left(1 + \frac{[\text{Al}^{3+}]}{C_{\text{Al,OH}}}\right)^{y_{\text{OH}}} * \left(1 + K_{\text{Si,OH}} * \left(\frac{[\text{Si}]}{C_{\text{Si,OH}^-}}\right)^{z_{\text{OH}}}\right) \quad (28)$$

552 where:

553 $C_{\text{BC},i}$ is the lower limiting base cation concentration in reaction i ,
 554 $C_{\text{Al},i}$ is the lower limiting aluminium concentration in reaction i ,
 555



556 C_{Si_i} is the lower limiting silica concentration in reaction i ,
 557 $P_{CO_2\text{limit}}$ is the lower limiting carbon dioxide partial pressure in reaction i ,
 558 $[R]_{\text{limit}}$ is the lower limiting organic acid concentration in reaction i as concentration of DOC,
 559 x_i is the base cation brake reaction order for i ,
 560 y_i is the aluminium brake reaction order for i
 561 z_i is the silica brake reaction order of i .
 562 K_{CO_2} is the CO_2 brake coefficient and set to 20.
 563 K_{Si_i} is the silica brake constant for reaction i , set to 100.
 564

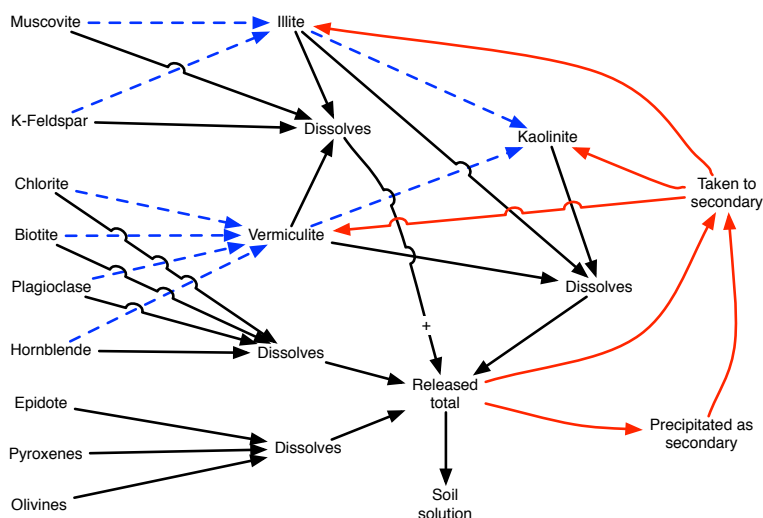
Table 2. Alteration series from muscovite, biotite and feldspars to clays, corresponding to Figure 11.

#	Mineral	Interlayer	Octahedral	Tetrahedral
Muscovite pathway				
1	Muscovite	K	Al ₂	Al _{1.0} Si _{3.0} O ₁₀ (OH) ₂
2	Illite 1	K _{0.5} Mg _{0.01} Ca _{0.01} Al _{0.05}	Al _{1.6} Fe _{0.25} Mg _{0.1} Ti _{0.04}	Al _{0.6} Si _{3.4} O ₁₀ (OH) ₂
3	Illite 2	K _{0.44} Mg _{0.01} Ca _{0.01} Al _{0.07}	Al _{1.6} Fe _{0.25} Mg _{0.1} Ti _{0.04}	Al _{0.6} Si _{3.4} O ₁₀ (OH) ₂
4	Illite 3	K _{0.39} Mg _{0.013} Ca _{0.013} Al _{0.06}	Al _{1.5} Fe _{0.32} Mg _{0.1} Ti _{0.08}	Al _{0.6} Si _{3.4} O ₁₀ (OH) ₂
5	Illitic vermiculite	K _{0.35} Mg _{0.03} Ca _{0.03} Al _{0.06}	Al _{1.63} Fe _{0.32} Mg _{0.08} Ti _{0.07}	Al _{0.6} Si _{3.4} O ₁₀ (OH) ₂
6	Kaolinite			Al _{2.0} Si ₂ O ₅ (OH) ₄
Chlorite pathway				
1	Chlorite	Ca _{0.5} Mg _{1.5}	Al _{1.0} Fe _{0.5} Mg _{1.5}	Al _{1.0} Si _{3.0} O ₁₀ (OH) ₂
2	Vermiculite 1	K _{0.32} Mg _{0.07} Ca _{0.09} Al _{0.05}	Al _{1.52} Fe _{0.35} Mg _{0.1}	Al _{0.6} Si _{3.4} O ₁₀ (OH) ₂
3	Vermiculite 2	K _{0.30} Mg _{0.05} Ca _{0.05} Al _{0.05}	Al _{1.55} Fe _{0.32} Mg _{0.05} Ti _{0.06}	Al _{0.6} Si _{3.4} O ₁₀ (OH) ₂
4	Vermiculite 3	K _{0.25} Mg _{0.04} Ca _{0.04} Al _{0.08}	Al _{1.55} Fe _{0.32} Mg _{0.05} Ti _{0.06}	Al _{0.6} Si _{3.4} O ₁₀ (OH) ₂
5	Al/OH interlayered vermiculite	K _{0.11} Mg _{0.04} Ca _{0.04} Al _{0.1}	Al _{1.52} Fe _{0.4} Mg _{0.05} Ti _{0.08}	Al _{0.5} Si _{3.5} O ₁₀ (OH) ₂
6	Kaolinite			Al _{2.0} Si ₂ O ₅ (OH) ₄
Biotite pathway				
1	Biotite	K _{1.0} Mg _{2.0}	Al _{0.5} Fe _{0.5} Mg _{1.0}	Al _{1.0} Si _{3.0} O ₁₀ (OH) ₂
2	Vermiculite 1	K _{0.32} Mg _{0.07} Ca _{0.09} Al _{0.05}	Al _{1.52} Fe _{0.35} Mg _{0.1}	Al _{0.6} Si _{3.4} O ₁₀ (OH) ₂
3	Vermiculite 2	K _{0.30} Mg _{0.05} Ca _{0.05} Al _{0.05}	Al _{1.55} Fe _{0.32} Mg _{0.05} Ti _{0.06}	Al _{0.6} Si _{3.4} O ₁₀ (OH) ₂
4	Vermiculite 3	K _{0.25} Mg _{0.04} Ca _{0.04} Al _{0.08}	Al _{1.55} Fe _{0.32} Mg _{0.05} Ti _{0.06}	Al _{0.6} Si _{3.4} O ₁₀ (OH) ₂
5	Al/OH interlayered vermiculite	K _{0.1} Mg _{0.04} Ca _{0.04} Al _{0.1}	Al _{1.52} Fe _{0.4} Mg _{0.05} Ti _{0.08}	Al _{0.5} Si _{3.5} O ₁₀ (OH) ₂
6	Kaolinite			Al _{2.0} Si ₂ O ₅ (OH) ₄
Feldspar pathway				
1	Feldspar	K, Na, Ca		Al ₁ Si ₃ O ₈
2	Sericite	Na _{0.1} K _{0.75}	Al _{1.9} Mg _{0.1}	Al _{0.84} Si _{3.16} O ₁₀ (OH) ₂
3	Sericitic vermiculite 1	K _{0.3} Mg _{0.02} Ca _{0.05}	Al _{0.02}	Al _{1.0} Si ₃ O ₁₀ (OH) ₂
4	Sericitic vermiculite 2	K _{0.1} Mg _{0.05} Ca _{0.02}	Al _{0.05}	Al _{1.0} Si ₃ O ₁₀ (OH) ₂
5	Al/OH interlayered vermiculite	K _{0.1} Mg _{0.04} Ca _{0.04} Al _{0.1}	Al _{1.52} Fe _{0.4} Mg _{0.05} Ti _{0.08}	Al _{0.5} Si _{3.5} O ₁₀ (OH) ₂
6	Kaolinite			Al _{2.0} Si ₂ O ₅ (OH) ₄

565
 566 **3.10. Secondary phases in the soil**
 567 A significant fraction of primary minerals dissolve incongruently to alteration minerals often referred to as
 568 secondary minerals and clays. Both terms are inconsistently used in the literature, and thus we define them as
 569 follows: We define clay minerals by their composition (kaolinite, gibbsite, quartz) and as listed in Table 3.
 570 This approach is thus not based on particle size, but on the molecular crystalline structure. Secondary minerals
 571 are formed in either two ways; a mineral that has been altered significantly in situ as is described in Table 2,
 572 for example when muscovite is altered through a series of illite and vermiculite phases and finally to kaolinite
 573 as the end product. Vermiculite, illite, montmorillonite are minerals of variable composition that are often
 574 called clays. In the soil, amorphous phases are composed of aluminium, silicate and soil organic substances.
 575 These amorphous phases slowly change composition as the organic matter decomposes and a more solid
 576 structure emerges. The alteration series from muscovite, biotite and feldspars to clays, are illustrated
 577 schematically in Figure 11 and listed in Table 2. The concept behind Table 2 is that as these minerals go
 578 through incongruent dissolution (alteration), they become depleted in certain ions (like Ca, Mg, K or Na, and
 579 depending on pH, in aluminium (at low pH) or silica (at high pH), but the crystal structure remains constant.
 580 Thus the crystal lattice destruction rate remains, but the base cation content of this structure becomes poorer,
 581 yielding less cations and less acidity neutralization. We have simplified this process down to 4 pathways, the
 582 muscovite pathway, the chlorite pathway, the biotite pathway and the feldspar pathway – see Table 2.
 583 Muscovite changes through a series of alteration reactions to illite and finally to kaolinite. Chlorite alters to
 584 vermiculites and finally to kaolinite. Biotite goes through a series of alterations to vermiculite and kaolinite.



585 Feldspars go through alterations, K-Feldspars through sericites and plagioclases to vermiculites (Holmqvist
586 2004, Holmqvist 2002, 2003).
587



588
589 *Figure 11. The alteration sequence developed for primary mineral towards alteration minerals, of which some*
590 *are clay minerals. All minerals that dissolve contribute to the precipitation of secondary minerals.*
591

592
593
594
595
596
597

3.11. The parameterization of the kinetic rate equations

The original PROFILE database had kinetic data for 59 different minerals, including about 25 different carbonates and some artificial silicates. New data from our own experiments (Sverdrup 1998, 1996, Sverdrup and Alveteg 1998, Holmqvist et al., 2002, 2003; Sverdrup and Holmqvist 2004) and from the literature² have

²Examples are the following list of articles and studies we have used, but not limited to: Ajemba and Onokwuli 2012, Alekseyev 2007, Alexeyev et al., 1997, Amram and Ganor 2005, Amrhein and Suarez 1992, Anbeek 1992a,b, Anbeek et al., 1994, Aradottir et al., 2013, Bandstra et al., 1998, Beig and Lüttge 2006, Bengtsson and Sjöberg 2009, Berg and Banwart 1994, 2000, Bibi et al., 2010, Bickmore et al., 2006, Blake and Walther 1996, Blum and Stillings 1995, Blum and Lasaga 1988, 1991, Blum 1994, Brady and Walther 1992, Bray et al., 2015, Brandt et al., 2005, Brantley 2003, 2008a,b, Brantley and Stillings 1994, 1996, Brantley and Chen 1995, Brantley and Conrad 2008, Brady and Walther 1992, Braun et al., 2016, Bray 2015, Cama et al., 2000, Carrol and Knauss 2005, Carrol and Westrich 1992, Chaïrat et al., 2007, Chen and Brantley 1997, 1998, 2000, Chin and Mills 1991, Critelli et al., 2015, 2014, Cotton 2008, Crundwell 2013, 2014a,b,c,d, 2015a,b, 2017, Daval et al., 2010a,b, 2013, Devidal et al., 1997, Diedrich et al., 2014, Dixit and Carrol 2007, Dove and Crerar 1990, Dorozhkin 2012, Dresel 1989, Drever et al., 1994, 1996, Drever and Clow 1995, Drever and Zobrist 1992, Drever and Stillings 1997, Dorozin 2012, Duckworth and Martins 2003a,b, Fernandez-Bastero et al., 2008, Fischer and Liebscher 2014, Finlay et al., 2010, Fouda et al., 1996a,b, Frogner and Schweda 1998, Fumuto et al., 2001, Gahrke et al., 2005, Ganor et al., 2005, Gautier et al., 1994, Gislason and Hans, 1987, Gislason and Oelkers 2003, Gislason et al., 1996, Godderis et al., 2006, Glover et al., 2003, Godderis et al., 2006, Golubev et al., 2004, 2005, Guidry and Mackenzie 2003, Goynes et al., 2006, Gudbrandsson et al., 2011, 2014, Gustafsson and Puigdomenech 2003, Hamilton et al., 2000, 2001, Hangx and Spiers 2009, Harouiyi et al., 2007, Harouiyi and Oelkers 2004, Haug et al., 2010, Hausrath et al., 2009, Hayashi and Yamada 1990, Helgeson et al., 1984, Hellmann 2007, 2006, 2010, Hilley et al., 2010, Holmqvist and Sverdrup 2001, Holmqvist et al., 1999, 2002, 2003, 2004, Hodson 2006a,b, Hodson and Langan 1999, Hodson et al., 1996, 1997, Hänchen et al., 2006, Huertas et al., 1999, 2001, Jin et al., 2011, Johnsson et al., 1992, Johnson et al., 2014, Jonckbloedt 1998, Jönsson et al., 1995, Kalinowski 1997, Kalinowski and Schweda 1995, Kalinowski et al., 1998, Knauss et al., 1993, Köhler et al., 2003, 2005, Kuwahara 2006a,b, 2008, Labat and Viville 2006, Lagache 1965, Langan et al., 1996a, b, Lartigue 1994, Lasaga 1995, 1998, Lowson et al., 2005, 2007, Lazaro et al., 2015, Lu et al., 2013, 2015, Ludwig et al., 2013, Maher 2010, Malmström and Banwart 1997, Malmström et al., 1996, Maurice et al., 2002, Mazer and Walther 1994, McCourt and Hendershot 1992, Metz et al., 2005, Meyer 2014, Mongeon et al., 2007, Murakami et al., 1998, Murphy and Helgeson 1987, Murphy et al., 1992, 1996, Nagy 1995, Nagy and Lasaga 1992, Nagy et al., 1991, Navarre-Sitchler and Thyne 2007, Nesbitt et al., 1991, Nyström-Claesson and Andersson 1996, Numan and Weaver 1969, Oelkers 2001a,b, Oelkers and Schott 1995a,b, 1998, 2001, Oelkers et al., 1994, 2008, Oelkers and Gislason 2001, Olsen 2007, 2008, Olsson 2007, Opolot and Finke 2015, Oxburgh 1991, Oxburgh et al., 1994, Paces 1983, Palandri and Kharkh 2004, Pokrowsky and Schott 2000a,b, 2002, Pokrowsky et al., 2004, Poulson et al., 1997, Prajapati et al., 2014, Price et al., 2005, Pigiobbe et al., 2009, Ragnarsdottir 1993, Ragnarsdottir and Graham 1996, Raschmann and Fedorockova 2008, Rietz 1995, Rimstidt et al., 2012, Ross 1969, Rosso and Rimstidt 1999, Rozalen et al., 2014, Running and Gower 1991, Saldi et al., 2007, Sanemasa and Katura 1973, Schnoor 1990, Schofield et al., 2015, Schott et al., 2009, 2012, Smith et al., 2013, Smits and



598 been considered to upgrade this database for this study. Care of these new data we have obtained rate
 599 parameters for about 107 different silicate or aluminium minerals and 6 generic carbonates. Of these minerals,
 600 the regression of ~20 have yet to be published. In due time, these will get their own proper publications, it is
 601 beyond the scope of this study to do them in detail. Data and records from unpublished experiments and
 602 experiment evaluations by Sverdrup and Holmqvist are available on paper records held in a large number of
 603 binders at the Inland University of Applied Sciences, at Hamar, Norway. These data are no longer available in
 604 digital form due to computer system changes and data filing format changes that have occurred during the last
 605 20 years. This documentation could be available in 1-2 years time, provided that funding for the redigitalization
 606 work can be obtained. Rather some selected examples are presented below. The estimation of rate parameters
 607 was performed using the complete rate equation 1 and equations 23-28. As such, for a successful regression
 608 of experimental data, the rate must be known, along with the concentrations of all reactants at the conditions
 609 that rate was observed including $[H^+]$, pCO_2 , $[R]$, $[OH^-]$, as well as the reaction products in solution potentially
 610 contributing to retarding the dissolution reaction; $[Ca^{2+}]$, $[Mg^{2+}]$, $[K^+]$, $[Na^+]$, $[Al^{3+}]$, $[Al(OH)_4^-]$, $[H_4SiO_4]$
 611 (Sverdrup 1990, Sverdrup and Warfvinge 1995). The experiments must have been performed over sufficient
 612 reaction conditions for the parameters in Equation 29 to be estimated. In some cases, the data from different
 613 experimental studies were combined to determine rate parameters or a reaction orders. During the regression
 614 process, experimental studies with insufficient data or documentation were omitted, unless the gap could be
 615 bridged with reasonable assumptions. Data regression was performed by rearranging equation (22) to:
 616

$$617 \quad k_H * \frac{[H^+]^{n_H}}{f_H} = r_{\text{Observed}} - \left(\frac{k_{H_2O}}{f_{H_2O}} + k_{CO_2} * \frac{P_{CO_2}^{n_{CO_2}}}{1 + K_{CO_2} * P_{CO_2}^{n_{CO_2}}} * \frac{1}{f_{CO_2}} \right. \\ 618 \quad \left. + k_R * \frac{[R]^{n_R}}{1 + K_R * [R]^{n_R}} * \frac{1}{f_R} + k_{OH} * \frac{[OH^-]^{n_{OH}}}{f_{OH}} \right) \quad (29)$$

619
 620 In the acid to neutral pH range, such as $pH < 7$, this equation can be simplified in most instances by removing
 621 the OH-reaction to get (Sverdrup 1990):
 622

$$623 \quad k_H * \frac{[H^+]^{n_H}}{f_H} = r_{\text{Observed}} - \left(\frac{k_{H_2O}}{f_{H_2O}} + k_{CO_2} * \frac{P_{CO_2}^{n_{CO_2}}}{1 + K_{CO_2} * P_{CO_2}^{n_{CO_2}}} * \frac{1}{f_{CO_2}} \right. \\ 624 \quad \left. + k_R * \frac{[R]^{n_R}}{1 + K_R * [R]^{n_R}} * \frac{1}{f_R} \right) \quad (30)$$

625 and the in the acid pH range ($pH < 4$), this may be reduced to:
 626

$$627 \quad k_H * \frac{[H^+]^{n_H}}{f_H} = r_{\text{Observed}} \quad (31)$$

628
 629 By entering the concentrations of H^+ , base cations, aluminium and silica into these equations, we can determine
 630 the rate coefficient, k_H , and f_{H^+} . When the experiment was performed in the absence of organic acids, as is
 631 often the case, Equation (29) reduces to:
 632

$$633 \quad k_H * \frac{[H^+]^{n_H}}{f_H} = r_{\text{Observed}} - \left(\frac{k_{H_2O}}{f_{H_2O}} + k_{CO_2} * \frac{P_{CO_2}^{n_{CO_2}}}{1 + K_{CO_2} * P_{CO_2}^{n_{CO_2}}} * \frac{1}{f_{CO_2}} \right) \quad (32)$$

634

Wallander 2016, Smits et al., 2014, Soler et al., 2008, Stephens and Hering 2003, Stillings and Brantley 1995, Stillings et al., 1996, Stockmann et al., 2008, Stumm and Wollast 1990, Stumm and Wieland 1990, Sverdrup 1990, 1996a,b, 1998, 2009, Sverdrup and Bjerle 1982, Sverdrup and Alveteg 1998, Sverdrup and Holmqvist 2016, Sverdrup and Warfvinge 1992a,b, 1995, Sverdrup et al., 1986, 1987, 1995,a,b, 1998, 2002, 2006, 2008, 2010, Traven et al., 2005, Swoboda-Collberg and Drever 1993, Taylor et al., 1999, 2000, Taylor and Blum 1995, Taylor et al., 2017, Techer et al., 2007, Terry et al., 2007, Terry 1983a,b,c, Terry and Monhemius 1983, Thom et al., 2013, Valsami-Jones et al., 1998, Turpault and Trotignon 1994, Valsami-Jones et al., 1998, Voltini et al., 2012, Wang and Giammar 2012, Wang et al., 2017, Warfvinge and Sverdrup 1992,a,b,c,d, 1993, 1995, Warfvinge et al., 1987, 1992, 1993, 1996, 2000, Weissbart and Rimstidt 2000, Welch and Ullman 1993, 1996, 2000, Westrich et al., 1993, White and Brantley 1995, 2003, White and Blum 1995, White et al., 1999, Whitfield et al., 2009, 2010, Wogelius and Walther 1991, 1992, Wolff-Boenisch et al., 2004a,b, 2011, Wood et al., 1999, Xie and Walter 1994, Yadaw and Chakrapani 2006, Yadaw et al., 2000, Yang and Steefel 2008, Yoo et al., 2009, Yu et al., 2016, 2017, Zabowski et al., 2007, Zhang and Bloom 1999a,b, Zhang et al., 1996, 2015, Zhang et al., 2013, Zhang and Lüttge 2017, 2009a,b, Zhu et al., 2010, Zassi 2009, Zavodsky et al., 1995, Zysset and Schindler 1996).



635 Some experiments were conducted at very low or with no dissolved CO₂ present and with organic ligands
 636 absent. In such cases, Equation (29) reduces to (Sverdrup 1990, Chin et al., 1991):
 637

$$638 \quad r_H = k_H * \frac{[H^+]^{n_H}}{f_H} = r_{\text{Observed}} - \frac{k_{H_2O}}{f_{H_2O}} \quad (33)$$

639
 640 In this latter case, two reactions influence mineral dissolution rates: 1) the H⁺ reaction, and 2) the water
 641 reaction. The variation of rates as a function of pH at such conditions consists of a ‘flat part’ where rates are
 642 controlled by the water reaction (Figure 12). At these conditions, by entering the concentrations of retarding
 643 base cations, aluminium and silica, the rate coefficients can be determined. In the semi-neutral region (pH 6-
 644 8), the expression may be a flat line and the rate expression is reduced to:
 645

$$646 \quad r_{\text{Observed}} = \frac{k_{H_2O}}{f_{H_2O}} + k_{CO_2} * \frac{P_{CO_2}^{n_{CO_2}}}{1 + K_{CO_2} * P_{CO_2}^{n_{CO_2}}} * \frac{1}{f_{CO_2}} + k_R * \frac{[R]^{n_R}}{1 + K_R * [R]^{n_R}} * \frac{1}{f_R} \quad (34)$$

647
 648 When neither organic ligands nor CO₂ is present, and in the pH range of 6-8, this is reduced to:
 649

$$650 \quad r_{\text{Observed}} = \frac{k_{H_2O}}{f_{H_2O}} \quad (35)$$

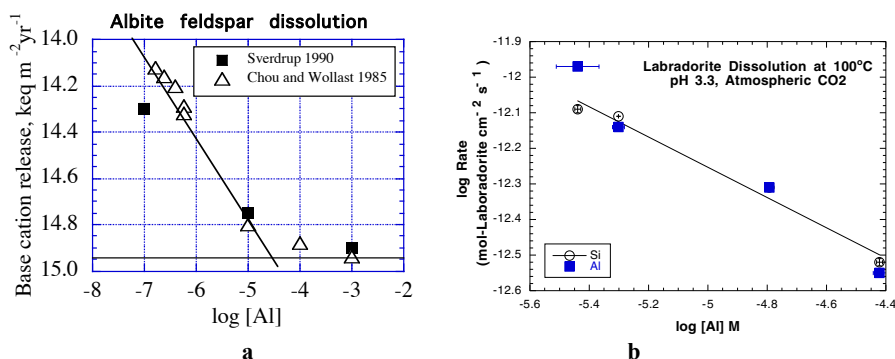
651
 652 With only organic acid ligands but no CO₂ present, and in the pH range of 6-8, the rate expression becomes:
 653

$$654 \quad r_{\text{Observed}} = \frac{k_{H_2O}}{f_{H_2O}} + k_R * \frac{[R]^{n_R}}{1 + K_R * [R]^{n_R}} * \frac{1}{f_R} \quad (36)$$

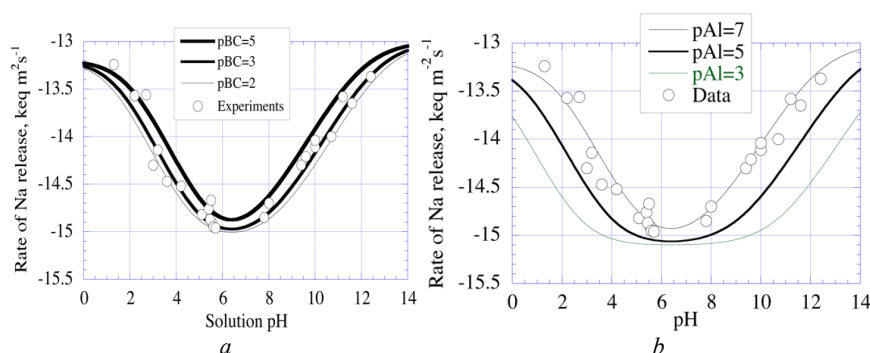
655
 656 In the far alkaline region (pH 10-14), where we may assume that the OH⁻ reaction will be dominant, the rate
 657 expression reduces to:
 658

$$659 \quad k_{OH} * \frac{[OH^-]^{n_{OH}}}{f_{OH}} = r_{\text{Observed}} \quad (33)$$

660
 661 By entering the concentrations of base cations, aluminium and silica, f_{OH} can be determined and the rate
 662 coefficient, k_{OH}, and reaction order, n_{OH} be determined. The reaction order n_H and the coupled n_{OH} for the H⁺
 663 and the OH⁻ reaction is derived from plots of the rate versus the solution pH

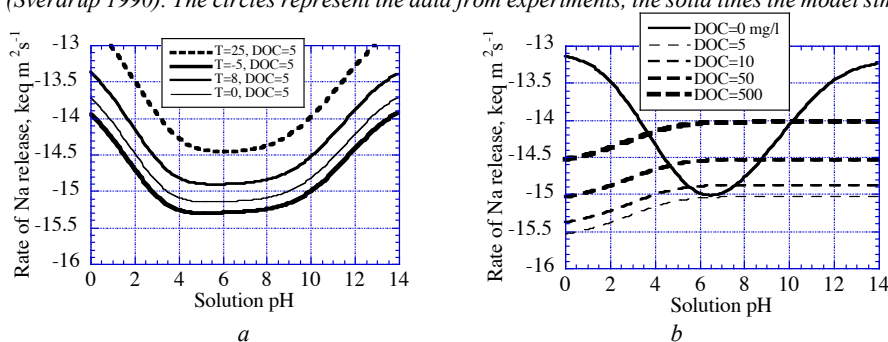


664
 665
 666 *Figure 12. Regression plots showing the retarding or ‘braking’ effect of aluminium on the dissolution rate of*
 667 *albite. The figures were adapted from Sverdrup (1990). The decrease of rates as a function of aqueous*
 668 *aluminium concentration (the aluminium brake) is very prominent in the range of log [Al³⁺] from -7 to -4.5.*
 669 *Aluminium concentrations are in kmol m⁻³. The figures were adapted from (a) Sverdrup et al. (1990) and from*
 670 *(b) Carroll and Knauss (2001). For further information, see Sverdrup (1990) and Sverdrup and Warfvinge*
 671 *(1995).*



672
673
674
675

Figure 13. The effect on the base cation (a) and the aluminium concentration (b) on the dissolution rate of albite. (Sverdrup 1990). The circles represent the data from experiments, the solid lines the model simulations.



676
677
678
679
680

Figure 14. The effect on the base cation (a) and the aluminium concentration (b) on the dissolution rate of albite. The solid line is the reaction rate without CO₂ or organic acid ligands.

Figure 13 shows diagrams used to quantify the retarding effect of aluminium on the dissolution rate of albite feldspar. The figures were adapted from Sverdrup (1990) and the work prepared for Sverdrup and Warfvinge (1995) and Sverdrup et al., (2009). Similar results for aluminium were found by Oelkers (2001), Oelkers and Gislsson (2001), Oelkers and Schott (2001, 1995a,b), Oelkers et al., (1999) for several minerals. The aluminium brake is very prominent in the range of log [Al] from -7 to -4.5. For further information, see Sverdrup (1990) and Sverdrup and Warfvinge (1995).

The reaction order for the organic acid reaction is derived from experiments where only the concentration of organic ligand, [R], has been varied. This was found to be $n_R=0.5$ on most experiments and this exponent value was universally adopted, suggesting a divalent ligand being the reactive agent (Sverdrup 1990, Sverdrup and Warfvinge 1995, Oelkers and Schott 1998).

The reaction order n_{CO_2} for the reaction with CO₂ is difficult to constrain, as very few experiments that allow it to be determined are available (Daval et al., 2013, Berg and Banwart 2000, Golubev et al., 2005, Fernandez-Bastero et al., 2008, Hangx and Spiers 2009, Lagache 1965, Wogelius and Walther 1991, Wolff-Boenisch et al., 2011, Stephens and Hering 2004, Sverdrup 1990). The few experiments that are available often gives conflicting results. Moreover, many experiments dealing with the effect of CO₂ on weathering do not have the required resolution to allow data regression. For the minerals where the CO₂ has little or no effect, this is fine, but for some it is. It was found to be $n_{CO_2}=0.6$ and was universally adopted. Sometimes these parameterizations can be determined by making single factor plots, but more often, the whole model must be used to recreate the experiments, taking many factors into account simultaneously. Figure 13 shows the effect on the base cation (a) and the aluminium concentration (b) on the dissolution rate of albite. Various plots were used to help data interpretation. Figure 14-15 illustrates how the model was used to plot different combinations of conditions, to investigate how distinct factors affect the weathering rates. The experimental data were overlaid in such diagrams (Figures 16-20) to help interpretation towards generating kinetic parameters (rate coefficients and reaction orders), for example the combination of different organic acid ligand concentrations and aluminium concentrations. The last diagram, on the lower right of Figure 15, shows the combination of different combinations of organic acid ligand concentrations and CO₂ pressures in atmospheres. Figure 16

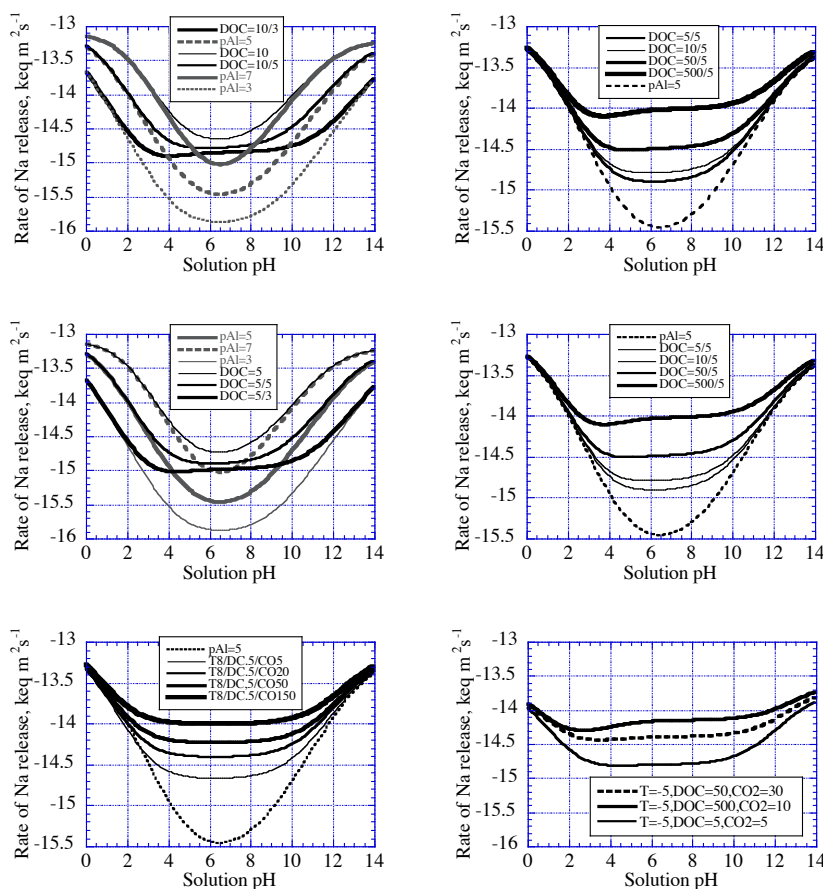


707 shows the effect on rates of the base cation (a) and the aluminium concentration (b) on the dissolution rate for
708 albite. The circles represent the data from experiments.

709 A further example of parameterization efforts is shown in Figure 16 for the case of hornblende
710 dissolution rate data reported by from Holmqvist and Sverdrup (2004) and Holmqvist et al. (2002, 2003).
711 Figure 16a and 16b shows these data as a function of pH. The figures were adapted from Holmqvist et al.,
712 2003). Figure 16c shows the retarding effect of aluminium on the dissolution rate of hornblende, adapted from
713 Holmqvist et al. (2003). Figure 16d shows a three-dimensional plot for the dissolution rate of hornblende, as
714 a function of solution pH and aluminium concentration (Sverdrup, 1990).

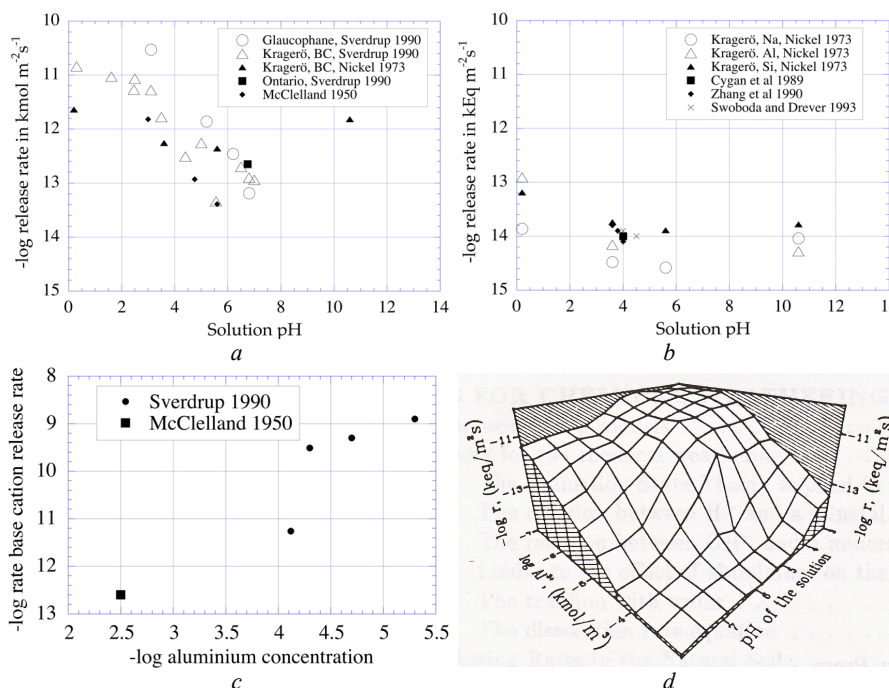
715 In total, the dissolution rate of hornblende is defined by at least 8 and perhaps 9 different chemical
716 factors including pH, Ca+Mg, K, Na, Al, DOC, CO₂, Si and sometimes Fe concentrations, and in addition to
717 mineral surface area, soil wetting degree and temperature. For example changes in the aluminium
718 concentration, can change the weathering rate by several orders of magnitude. Additional examples are
719 presented in Figs. 17-21.

720



721
722 *Figure 15. The weathering rate model was used to plot different combinations of conditions, to investigate the*
723 *different shapes the weathering rate dependency can change (See Figure 7 and 9 for how the principle works).*
724 *The experimental data were overlaid in such diagrams, to help retrieve kinetic parameters (e.g. rate*
725 *coefficients and reaction orders). The last diagram, lower right, shows the combination of different*
726 *combinations of organic acid ligand concentrations and CO₂ pressures in atmospheres.*

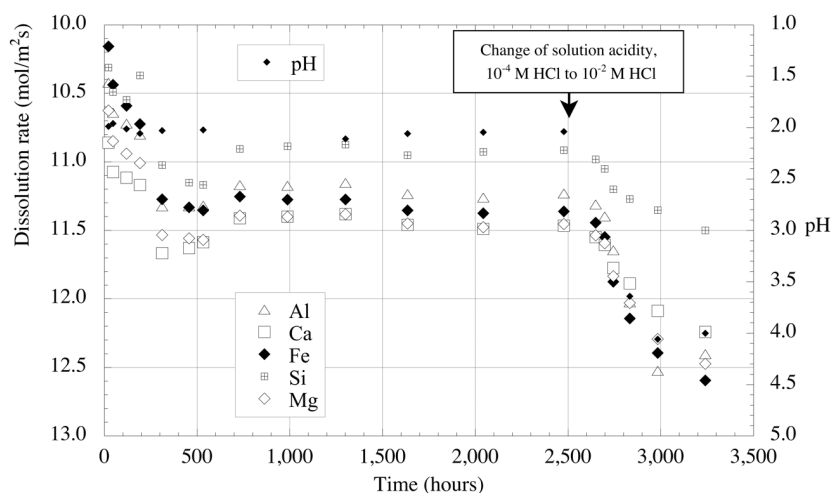
727
728 Figure 17 shows a typical example of data generated for different minerals during the 1996-2002 field
729 seasons using a continuous, flow through, fluidized bed, with constant concentration feed solutions. Figure 18
730 shows the experimentally measured dissolution rates of epidote, after Holmqvist et al. (2003), as a function of
731 pH according to a number of weathering experiments.



732
733

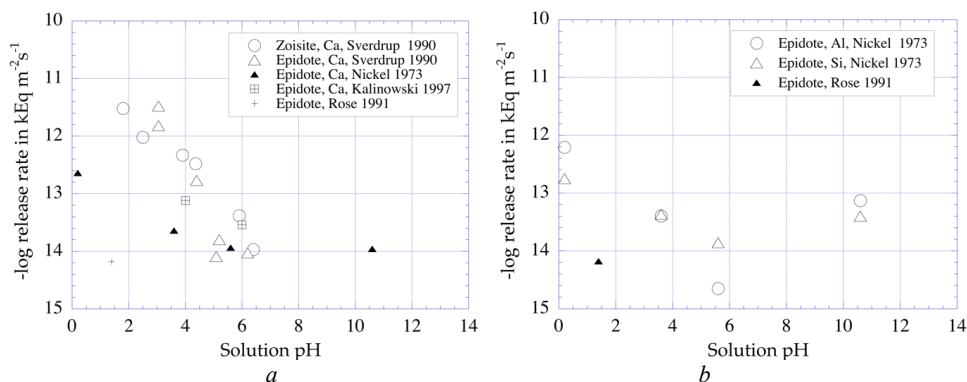
734
735
736
737
738
739
740
741
742

Figure 16. Diagram (a) shows the dissolution rate of minerals presented as base cation release rates as a function of pH and (b) shows the dissolution rate for hornblende as a function of solution pH, but under different experimental conditions (Adapted from Sverdrup, 1990). Diagram (c) shows the retarding effect of aluminium on the dissolution rate of hornblende. (Adapted from Holmqvist et al., 2003). Diagram (d) shows a three-dimensional plot for the dissolution rate of hornblende, as a function of solution pH and aluminium concentration (Adapted from Sverdrup, 1990).



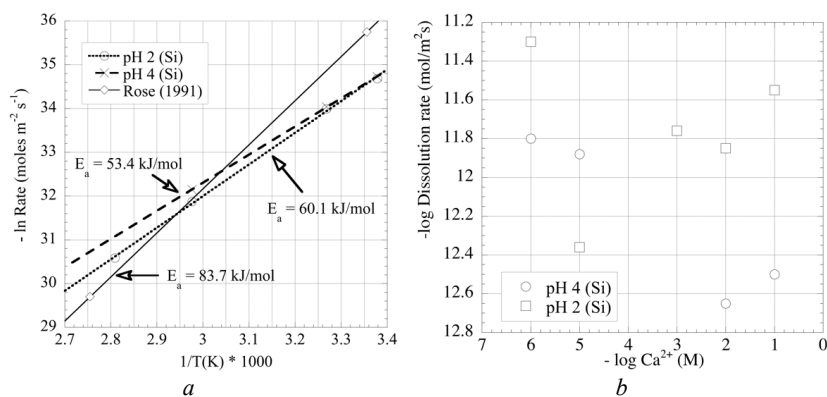
743
744
745
746

Figure 17. Typical example of dissolution rate data generated for epidote during 1996-2002 using a continuous, flow through, fluidized bed, with constant concentration feed solutions (Holmqvist 2002, 2003). All relevant constituents of the mineral were monitored in the aqueous solution in the experiment.



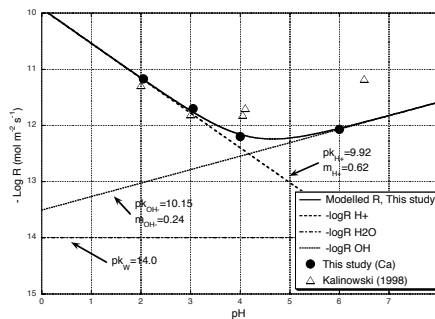
747
 748
 749
 750
 751

Figure 18. Epidote dissolution rate versus pH according to experiments reported by Holmqvist and Sverdrup and other literature sources data.



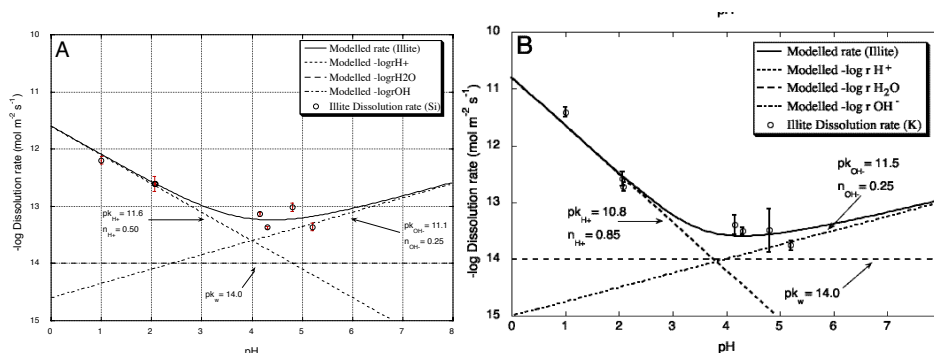
752
 753
 754
 755
 756

Figure 19. a) Estimates of the energy of activation for the dissolution of epidote. (b) the dependence of the rate of epidote on the calcium concentration at pH 2 and pH 4 (From one series of experiments by the authors).



757
 758
 759
 760

Figure 20. Hornblende dissolution rate data from Holmqvist and Sverdrup (2004) and Holmqvist et al. (2002, 2003) suggests that an arithmetic addition gives a good fit to the data.



761
762 *Figure 21. Diagram A show regression results from hornblende dissolution rates, diagram (B) shows*
763 *regression results from a natural illite mineral dissolution extracted from an agricultural soil sample taken at*
764 *the agricultural research site at Lanna, Uppsala, Sweden. Data from Holmqvist and Sverdrup (2004) and*
765 *Holmqvist et al. (2002, 2003)*

766
767 The release of all relevant ions was monitored by frequent sampling during the experiments. Figure
768 19a shows the activation energy for the dissolution of epidote. The dependence of the dissolution rate of
769 epidote on the calcium concentration at pH 2 and pH 4 is shown in Figure 19b. Figure 20 and 21 shows data
770 from Holmqvist and Sverdrup (2004) and Holmqvist et al. (2002, 2003) confirming that an arithmetic addition
771 of the various rate contributions gives the best fit of the data, consistent with the principle shown in Figure 7.
772 Figure 21 shows results from hornblende, the bottom diagrams (A, B) shows results from a natural illite
773 mineral extracted from an agricultural soil sample taken at the agricultural research site at Lanna, Swedish
774 Agricultural University, Uppsala, Sweden. Model lines were fitted to the data points to set the rate coefficients
775 and reaction orders. Note that a complete set of kinetic parameters could not be directly generated for all
776 minerals due to incomplete experimental data sets.

777 Estimates for some of the rate coefficients in Table 3 were based on mineral crystal structure analogies
778 (Sverdrup 1990, Holmqvist 2003, Sverdrup and Stiernquist 2002, Crundwell 2014a,b, 2016), crystal bond
779 energies (Sverdrup 1990, Velbel 1999, Crundwell 2014b, 2016) and comparison with analogue minerals. For
780 many of the minerals, the dissolution kinetics patterns are very consistent. The dissolution rate curve shapes
781 of feldspars, garnets, olivines, zoisites allow for this, but also muscovite to illite alteration series, K-feldspar
782 to sericite alteration series.

783 For example, for the feldspars, we have sufficient data to parameterize the H^+ reaction for 5 different
784 plagioclases, the mixed composition plagioclases from albite to anorthite. A plagioclase with a different
785 composition will be interpolated between these as shown in Figure 22. We have the same situation for K-
786 feldspars with increasing contents of Na and Ca, giving a systematic shift in parameter values. The pattern is
787 very consistent as can be seen from the diagrams shown in Sverdrup (1990). However, for the OH^- reaction
788 we have less information. The OH^- rate equation is theoretically linked to the H^+ reaction, but more sensitive
789 to the concentration of the same base cation as in the mineral (Na, K, Ca). With the available data and the
790 theoretical link, we can estimate the missing parameters for some of the feldspars. There is a similar situation
791 for the H_2O reaction. We have the experiments that allow it to be constrained for most of the feldspars, and
792 the shifts between the feldspars are systematic and consistent.

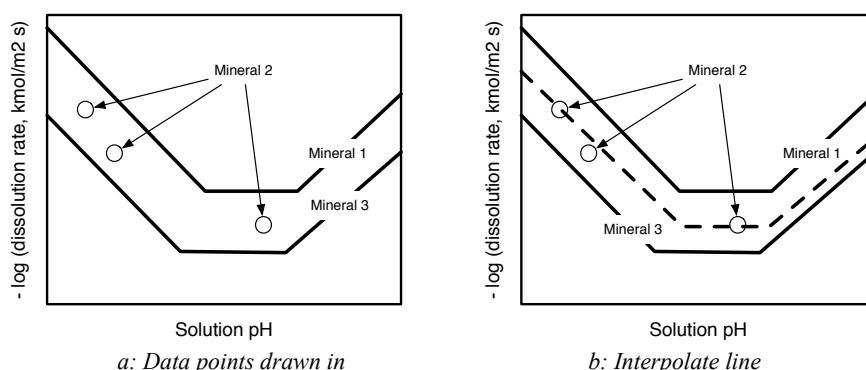
793 For the reaction with organic acid ligands, the situation is more complex. Many of the dissolution
794 experiments run with organic acids were poorly documented, and getting accurate parameterization from them
795 is not possible. For some minerals like feldspars and olivine, some experimental results are available (Stillings
796 et al., 1996 is one example for feldspar) that allow for kinetic parameter estimation. They found $n_R=0.75$ in
797 the range pH 3-7. For other minerals, we have only single experiments, scattered among some few minerals.
798 Few experiments are available, and for only a few types of minerals. These provide suggestions on what the
799 parameter values probably would be. The situation is similar for the reaction between the mineral surface and
800 CO_2 . The reaction seems to be weak, and only play a role at elevated pressures. For example, Wang (2013),
801 based on the experimental results of Hanchen et al. (2006) concluded there was no effect of the CO_2 reaction
802 on olivine dissolution rates beyond the effect caused by CO_2 on pH.

803 Retrieved kinetic parameters are provided in Table 3. Parameters that are derived directly from of one
804 or more set of experimental data are given in **bold** font. The kinetic parameters that were estimated are shown
805 in roman font. The minerals in this table are divided into 11 groups of basic crystalline structures. Some of the



806 minerals inside each group have large commonalities with respect to how they dissolve, and this was of great
807 help in parameter estimation table.

808 For feldspars, nesosilicates and phyllosilicates, the amount of experimental data available makes the
809 retrieved parameters robust. If three different compositions of basically the same type of mineral, A, B and C,
810 are known to have relative rates $A > B > C$, and we have the kinetic parameters for A and C, then we can be
811 fairly certain that the values for the kinetic parameters for B are constrained between A and C (see Figure 22).
812 If they are close, then we would be able to set parameters for B fairly accurately, even with sparse experimental
813 data for B. This is the case for many minerals (In particular feldspars, nesosilicates, phyllosilicates), and is a
814 way to get more parameterization from limited experimental data sets. For the pyroxenes and amphiboles, the
815 experiments indicate that the minerals behave with some variety depending on their composition, making the
816 estimates less accurate. But, many pyroxenes are mixtures of definable end members and this was utilized to
817 interpolate and estimate missing parameters.
818



819
820
821 *a: Data points drawn in* *b: Interpolate line*
822 *Figure 22. Some mineral groups have very similar dissolution rate behaviours. Such similarities can be used*
823 *to interpolate between them (b) when we have intermediate minerals with only a few data points available (a).*

824 Nevertheless all parameters in Table 3 together with their kinetic expressions should be further validated as
825 additional experimental data become available. The ultimate test of the kinetics equations and parameters are
826 how well they describe both laboratory experiments and field data where independent estimates of the
827 weathering rate are available. Such tests have been generally successful (see the publications referred to earlier,
828 and Erlandsson Lampa et al., 2016, 2019), suggesting that the combined methodology (experiments, analogues,
829 interpolations, estimates based on theoretical rescaling, predictions made based on crystal bond
830 energies) have captured the kinetics sufficiently well. More on this will be forthcoming in future publications.
831

832 4. Results

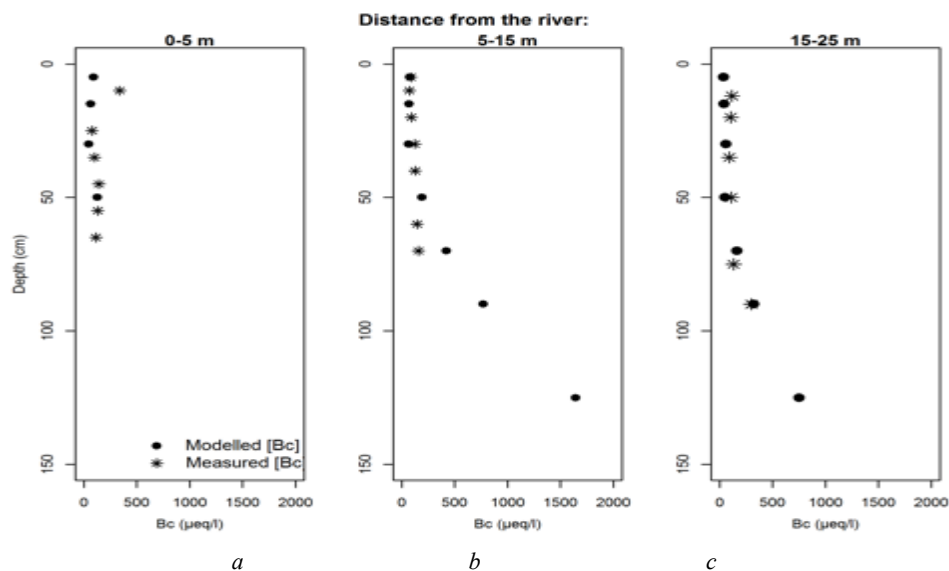
833 4.1. Kinetics and parameterization

834 The tabulated kinetic coefficients are the major result of this report and they are provided in the Tables
835 1, 3 and 4. In total the dissolution kinetics parameterization for 112 minerals are provided. Erlandsson-Lampa
836 et al. (this volume) tested the application of these values using the parameters on the Svartberget research site
837 as a field evaluation.

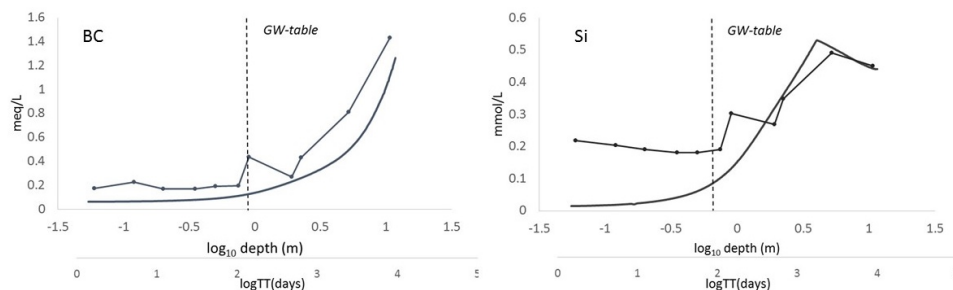
838 The parameters in Table 3 are for a temperature of 8°C and standard atmospheric pressure.. The
839 following default approximations were adopted due to the lack of data; C_{A1} for the H^+ -reaction is taken to be
840 equal to $\frac{1}{3}$ of the C_{A1} for the OH^- -reaction. C_{BC} for the H^+ -reaction is taken to be $\frac{1}{3}$ of the C_{BC} for the OH^- -
841 reaction. The retarding reaction orders for base cations (x), aluminium (y) and silicate (z) have been extracted
842 from separate datasets and experiments where it was possible to separate out the effect of silicate alone, having
843 subtracted the effect of base cations and aluminium first. Default values were computed and scaled with
844 Madelung crystal lattice site energy (See Sverdrup 1990 and Velbel 1999 for how a-priori weathering rate
845 coefficient estimates are made from crystal properties). Irreversible dissolution implies that the mineral cannot
846 be formed from solution under soil conditions, and that there is no saturation concentration or back reaction.
847 Pokrovsky and Schott (2000) and Rosso and Rimstidt (2000) reports a reaction order of $n_{H^+}=0.5$ for forsterite,
848 but others report $n_{H^+}=1.0$ (Grandstaff 1986, Blum and Lasaga 1988, Siegel and Pfannkuch 1984, Sverdrup
849 1990). $n_{H^+}=1.0$ seems to be a property of the nesosilicate group, but there is a possibility that presence of
850 impurities such as pyroxenes or feldspars in the nesosilicate may give it a different crystal structure and thus
851 a different n_{H^+} . Others, Berg and Banwart (2000), report n_{H^+} in the range 0.5 to 1, depending on pH.



852 Table 4 shows the temperature dependencies of the dissolution rates. All variations of rates on
 853 temperature are computed using a modified Arrhenius equation (Sverdrup 1990, 1998, Sverdrup and
 854 Warfvinge 1988, 1992, 1995). Parameters for this equation generated from experimentally measured rates are
 855 shown in bold. Where experimental data were not available, estimates were computed and scaled with
 856 Madelung crystal lattice site energy from garnet (Sverdrup 1990, Velbel 1999). Values in normal font were
 857 estimated from the lattice energies and the properties of the mineral surface. Table 5 shows the stoichiometry
 858 of the minerals considered in this study.
 859
 860



861
 862
 863 Figure 23. Comparison of calculated with measured base cation concentrations at the Svartberget field site,
 864 (Zanchi et al., 2016). Note the base cation concentrations ([Bc]) refer to the sum of the concentrations of Na,
 865 H, Ca, and Mg in units of microequivalents per litre.
 866



867
 868
 869 Figure 24. Modelled base cation (a) and Si (b) concentrations plotted against \log_{10} of water transit time
 870 (smooth lines) at the Svartberget field site (See Erlandsson-Lampa et al., 2016, 2019 for a full description of
 871 the field test of the model). Overlain are the observed base cation and Si-concentrations from the soil profile,
 872 plotted against \log_{10} of soil depth (straight lines with symbols).
 873

874 4.2. Testing the kinetic model

875 The most recent comparison between the kinetic weathering model results and field observations
 876 follows in the article by Erlandsson-Lampa et al. (This issue). The research catchment where many of the
 877 model applications have been tested is located in Northern Sweden. A few examples are shown in Figure 23
 878 and 24. Figure 23 shows a comparison between calculated and observed base cation concentrations at the



879 Svartberget research site. The model results reproduce the observed concentration pattern (Zanchi et al., 2016).
880 Figure 23a shows the modelled base cation (Bc)³ concentration and Figure 23b shows the Si concentrations,
881 plotted against log₁₀ of water transit time (smooth lines). Overlaid are the observed Bc and Si-concentrations
882 from the soil profile, plotted against log₁₀ of soil depth (solid lines with markers) in Figure 23c. The weathering
883 model considers all soil processes including ion exchange, vegetation interactions, decomposition of organic
884 matter, water transport in the catchment in both the horizontal and vertical directions (Belyazid et al., 2004,
885 2011a,b, 2010a,b, 2015, 2019, Erlandsson-Lampa et al., 2019, Sverdrup et al., 1995, 2002). The model
886 reproduces the observed field observations as a function of depth (Zanchi et al., 2016). The close
887 correspondence between the calculated dissolved metal concentrations and the field observation are notable
888 considering that we employed a silicate dissolution rate model based on laboratory measurements to determine
889 the composition of the aqueous phase in the soil.

890

891 4.3. Discussion

892 The detailed comparisons between laboratory measured and field determined weathering rates
893 generated using the kinetic models described above coupled to soil processes performed using PROFILE and
894 ForSAFE stand out in stark contrast to the traditional geochemical models, which give results that are several
895 orders of magnitude different from field observations (Erlandsson-Lampa et al., 2019). It was discovered that
896 past efforts to describe field weathering rates using laboratory measured dissolution rates without consideration
897 of the coupling of rates to the major soil processes yielded inaccurate results – see Erlandsson Lampa et al.
898 (2016) and Nyström-Claesson and Andersson, (1996). Such observations demonstrate a need to take into
899 account the complete set of processes occurring in the soil. Note that the mineral dissolution ‘brake functions’
900 used in this approach act differently on the weathering rates that the equilibrium expressions used in earlier
901 models (Aagaard and Helgeson 1982, Murphy et al., 1987, Alekseyev et al., 1997, 2004, 2007, Oelkers, 2001,
902 Oelkers et al., 1994, 2001, 2008). The preference for using the brakes rather than the traditional rate expression
903 based on a slowing of rates as equilibrium is approached between the surface and the liquid is that equilibrium
904 is not approached for many primary silicate minerals and thus the weathering process is irreversible.

905

906 7. Conclusions

907 The complex nature of weathering in the field is nearly impossible to interpret without a
908 comprehensive model for the whole process. A first step to such interpretations can be the quantitative
909 description of the dissolution rates of the major rock forming minerals. Even the dissolution rates of an
910 individual mineral can involve several simultaneous reactions. Thus, experimentally measured rates results
911 can only be accurately interpreted when a full system model is used. Under field conditions, mineral dissolution
912 is coupled to other soil processes, and thus a full ecosystem system model is needed for their interpretation.
913 The apparent difference between field and laboratory dissolution rates arise from the coupling of these
914 processes, and disappear once a full model is employed. Use of a fully coupled model shows these differences
915 to be negligible (Keegan and Laskow-Lehey 2014).

916 Taking account the vast literature reporting experimentally measured mineral dissolution rates, it was
917 possible to create a fully parameterized kinetic database for about 100 minerals. About 40% of the kinetic
918 parameters were determined directly from experiment interpretations, and the rest were determined from inter-
919 mineral interpolations and using of analogues.

920 The adjustment of the aluminium ‘brake function’ and the introduction of a silica “brake function” as
921 described in this work were necessary to improve the description of weathering rates in the lower part of the
922 soil, below 1 meter depth. The test at the Svartberget catchment suggests that this revised mineral dissolution
923 model works adequately as can be seen from Figures 24-25.

924

925 8. Acknowledgements

926 This work is based upon that of Prof. Dr. Harald Sverdrup and Prof. Dr. Per Warfvinge who initiated the new
927 model approaches in the 1980’s. Since then major contributions have been made by Dr. Matthias Alveteg (Uncertainty,
928 programming the code), Prof. Per Warfvinge (Programming the code), Dr. Cecilia Akselsson (Regional
929 parameterizations, geostatistics), Dr. Salim Belyazid (Programming the code, applying the model) and Daniel Kurz
930 (Adaption of the mineral stoichiometry, adaptation to Switzerland). Dr. Johan Holmqvist and Harald Sverdrup were
931 instrumental in taking up a second long campaign in weathering experiments, generating more kinetic data during 1997-
932 2004. Dr. Johan Holmqvist carefully worked out the geostatistics of landscape sampling and robustness of regional
933 parameterizations and creating geostatistically sound regional weathering rate maps), Dr. Salim Belyazid is the present
934 head code editor of the PROFILE and ForSAFE models.



935 This study was a part of the QWARTZ Project, coordinated by Prof. Kevin Bishop, Uppsala University, Sweden.
936 Dr. Salim Beliaïd, Natural Geography and Quaternary Geology, Stockholm University, Sweden, Dr. Martin Erlandsson
937 Lampa, Institute of Hydrology, University of Uppsala, Sweden, Dr. Cecilia Akselsson, Earth Sciences, Lund University,
938 Lund, Sweden, Daniel Kurz, EKG Geoscience, Bern, Switzerland, Dr. Max Posch, CCE, RIVM, Bilthoven, Netherlands,
939 Dr Julian Aherne, Ecology, University of Trent, Canada, Dr. Jennifer Phelan, RTI Inc, Triangle Park, North Carolina,
940 United States of America and Professor Harald Sverdrup, Industrial Engineering, University of Iceland, Reykjavik,
941 Iceland (Earlier at Lund University) took part in the parameterization workshops, with the aim to have this updated
942 kinetics database completed.

943 Professor Dr. Eric Oelkers was external advisor to the project, which turned out to be a good choice. He
944 participated very willingly, eagerly and with excellent advice to the research process and in writing this paper.
945

946 9. References

- 947 Aagard, P. and H. C. Helgeson, Thermodynamic and kinetic constraints on reaction rates among minerals and aqueous solutions: I.
948 Theoretical considerations. *American Journal of Science* 282: 237-285. 1982.
- 949 Adebayo, A.O., Ipinmoroti, K.O., Ajayi, O.O., Dissolution Kinetics of Chalcopyrite with Hydrogen Peroxide in Sulphuric acid Medium
950 *Chem. Biochem. Eng. Q.* 17, 213–218. 2003
- 951 Ajemba, R.O., and Onukwuli, O.D. Dissolution kinetics and mechanisms of reaction of Udi clay in nitric acid solution *American*
952 *Journal of Scientific and Industrial Research.* 3, 115-121. 2012
- 953 Alekseyev, V.A. Equations for the Dissolution Reaction Rates of Montmorillonite, Illite, and Chlorite. *Geochemistry International*,
954 45: 770–78. 2007
- 955 Alekseyev, V.A., Medvedeva, L.S., Prisyagina, N.I., Meshalkin, S.S., Balabin, A.I. Change in the dissolution rates of alkali feldspars
956 as a result of secondary mineral precipitation and approach to equilibrium. *Geochimica et Cosmochimica Acta* 61, 1125–
957 1142. 1997
- 958 Akselsson, C., Holmqvist, J., Alveteg, M., Kurz, D., Sverdrup, H. Scaling and mapping regional calculations of soil chemical
959 weathering. *Water, Air and Soil Pollution Focus* 4:671-681. 2004
- 960 Akselsson, C., Sverdrup, H., Holmqvist, J. Estimating weathering rates of Swedish forest soils in different scales, using the PROFILE
961 model. *Journal of Sustainable Forestry.* 21:119-131. 2005
- 962 Akselsson, C., Holmqvist, J., Kurz, D., Sverdrup, H. Relations between elemental content in till, mineralogy of till and bedrock
963 mineralogy in the province of Småland, Southern Sweden. *Geoderma* 136:643-659. 2006
- 964 Akselsson, C., and Sverdrup, H. Uthålligt skogsbruk i Sverige-räcker baskajonvittringen till? In: Melkerud, P., Markdagen 2004, Nytt
965 från forskningsfronten. 43-50. 2004
- 966 Akselsson, C., Westling, O., Sverdrup, H., Holmqvist, J., Thelin, G., Ugglä, E., Malm, G. Impact of harvest intensity on long term
967 base cation budgets in Swedish forest soils. *Water, Air and Soil Pollution: Focus* 7:201-210. 2007
- 968 Akselsson, C., Westling, O., Sverdrup, H., Holmqvist, J., Thelin, G., Ugglä, E., Malm, G. Impact of Harvest Intensity on Long-Term
969 Base Cation Budgets in Swedish Forest Soils. *Water, Air, and Soil Pollution: Focus* 7: 201-210. 2007
- 970 Akselsson, C., Fölster, J., Rapp, L., Alveteg, M., Belyazid, S., Westling, O., Sverdrup, H., Stendahl, J. Bara naturlig försurning.
971 Underlagsrapport reviderade beräkningar av kritisk belastning för försurning. I: Naturvårdsverkets *Rapport* 5780, Bara
972 naturlig försurning Bilagor til underlagsrapport fördjupad utvärdering av miljömålen, Bilaga 7:103-147. 2007
- 973 Akselsson, C., Westling, O., Alveteg, M., Thelin, G., Fransson, A.M., Hellsten, S., The influence of N load and harvest intensity on
974 the risk of P limitation in Swedish forest soils. *Science of the Total Environment.* 404, 284-289. 2008
- 975 Akselsson, C., Westling, O., Alveteg, M., Thelin, G., Fransson, A-M., Hellsten, S., The influence of N load and harvest intensity on
976 the risk of P limitation in Swedish forest soils. *Science of The Total Environment.* 404, 284-289. 2008
- 977 Akselsson, C., Belyazid, S. Critical biomass harvesting – Applying a new concept for Swedish forest soils. *Forest Ecology and*
978 *Management* 409, 67-73. 2018
- 979 Akselsson, C., Olsson, J., Belyazid, S., René Capell, R. Can increased weathering rates due to future warming compensate for base
980 cation losses following whole-tree harvesting in spruce forests? *Biogeochemistry* 128:1-2, 89-105. 2016
- 981 Albin, S., Building a system dynamics model; Part 1; Conceptualization. MIT System Dynamics Education Project (J. Forrester (Ed)).
982 MIT, Boston. 34pp. [https://ocw.mit.edu/courses/sloan-school-of-management/15-988-svstem-dynamics-self-study-fall-1998-
983 spring-1999/readings/building.pdf](https://ocw.mit.edu/courses/sloan-school-of-management/15-988-svstem-dynamics-self-study-fall-1998-spring-1999/readings/building.pdf). 1997
- 984 Alveteg, M., and Sverdrup, H. Gothenburg Protocol: Uncertainty as to effects, *Acid News* 2, June 2000.
- 985 Alveteg, M., Sverdrup, H., Warfvinge, P., Regional assessment of dynamic aspects of soil acidification in southern Sweden. *Water,*
986 *Air and Soil Pollution* 85:2509-2514. 1996
- 987 Alveteg, M., Walse, C., Sverdrup, H. Evaluating simplifications used in regional applications of SAFE and MAKEDEP models.
988 *Ecological Modelling* 107:265-277. 1998
- 989 Alveteg, M., Barkman, A., Sverdrup, H. Integrated Environmental Assessment Modelling - Uncertainty in Critical Load Assessments.
990 Final Report of the Swedish Subproject, EU/LIFE project. *Reports in Ecology and Environmental Engineering* 2000:1-163.
- 991 Alveteg, M., Sverdrup, H., Warfvinge, P. 1995 Developing a kinetic alternative in modelling soil aluminum. *Water, Air and Soil*
992 *Pollution,* 79:377–389
- 993 Ameli, A.A., Beven, K., Erlandsson, M., Creed, I.F., McDonnell J.J., Bishop, K. Primary weathering rates, water transit times, and
994 concentration-discharge relations: A theoretical analysis for the critical zone, *Water Resources Research* 53, 942–960, 2017
- 995 Amram, K. and Ganor, J. The combined effect of pH and temperature on smectite dissolution rate under acidic conditions. *Geochimica*
996 *et Cosmochimica Acta* 69, 2535–2546. 2005
- 997 Amrhein, C. and Suarez, D.L. Some factors affecting the dissolution kinetics of anorthite at 25 8C. *Geochimica et Cosmochimica*
998 *Acta* 56, 1815–1826. 1992
- 999 Anbeek, C. The dependence of dissolution rates on grain size for some fresh and weathered feldspars. *Geochimica et Cosmochimica*
1000 *Acta* 56, 3957–3970. 1992a
- 1001 Anbeek, C. Surface roughness of minerals and implications for dissolution studies. *Geochimica et Cosmochimica Acta* 56, 1461–
1002 1469. 1992b



- 1003 Anbeek, C., van Breemen N., Meijer E.L., van der Plas, L. The dissolution of naturally weathered feldspar and quartz. **Geochimica et Cosmochimica Acta** 58, 4601–4614. 1994
- 1004
- 1005 Andersson, B., Bishop, K., Borg, G.C., Gielser, R., Hultberg, H., Huse, M., Moldan, F., Nyberg, L., Nygaard, P.H., Nyström, U. The covered catchment site: A description of the physiography, climate and vegetation of three small coniferous forest catchments at Gårdsjön, South-west Sweden. In: Hultberg H. and Skeffington R. (Eds.) *Experimental reversal of acid rain effects; The Gårdsjön roof project*: 25-70. John Wiley Science. 1998
- 1006
- 1007
- 1008
- 1009 Aradóttir, E.S.P., Sigfusson, B., Sonnenthal, E.L., Björnsson, G., Jonsson, H. Dynamics of basaltic glass dissolution – Capturing microscopic effects in continuum scale models. **Geochimica et Cosmochimica Acta** 121: 311–327. 2013.
- 1010
- 1011 Augustin, F., Houle, D., Gagnon, C., Courchesne, F. Evaluation of three methods for estimating rates of base cations in forested catchments. **Catena** 144, 1-10. 2006.
- 1012
- 1013 Ballesta, R., Cabrero, B., Sverdrup, H., Critical loads for different soils of the Mediterranean environment. **The Science of the Total Environment** 181:65-71. 1996
- 1014
- 1015 Balogh-Brunstad, Z., Keller, C.K., Bormann, B.T., O'Brien, R., Wang, D., Hawley, G. Chemical weathering and chemical denudation dynamics through ecosystem development and disturbance, *Global Biogeochem. Cycles*, 22, GB1007, doi:10.1029/2007GB002957. 2008
- 1016
- 1017
- 1018 Bandstra, J.Z., Buss, H.L., Campen, K., Liermann, L.J., Moore J., Hausrath, E.M., Navarre, A.K., Jang, J-H., Brantley, S.L. *Appendix: Compilation of Mineral Dissolution Rates*, in *Kinetics of Water-Rock Interaction*, S. L. Brantley, J. D. Kubicki and A. F. White (eds). Springer, New York, 731-808. 1998
- 1019
- 1020
- 1021 Barkman, A., Schlyter, P., Lejonklev, M., Alveteg, M., Warfvinge, P., Sverdrup, H., Arnström T. Uncertainties in high resolution critical load assessment for forest soils - possibilities and constraints of combining distributed soil modelling and GIS. **Environmental and Geographical Modeling**, 3:2:125-143, 1999
- 1022
- 1023
- 1024 Barkman, A., and Sverdrup, H., Critical loads of acidity and nutrient imbalance for forest ecosystems in Skåne. *Reports in Environmental Engineering and Ecology*, 1:96, Chemical Engineering II, Box 124, Lund University. 221 00 Lund, Sweden, 1996
- 1025
- 1026
- 1027 Barkman, A., and Alveteg, M., Identifying potentials for reducing uncertainty in critical load calculations using the PROFILE model. **Water, Air and Soil Pollution**. 125, 35-54 2001.
- 1028
- 1029 Beig M.S., and Lüttge A. Albite dissolution kinetics as a function of distance from equilibrium: implications for natural feldspar weathering. **Geochimica et Cosmochimica Acta** 70:1402–1420. 2006
- 1030
- 1031 Bélanger, N., Côté, B., Courchesne, F., Fyles, J.W., Warfvinge, P. and Hendershot, W. H. Simulation of soil chemistry and nutrient availability in a forested ecosystem of southern Quebec. I. Reconstruction of time-series files of nutrient cycling using the MAKEDEP model. **Environ. Model. Soft.** 17: 427–445. 2002a
- 1032
- 1033
- 1034 Bélanger, N., Courchesne, F., Côté, B., Fyles, J.W., Warfvinge, P., Hendershot, W.H. Simulation of soil chemistry and nutrient availability in a forested ecosystem of southern Quebec. Part II. Application of the SAFE model. **Environ. Mod. Soft.** 17: 447–465. 2002b.
- 1035
- 1036
- 1037 Belyazid, S., Sverdrup, H., Alveteg, M. The biogeochemical models family of the biogeochemistry group at Lund University. Proceedings from a UN/ECE conference held in Pushino, Russia September 16-18, 2004. Institute of Soils Science and Phytobiology, Nauka, September 2004.
- 1038
- 1039
- 1040 Belyazid, S., Westling, O. Sverdrup, H. Modelling changes in soil chemistry at 16 Swedish coniferous forest sites following deposition reduction. **Environmental Pollution** 144:596-609. 2006
- 1041
- 1042 Belyazid, S., Bailey, S., Sverdrup H. Past and Future Effects of Atmospheric Deposition on the Forest Ecosystem at the Hubbard Brook Experimental Forest: Simulations with the Dynamic Model ForSAFE In: *Modelling of Pollutants in Complex Environmental Systems*, Volume II: 357-377, Hanrahan. G. (Ed.) ILM Publications, International Labmate Limited. 2010
- 1043
- 1044
- 1045 Belyazid, S., Sverdrup, H., Kurz, D., Braun, S. Exploring ground vegetation change for different scenarios and methods for estimating critical loads for biodiversity using the ForSAFE-VEG model in Switzerland and Sweden. **Water, Air and Soil Pollution**, 216:289-317. 2011
- 1046
- 1047
- 1048 Belyazid, S., Kurz, D., Braun, S., Sverdrup, H., Rihm, B., Hettelingh, J.P. A dynamic modelling approach for estimating critical loads of nitrogen based on plant community changes under a changing climate. **Environmental Pollution** 159:789-801. 2011
- 1049
- 1050 Belyazid S., Phelan J., Clark C., Sverdrup H., Nihlgård B., Driscoll C., Fernandez I., Robin Dennis, R., Aherne J. Assessing the effect of climate and air pollution on plant diversity and biogeochemistry in the Northeastern US broadleaf forests testing the ForSAFE-VEG model at three sites. In press **Water, Air and Soil Pollution**. 2015
- 1051
- 1052
- 1053 Belyazid, S., Kurz, D., Braun, S., Sverdrup, H., Rihm, B., Hettelingh, J.P. A dynamic modelling approach for estimating critical loads of nitrogen based on plant community changes under a changing climate. **Environmental Pollution** 159:789-801. 2011
- 1054
- 1055 Belyazid, S., Bailey, S., Sverdrup H. Past and Future Effects of Atmospheric Deposition on the Forest Ecosystem at the Hubbard Brook Experimental Forest: Simulations with the Dynamic Model ForSAFE In: *Modelling of Pollutants in Complex Environmental Systems*, Volume II: 357-377, Hanrahan. G. (Ed.) ILM Publications, International Labmate Limited. 2010
- 1056
- 1057
- 1058 Belyazid, S., Sverdrup, H., Akselsson, C., Kurz D. Synergies and conflicts in addressing climate change and nitrogen deposition in terrestrial ecosystems. Proceedings from the Nitrogen 2011 Conference held at the Edinburgh International Conference Centre. 11-14 April 2011. Edited by M. Sutton. http://www.nitrogen2011.org/oral_presentations/S17_2_Belyazid.pdf 2011.
- 1059
- 1060
- 1061 Belyazid, S., Sverdrup, H.U., Kurz, D., Braun, S. Use of an integrated deterministic soil-vegetation model to assess impacts of atmospheric deposition and climate change on plant species diversity. In W. de Vries, J-P. Hettelingh, M. Posch (Eds) *Critical Loads and Dynamic Risk Assessments: Nitrogen, Acidity and Metals in Terrestrial and Aquatic Ecosystems*: 327-358. Springer Verlag. 2015.
- 1062
- 1063
- 1064
- 1065 Belyazid, S.; Phelan, J., Nihlgård, B., Sverdrup, H., Driscoll, C. Fernandez, I., Aherne, J., Teeling-Adams, L.M., Arsenault, M., Cleavitt, N., Engstrom, B., Dennis, R., Sperduto, S., Werier, D., Clark, C. Assessing the Effects of Climate Change and Air Pollution on Soil Properties and Plant Diversity in Northeastern U.S. hardwood forests: Model Setup and Evaluation. **Water, Air and Soil Pollution**. In review. 2019
- 1066
- 1067
- 1068
- 1069 Bengtsson, Å. and Sjöberg, S., Surface complexation and proton-promoted dissolution in aqueous apatite systems. **Pure Appl. Chem.**, 81. 1569–1584, 2009.
- 1070
- 1071 Berg A. and Banwart, S.A. Carbon dioxide mediated dissolution of Ca-feldspar: implications for silicate weathering. **Chemical Geology** 163, 25–42. 2000
- 1072



- 1073 Berg, A. and Banwart, A.S., Anorthite surface speciation and weathering reactivity in bicarbonate solutions at 25°C. Proceedings of
1074 the workshop “CO₂ Chemistry”, Hemavan, Sweden, Sept. 13–16, 1993. Proceedings of the English Royal Society of
1075 Chemistry. 1994
- 1076 Bibi, I., Singh, B., Silvester, E., Dissolution of phyllosilicates under saline acidic conditions. 19th World Congress of Soil Science, Soil
1077 Solutions for a Changing World, 1 – 6 August 2010, Brisbane, Australia. 4 pages. Published on DVD. 2010
- 1078 Bickmore, B.R., Nagy, K.L., Gray, A.K., Brinkerhoff, A.R. The effect of Al(OH)₃ on the dissolution rate of quartz. **Geochimica et**
1079 **Cosmochimica Acta**, 70, 290–305. 2006
- 1080 Binder, T., Vox, A., Belyazid, S., Haraldsson, H., Svensson, M. Developing system dynamics models from causal loop diagrams. 21
1081 pp. <https://www.semanticscholar.org/>. <https://pdfs.semanticscholar.org/cf00/b9084b05ba357bf0c5fa7a5b9cc1b5695015.pdf>
1082 2003.
- 1083 Blake, R.E. and Walter, L.M. Effects of organic acids on the dissolution of orthoclase at 80°C and pH 6. **Chemical Geology** 132, 91–
1084 102. 1996
- 1085 Bobbink, R., Draaijers, G., Erisman, J.W., Gregor, H.D. (Ed) Henriksen, A., Hornung, M., Iversen, T., Kucera, V., Posch, M., Rihm,
1086 B., Spranger, T., Sverdrup, H., de Vries, W., Werner, B., (Ed) Manual on methodologies and criteria for mapping critical
1087 levels/loads and geographical areas where they are exceeded. **Umweltbundesamt Texte** 71:96, issn 0722-186X. 1996
- 1088 Bonten, L.T.C., Reinds, G.J., Groenenberg, J.E., de Vries, W., Posch, M. Evans; C.D. Belyazid, S., Braun S., Moldan, F., Sverdrup,
1089 H.U. Kurz, D.. Dynamic geochemical models to assess deposition impacts and target loads of acidity for soils and surface
1090 waters. In: W. de Vries, J-P. Hettelingh, M. Posch (Eds) Critical Loads and Dynamic Risk Assessments: Nitrogen, Acidity
1091 and Metals in Terrestrial and Aquatic Ecosystems: 225-251. Springer Verlag. 2015
- 1092 Bortoluzzi, E., Belyazid, S., Alard, D., Corcket, T., Gauquelin, T., Gégout, J.C., Nihlgard, B., Party, J.P., Sverdrup, H., Probst, A.
1093 Modélisation dynamique de l’impact des dépôts atmosphériques azotés sur la biodiversité forestière: évaluation des charges
1094 critiques. Session 28: Modélisation mécaniste: réponses aux perturbations environnementales, de l’individu à la population.
1095 In: (Eds.) Bertrand, J.C., Bonis, A., Caquet, T., Franc, A., Garnier, E., Olivier, I., Thébaud, C., Roy, J. Proceedings of the
1096 Colloque Ecologie 2010 Montpellier 2-4 septembre 2010. A l’initiative des réseaux: AFEM - COMEVOU - ECOVEG - JEF
1097 - PPD - REID - SFE – TRAITTS. 2010.
- 1098 Blum A.E. Feldspars in weathering. In Feldspars and their Reactions (ed. I. Parsons). Kluwer Academic, Dordrecht, Boston. 595–630.
1099 1994
- 1100 Blum A.E. and Lasaga A.C. The role of surface speciation in the dissolution of albite. **Geochimica et Cosmochimica Acta** 55, 2193–
1101 2201. 1991
- 1102 Blum A.E. and Stillings L.L. Feldspar dissolution kinetics. **Reviews in Mineralogy** 31, 291–331. 1995
- 1103 Bossel, H. Earth at the crossroads. Paths to a sustainable future. Cambridge University Press, 387 pages. 1998.
- 1104 Brady P.V. and Walther J.V. Surface chemistry and silicate dissolution at elevated temperatures. **American Journal of Science** 292,
1105 639. 1992
- 1106 Brady, P.V., Carroll, S.A., Direct effect of CO₂ and temperature on silicate weathering: possible implications for climate control.
1107 **Geochimica et Cosmochimica Acta** 58, 1853–1856. 1994.
- 1108 Brady, P.V., Gislason, S.R., Seafloor weathering controls or atmospheric CO₂ and global climate. **Geochimica et Cosmochimica**
1109 **Acta** 61, 965–973. 1997
- 1110 Bray, A.W., Oelkers, E.H., Bonneville, S., Wolff-Boenisch, D., Potts, N.J., Fones, G., Benning, L.G. The effect of pH, grain size and
1111 organic ligands on biotite weathering rates. **Geochimica et Cosmochimica Acta** 164, 127–145. 2015
- 1112 Bray, A.W., Benning, L.G., Bonneville, S., Oelkers E.H., Biotite surface chemistry as a function of aqueous fluid composition. Biotite
1113 surface chemistry as a function of aqueous fluid composition **Geochimica et Cosmochimica Acta** 128, 58-70. 2013
- 1114 Brandt F., Bosbach, D., Krawczyk-Bärsch, R., Arnold, T., Bernhard, G. Chlorite dissolution in the acid pH range: A combined
1115 microscopic and macroscopic approach. **Geochimica et Cosmochimica Acta**, 67: 1451-1461. 10.1016/S0016-
1116 7037(02)01293-O. 2005
- 1117 Brantley, S. Reaction kinetics of primary rock-forming minerals under ambient conditions. In: Treatise on Geochemistry, Volume 5.
1118 Editor: James I. Drever. Executive Editors: Heinrich D. Holland and Karl K. Turekian. ISBN 0-08-043751-6. Elsevier, 73-
1119 117. 2003
- 1120 Brantley, S. Chapter 5: Kinetics of mineral dissolution. 151-263. In: Kinetics of water-rock interaction. Edited by Brantley, S.L.,
1121 Kubicki, J.D., White, A.F., Springer Verlag. ISBN 978-0-387-73562-7. 2008b
- 1122 Brantley S. L. Kinetics of Water–Rock Interaction. Springer. 2008.
- 1123 Brantley, S.L., Conrad, C.F. Analysis of Rates of Chemical Reactions, in Kinetics of Water-Rock Interaction, S.L. Brantley, J.D.
1124 Kubicki, & A.F. White (eds.), Springer, New York, Chapter 1, 1-37. 2008
- 1125 Brantley, S.L. Kinetics of Mineral Dissolution, in: Kinetics of Water-Rock Interaction. S.L. Brantley, J.D. Kubicki, & A.F. White
1126 (eds.), Springer, New York, Chapter 5, 151-210. 2008.
- 1127 Brantley S.L. and Chen Y. Chapter 4: Chemical weathering rates of pyroxenes and amphiboles. In Chemical Weathering Rates of
1128 Silicate Minerals (eds. A.F. White and S.L. Brantley). Mineralogical Society of America, Washington, DC, **Reviews in**
1129 **Mineralogy** 31, 119–172. 1995
- 1130 Brantley S.L., and Stillings L., An integrated model for feldspar dissolution under acid conditions. **Mineralogical Magazine** A 58,
1131 117–118. 1994
- 1132 Brantley S.L. and Stillings L.L. Feldspar dissolution at 25°C and low pH. **American Journal of Science** 296, 101–127. 1996
- 1133 Braun, J., Mercier, J., Guillocheau, F., Robin, C., A simple model for regolith formation by chemical weathering. **Journal of**
1134 **Geophysical Research: Earth Surface** 121: 2140-217. 2016,
- 1135 Bricker, O., Paces, T., Johnson, C., Sverdrup, H., Weathering and erosion aspects of small catchment research. In: Cerny, J. (Ed.)
1136 *Biogeochemistry of small catchments*, 51:85–106. John Wiley and sons. 1996
- 1137 Burch, T.E., Nagy, K.L., Lasaga, A.C. Free energy dependence of albite dissolution kinetics at 80 °C and pH 8.8. **Chemical Geology**
1138 105:137–162. 1993
- 1139 Cama J., Ganor J., Ayora C. and Lasaga A.C. Smectite dissolution kinetics at 80° and pH 8.8. **Geochimica et Cosmochimica Acta**
1140 64, 2701–2717. 2000
- 1141 Carroll S.A. and Knauss K.G. Dependence of labradorite dissolution kinetics on CO₂(aq), Al(aq) and temperature. Lawrence
1142 Livermore National Laboratory. Report from Technical Information Department’s Digital Library



- 1143 <http://www.llnl.gov/tid/Library.html> 17 pp. 2001
- 1144 Carroll S.A. and Knauss K.G. Dependence of labradorite dissolution kinetics on CO₂(aq), Al(aq) and temperature. **Chemical Geology**
- 1145 217, 213–225. 2005
- 1146 Carroll, S.A. and Smith, S. Chlorite Dissolution Kinetics at Variable pH and Temperatures up to 275°C. Lawrence Livermore National
- 1147 Laboratory. LLNL-TR-644422. 12 pages. 2013.
- 1148 Carroll, S.A. and Walther, J.V. Kaolinite dissolution at 25, 60, and 80°C. **American Journal of Science**, 290, 797–810. 1990
- 1149 Casey W.H., Westrich H.R., Holdren G.R. Dissolution rates of plagioclase at pH = 2 and 3. **American Mineralogist** 76, 211–217.
- 1150 1991
- 1151 Casey, W.H. and Sposito, G. On the temperature dependence of mineral dissolution rates. **Geochimica et Cosmochimica Acta**, 56,
- 1152 3825–3830. 1992
- 1153 Casey, W.H., On the relative dissolution rates of some oxides and orthosilicate minerals. **J. Colloid Interface Science** 146, 586–589.
- 1154 1991
- 1155 Casey W.H. and Westrich, H.R. Control of dissolution rates of orthosilicate minerals by divalent metal-oxygen bonds. **Nature** 355:
- 1156 157–159. 1992
- 1157 Casey, W.H., Westrich, H.R., Arnold, G.W., Surface chemistry of labradorite feldspar reacted with aqueous solutions at pH 2.3, and
- 1158 12. **Geochimica et Cosmochimica Acta** 52: 2795–2807. 1988
- 1159 Casetou-Gustafson, S., Hillier, S., Akselsson, C., Simonsson, M., Stendahl, J., Olsson, B. Comparison of measured (XRPD) and
- 1160 modeled (A2M) soil mineralogies: A study of some Swedish forest soils in the context of weathering rate predictions.
- 1161 **Geoderma**. 310. 77–88. 2018.
- 1162 Chaïrat, C., Schott, J., Oelkers, E.H., Lartigue, J-E., Harouiya, N. Kinetics and mechanism of natural fluorapatite dissolution at 25°C
- 1163 and pH from 3 to 12. **Geochimica et Cosmochimica Acta** 71:5901–5912. 2007
- 1164 Chen, Y., and Brantley, S.L. Dissolution of forsterite olivine at 65°C and 2<pH < 5. **Chemical Geology** 165; 267–281. 2000
- 1165 Chen, Y., and Brantley, S.L. Temperature- and pH-dependence of albite dissolution rate at acid pH. **Chemical Geology** 135, 275–290.
- 1166 1997.
- 1167 Chen, Y., and Brantley, S.L. Diopside and anthophyllite dissolution at 25° and 90°C and acid pH. **Chemical Geology** 147: 233–248,
- 1168 1998
- 1169 Chin, P. K. F. and Mills, G. L.. Kinetics and Mechanisms of Kaolinite Dissolution - Effects of Organic-Ligands. **Chemical Geology**
- 1170 90, 307–317. 1991
- 1171 Critelli, T., Marini, L., Schott, J., Mavromatis, V.M., Apollaro, C., Rinder, T., de Rosa, R., Oelkers, E.H. Dissolution rate of antigorite
- 1172 from a whole-rock experimental study of serpentinite dissolution from 2<pH<9 at 25°C: Implications for carbon mitigation
- 1173 via enhanced serpentinite weathering. **Applied Geochemistry** 61: 259–271. 2015
- 1174 Critelli, T., Marini, L., Schott, J., Mavromatis, V., Apollaro, C., Rinder, T., De Rosa, R., Oelkers, E.H. Dissolution rates of actinolite
- 1175 and chlorite from a whole-rock experimental study of metabasalt dissolution from pH 6–12 at 25°C. **Chemical Geology** 390,
- 1176 100–108. 2014
- 1177 Cory, N., Laudon, H., Köhler, S., Seibert, J., Bishop, K. Evolution of soil solution aluminium during transport along a forested boreal
- 1178 hillslope. **J. Geophys Res-Biogeophys** 112(G3). Artn G0301410.1029/2006jg000387. 2007
- 1179 Cotton, A. Dissolution kinetics of clinoptilolite and heulandite in alkaline conditions. **Bioscience Horizons**, 1:38–44. 2008
- 1180 Crundwell, F.K., The dissolution and leaching of minerals: Mechanisms, myths and misunderstandings. **Hydrometallurgy** 139, 132–
- 1181 148. 2013.
- 1182 Crundwell, F.K., The mechanism of dissolution of minerals in acidic and alkaline solutions: Part I — A new theory of non-oxidation
- 1183 dissolution. **Hydrometallurgy** 149: 252–264. 2014a.
- 1184 Crundwell, F.K., The mechanism of dissolution of minerals in acidic and alkaline solutions: Part II — Application to silicates.
- 1185 **Hydrometallurgy** 149, 265–275. 2014b.
- 1186 Crundwell, F.K., The mechanism of dissolution of minerals in acidic and alkaline solutions: Part III — Application to oxides and
- 1187 sulfides. **Hydrometallurgy** 149, 71–81. 2014c.
- 1188 Crundwell, F.K., The mechanism of dissolution of forsterite, olivine and minerals of the orthosilicate group. **Hydrometallurgy** 150:
- 1189 68–82. 2014d.
- 1190 Crundwell, F. K. The Mechanism of dissolution of the feldspars: Part I Dissolution at conditions far from equilibrium.
- 1191 **Hydrometallurgy** 151, 151–162. 2015a
- 1192 Crundwell, F. K. The Mechanism of dissolution of the feldspars: Part II Dissolution at conditions close to equilibrium.
- 1193 **Hydrometallurgy** 151, 163–171. 2015b
- 1194 Crundwell, F.K., The mechanism of dissolution of minerals in acidic and alkaline solutions: Part VI a molecular viewpoint.
- 1195 **Hydrometallurgy** 161, 34–44. 2016.
- 1196 Crundwell, F.K., On the mechanism of the dissolution of quartz and silica in aqueous solutions **ACS Omega**: 2:1116–1128. 2017.
- 1197 Cubillas, P., Köhler, S., Prieto, M., Chaïrat, C., Oelkers, E.H. Experimental determination of the dissolution rates of calcite, aragonite,
- 1198 and bivalves. **Chemical Geology** 216, 59–77. 2016
- 1199 Dambrinne, E., Sverdrup, H., Warfvinge, P. Atmospheric deposition; Forest management and soil nutrient availability; A modelling
- 1200 exercise. In: Bonneau M. Landmann, G., (Ed.), *Forest Decline and Acidification Effects in the French Mountains*, 259–269.
- 1201 Springer Verlag, Berlin. 1995
- 1202 Daval, D., Testemale, D., Reham, N., Tarascon, J.M., Siebert, J., Martinez, I., Guyot, F. Fayalite (Fe₂SiO₄) dissolution kinetics
- 1203 determined by X-ray absorption spectroscopy. **Chemical Geology** 275, 161–175. 2010a
- 1204 Daval, D., Hellmann, R., Corvisier, J., Tisserand, D., Martinez, I., Guyot, F. Dissolution kinetics of diopside as a function of solution
- 1205 saturation state: Macroscopic measurements and implications for modeling of geological storage of CO₂ **Geochimica et**
- 1206 **Cosmochimica Acta** 74: 2615–2633. 2010b
- 1207 Daval, D., Hellmann, R., Marinez, I., Gangloff, S., Guyot, F. Lizardite serpentine dissolution kinetics as a function of pH and
- 1208 temperature, including effects of elevated pCO₂. **Chemical Geology** 351: 245–256. 2013
- 1209 Declercq, J., Bosc, O., Oelkers E.H., Do organic ligands affect forsterite dissolution rates? **Applied Geochemistry** 39, 69–77. 2013
- 1210 Declercq, J., Diedrich, T., Perrot, M., Gislason, S.R., Oelkers, E.H., . Experimental determination of rhyolitic glass dissolution rates
- 1211 at 40–200°C and 2< pH< 10.1 **Geochimica et Cosmochimica Acta** 100, 251–263 2013.
- 1212 Denbigh, K., *The Principles of Chemical Equilibrium*, Cambridge University Press, Cambridge (U.K.). 1971



- 1213 Devidal J.-L., Schott J., Dandurand J.-L. An experimental study of kaolinite dissolution and precipitation kinetics as a function of
1214 chemical affinity and solution composition at 150°C, 40 bars, and pH 2, 6.8, and 7.8. **Geochimica et Cosmochimica Acta**
1215 61: 5165–5186. 1997
- 1216 Diedrich, T., Schott, J., Oelkers, E.H. An experimental study of tremolite dissolution rates as a function of pH and temperature:
1217 implications for tremolite toxicity and its use in carbon storage. **Mineralogical Magazine** 78: 1449–1464. 2014
- 1218 Dixit S. and Carroll S.A. Effect of solution saturation state and temperature on diopside dissolution. **Geochemical Transactions** 8.
1219 2007
- 1220 Dixon J.L. and von Blanckenburg, F., Soils as pacemakers and limiters of global silicate weathering. **Comptes Rendus Geoscience**,
1221 344:597–609. 2012
- 1222 Dresel P.E. The dissolution kinetics of siderite and its effect on acid mine drainage. Ph.D. thesis. Pennsylvania State University. 1989
- 1223 Drewer, J., Murphy, K.M., Clow, D.W. Field weathering rates versus laboratory dissolution rates: an update. Goldschmidt conference
1224 Edinburgh 1994. 239–240. 1994
- 1225 Drever J.I., Poulson S.R., Stillings L.L., Sun Y. The effect of oxalate on the dissolution rate of quartz and plagioclase feldspars at 20–
1226 25°C. **Geochemistry of Crustal Fluids: Water/Rock Interaction during Natural Processes**, 39. 1996
- 1227 Drever, J.I. and Clow, D.W. Weathering rates in catchments. In A. F. White and S. L. Brantley, (Eds), Chemical weathering rates of
1228 silicate minerals. Mineralogical Society of America, Washington D. C. **Reviews in mineralogy** 31:463–483. 1995
- 1229 Drever, J.I. and Zobrist, J., Chemical weathering of silicate rocks as a function of elevation in the southern Swiss Alps. **Geochimica**
1230 **et Cosmochimica Acta**, 56:3209–3216. 1992
- 1231 Drever, J., and Stillings, L. The role of organic acids in mineral weathering, **Colloids Surf. A**, 120: 167–181. 1997,
- 1232 Drever, J.I., **The Geochemistry of Natural Waters**, Prentice Hall, Englewood Cliffs, N.J. 1988
- 1233 Drever, J.I., The effect of land plants on weathering rates of silicate minerals, **Geochimica et Cosmochimica Acta** 58, 2325–2332.
1234 1994
- 1235 Dorozhkin, S. Dissolution mechanism of calcium apatite in acids: A review of literature. **World Journal of methodology** 26:1–17.
1236 2012
- 1237 Dove, P.M., and Crerar, D.A. Kinetics of quartz dissolution in electrolyte solutions using a hydrothermal mixed flow reactor. **Geochim**
1238 **et Cosmochim Acta**, 54:955–969. 1990.
- 1239 Duan, L., Hao, J., Xie, S., Zhou, Z., Xuemei Ye. Determining weathering rates of soils in China. **Geoderma** 110, 205–225. 2002
- 1240 Duckworth, O.W., and Martin, S.T. Role of molecular oxygen in the dissolution of siderite and rhodochrosite. **Geochimica et**
1241 **Cosmochimica Acta**, 68, 607–621. 2003
- 1242 Duckworth, O.W. and Martin, S.T. Connections between surface complexation and geometric models of mineral dissolution
1243 investigated for rhodochrosite. **Geochim. Cosmochim. Acta** 67, 1787–1801. 2003
- 1244 Erlandson, M., Oelkers, E.H., Bishop, K., Sverdrup, H.U., Belyazid, S., Ledesma, J.L.J., Köhler, S.J., Spatial and temporal variations
1245 of base cation release from chemical weathering on a hillslope scale **Chemical Geology** 441, 21:1–13. 2016
- 1246 Erlandson, M., Sverdrup, H.U., M., Bishop, K., Belyazid, S., Ameli, A., Köhler, S.J., Catchment export of base cations: Improved
1247 mineral dissolution kinetics influence the role of water transit time (This issue) **Soil** 1–19. 2019.
- 1248 Fernandez-Bastero, S., Gil-Lozano, C., Briones, M.J.I., Gago-Duport, L. Kinetic and structural constraints during glauconite
1249 dissolution: implications for mineral disposal of CO₂ **Mineralogical Magazine** 72, 27–31. 2008
- 1250 Fischer, S., and Liebscher, E., Dissolution Kinetics of Iron Carbonate, Illite and Labradorite – CO₂-Saline Fluid- mineral Experiments
1251 within the GaMin’11 Inter-laboratory Comparison Exercise. - **Energy Procedia**, 63, 5461–5466. A. 2014
- 1252 Finlay, R., Wallander, H., Smits, M.M., Holmström, S., van Hees, P., Lian, B., Rosling, A. The role of fungi in biogenic weathering
1253 in boreal forest soils. **Fungal Biology Review** 23: 101–106. 2010
- 1254 Flaathen, K., Gislason, S.R., Oelkers, E.H. The effect of aqueous sulphate on basaltic glass dissolution rates. **Chemical Geology** 277,
1255 345–354. 2010
- 1256 Forrester, J. W. **Industrial Dynamics**. Pegasus Communications. ISBN 1-883823-36-6. 1961.
- 1257 Forrester, J. W. **Urban Dynamics**. Pegasus Communications. ISBN 1-883823-39-0. 1969.
- 1258 Forrester, J., **World dynamics**. Pegasus Communications, Waltham MA. 1971.
- 1259 Forsius, M., Alveteg, M., Jenkins, A., Johansson, M., Kleemola, S., Lükewille, A., Posch, M. Sverdrup. H. MAGIC, SAFE and
1260 SMART model application at integrated monitoring sites: Effects of emission reduction scenarios. **Water, Air and Soil**
1261 **Pollution** 195:2–30. 1998.
- 1262 Fouda, M.F.R., Amin, R.E.-S., Abd-Elzaher, M.M. Extraction of magnesia from Egyptian serpentine ore via reaction with different
1263 acids. I. Reaction with sulfuric acid. **Bull. Chem. Soc. Jpn.** 1907–1912. 1996a.
- 1264 Fouda, M.F.R., Amin, R.E.-S., Abd-Elzaher, M.M. Extraction of magnesia from Egyptian serpentine ore via reaction with differ- ent
1265 acids. II. Reaction with nitric and acetic acids. **Bull. Chem. Soc. Jpn.** 69, 1913–1916. 1996b.
- 1266 Frogner, P and Schweda, P. Hornblende dissolution kinetics at 25°C. **Chemical Geology** 151, 169–179. 1998.
- 1267 Fu, Q., Lu, P., Konishi, H., Dilmore, R., Xu, H., Seyfried, W.E. Jr, Zhu, C. Coupled alkali feldspar dissolution and secondary mineral
1268 precipitation in batch systems: I. New experiments at 200 °C and 300 bars **Chemical Geology** 258, 125–135 2009
- 1269 Fumuto, T., Shindo, J., Oura, N., Sverdrup, H. Adapting the PROFILE model to calculate the critical loads for East Asian soils by
1270 including volcanic glass weathering and alternative aluminium solubility system. **Water, Air and Soil Pollution** 130:1247–
1271 1252. 2001
- 1272 Gahrke, T., Pina P.S., Cornell, R.M., Dissolution kinetics of montmorillonite in hydrochloric and oxalic acid. **Journal of the**
1273 **American Society** 114, 102 – 112. 2005.
- 1274 Galeczka, I., Wolff-Boenisch, D., Oelkers, E.H., Gislason, S.R., An experimental study of basaltic glass–H₂O–CO₂ interaction at 22
1275 and 50°C: implications for subsurface storage of CO₂. **Geochimica et Cosmochimica Acta** 126, 123–145. 2014
- 1276 Ganor, J., Roueff, E., Erel, Y., Blum, J. The dissolution kinetics of a granite and its minerals – implications for comparison between
1277 laboratory and field dissolution rates. **Geochimica et Cosmochimica Acta** 69, 2043–2056. 2005
- 1278 Ganor, J., Lu, P., Zheng, Z., Zhu, C. Bridging the gap between laboratory measurements and field estimations of weathering using
1279 simple calculations. **Environ Geol** 53:599–610. 2007
- 1280 Gainey, S.R., Hausrath, E.M., Hurowitz, J.A., Milliken, R.E., Nontronite dissolution rates and implications for Mars. **Geochimica et**
1281 **Cosmochimica Acta** 126: 192–211 2014.



- 1282 Gautier, J. M., Oelkers, E. and Schott, J., Experimental study of K-feldspar dissolution rate as a function of chemical affinity at 150°C
1283 and pH 9. **Geochimica et Cosmochimica Acta** 58, 4549-4560. 1994
- 1284 Gaudio, N., Belyazid, S., Gendre, X., Mansat, A., Nicolas, M., Rizzetto, S., Sverdrup, H., Probst, A. Combined effect of atmospheric
1285 nitrogen deposition and climate change on temperate forest soil biogeochemistry: a modeling approach. **Ecological Modelling**
1286 30, 624-634. 2015.
- 1287 Gautelier, M., Oelkers, E.H., Schott, J., An experimental study of dolomite dissolution rates as a function of pH from 0.5 to 5 and
1288 temperature from 25 to 80°C. **Chemical Geology** 157, 13-26, 1999
- 1289 Gislason S.R. and Hans P.E. Meteoric water-basalt interactions. I: A laboratory study. **Geochimica et Cosmochimica Acta** 51, 2827–
1290 2840. 1987
- 1291 Gislason, S.R., Oelkers, E.H. Mechanism, rates, and consequences of basaltic glass dissolution: II. An experimental study of the
1292 dissolution rates of basaltic glass as a function of pH and temperature. **Geochimica et Cosmochimica Acta** 67, 3817–3832.
1293 2003
- 1294 Gislason, S.R., Arnorsson, S., Armannsson, H., Chemical weathering of basalt in southwest Iceland: effects of runoff, age of rocks
1295 and vegetative/glacial cover. **American Journal of Science** 296, 837 – 907. 1996.
- 1296 Glover, E., Faanu, A., Fianko, J.R. Dissolution Kinetics of Stilbite at Various Temperatures under Alkaline Conditions. **West African**
1297 **Journal of Applied Ecology**, 16: 95-105. 2010
- 1298 Godderis, Y., Francois, L.M., Probst, A., Schott, J., Moncoulon, D., Labat, D., Viville, Didier. Modelling weathering processes at the
1299 catchment scale: The WITCH numerical model. **Geochimica et Cosmochimica Acta**, 70, 1128-1147. 2006
- 1300 Golubev, S.V., Pokrovsky, O.S., Schott, J. Laboratory weathering of Ca- and Mg-bearing silicates: weak effect of CO₂ and organic
1301 ligands. **Geochimica et Cosmochimica Acta**, A418. 2004.
- 1302 Golubev S. V., Pokrovsky O. S. and Schott J. 2005 Experimental determination of the effect of dissolved CO₂ on the dissolution
1303 kinetics of Mg and Ca silicates at 25°C. **Chemical Geology** 217, 227– 238.
- 1304 Guidry M.W. and Mackenzie F.T. Experimental study of igneous and sedimentary apatite dissolution: control of pH, distance from
1305 equilibrium, and temperature on dissolution rates. **Geochimica et Cosmochimica Acta** 67, 2949–2963. 2003
- 1306 Goynes, K.W., Brantley, S.L., Chorover, J. Effects of organic acids and dissolved oxygen on apatite and chalcocyanite dissolution:
1307 Implications for using elements as organomarkers and oxymarkers. **Chemical Geology** 234:28-45. 2006
- 1308 Gudbrandsson, S., Wolff-Boenisch, D., Gislason, S.R., Oelkers, E.H. An experimental study of crystalline basalt dissolution from
1309 2<pH<11 and temperatures from 5 to 75°C. **Geochimica et Cosmochimica Acta** 75, 5496–5509. 2011
- 1310 Gudbrandsson, S., Wolff-Boenisch, D., Gislason, S.R., Oelkers, E.H. Experimental determination of plagioclase dissolution rates as
1311 a function of its composition and pH at 22°C. **Geochimica et Cosmochimica Acta** 139:154–172. 2014
- 1312 Guidry, M.W., and Mackenzie, F.T. Experimental Study of Igneous and Sedimentary Apatite Dissolution: Control of pH, Distance
1313 from Equilibrium, and Temperature on Dissolution Rates. **Geochimica et Cosmochimica Acta**, 67, 2949–2963. 2003
- 1314 Gustafsson A.B., Puigdomenech, L. The effect of pH on chlorite dissolution rates at 25°C. **Materials Res Soc Symp Proc**, 757:649-
1315 655. 2003
- 1316 Hamilton J.P., Pantano C.G., Brantley S.L. Dissolution of albite glass and crystal. **Geochimica et Cosmochimica Acta** 64, 2603–
1317 2615. 2000
- 1318 Hamilton, J.P., Brantley, S.L., Pantano, C.G., Criscenti, L.J., Kubicki, J.D., Dissolution of nepheline, jadeite, and albite glasses:
1319 towards better models for aluminosilicate dissolution. **Geochimica et Cosmochimica Acta** 65, 3683–3702. 2001.
- 1320 Hangx, S.J. and Spiers, C.J. Reaction of plagioclase feldspars with CO₂ under hydrothermal conditions. **Chemical Geology** 265, 88–
1321 98. 2009
- 1322 Hansley, P.L., and Briggs, P.H., Garnet Dissolution in Oxalic Acid-A Possible Analog for Natural Etching of Garnet by Dissolved
1323 Organic Matter. U.S. Geological Survey Bulletin 2106. United States Government Printing Office, Washington: 1994
- 1324 Haraldsson, H., Sverdrup, H., Belyazid, S., Sigurdsson, B., Halldorsson, G. Assessment of effects of afforestation on soil properties in
1325 Iceland, using systems analysis and system dynamics methods. **Icelandic Agricultural Science** 20:107-123. 2007
- 1326 Haraldsson, H. 2004 Introduction to systems thinking and causal loop diagrams. Reports in Ecology and Environmental Engineering
1327 1:2004, 5th edition. Lund University, Lund, Sweden.
- 1328 Haraldsson H. and Sverdrup, H., 2005, On aspects of systems analysis and dynamics workflow. Proceedings of the systems dynamics
1329 society, July 17-21, 2005 International Conference on systems dynamics, Boston, USA. 1-10 pages.
1330 <http://www.systemdynamics.org/conferences/2005/proceed/papers/HARAL310.pdf>
- 1331 Harouiya, N., Chaïrat, C., Köhler, S.J., Gout, R., Oelkers, E.H. The dissolution kinetics and apparent solubility of natural apatite in
1332 closed reactors at temperatures from 5 to 50°C and pH from 1 to 6. **Chemical Geology** 244: 554–568. 2007
- 1333 Harouiya, N. and Oelkers, E.H. An experimental study of the effect of aqueous fluoride on quartz and alkali-feldspar dissolution rates.
1334 **Chemical Geology** 205, 155–167. 2004
- 1335 Haug, T.A., Kleiv, R.A., Munz, I.A., Investigating dissolution of mechanically activated olivine for carbonation purposes. **Applied**
1336 **Geochemistry** 25, 1547–1563. 2010.
- 1337 Hausrath, E.M., A. Neaman, S.L. Brantley. Elemental release rates from dissolving basalt and granite with and without organic ligands.
1338 **American Journal of Science** 309, 633-660. 2009.
- 1339 Hayashi, H., and Yamada, M. Kinetics of dissolution of non-crystalline oxides and crystalline clay minerals in a basic ion solution.
1340 **Clay and Clay Minerals** 38:308-3114. 1990
- 1341 van der Heijden, G., Belyazid, S. LU ; Dambrine, E.; Ranger, Jacques and Legout, A. NutsFor a process-oriented model to simulate
1342 nutrient and isotope tracer cycling in forest ecosystems **Environmental Modelling and Software** 9:365-380. 2017
- 1343 Helgeson, H., Murphy, W., Aagaard, P.: Thermodynamics and kinetic constraints on reaction rates among minerals and aqueous
1344 solutions: II. Rate constants, effective surface area and the hydrolysis of feldspar. **Geochimica et Cosmochimica Acta** 48,
1345 2405-2432. 1984,
- 1346 Hellmann, R., Daval, D., Tisserand, D., Renard, F. Albite feldspar dissolution kinetics as a function of the Gibbs free energy at high
1347 pCO₂. In Water Rock Interaction (Bullen, T.D., Wang, Y., eds.), Taylor & Francis, London, 591-595. 2007
- 1348 Hellmann, R. and Tisserand, D. Dissolution kinetics as a function of the Gibbs free energy of reaction: An experimental study based
1349 on albite feldspar. **Geochimica et Cosmochimica Acta** 70: 364-383. 2006
- 1350 Hellmann, R., Daval, D., Tisserand, D. The dependence of albite feldspar dissolution kinetics on fluid saturation state at acid and basic
1351 pH: Progress towards a universal relation. **Geoscience** 342: 676–684. 2010



- 1352 Hettelingh, J.P., Posch, M., de Vries, W., Bull, K., Sverdrup, H. Guidelines for the computation and mapping of nitrogen critical loads
1353 and exceedance in Europe. In: Grennfelt, P.-I. and Lövblat, G. (Eds) *Critical Loads for Nitrogen — A workshop report*: 287–
1354 303. Nordic Council of Ministers. 1992
- 1355 Hettelingh, J.P., Chadwick, M., Sverdrup, H., Zhou, D. Assessment of environmental effects of acid deposition. In: RAINS-ASIA; *An*
1356 *assessment model for air pollution in Asia*. W. Foell, M. Ammann, G. Carmichael, M. Chadwick, J. P. Hettelingh, L. Hordijk,
1357 D. Zhou (eds). Chapter V:1-59, World Bank. 1995
- 1358 Hettelingh, J.P., Sverdrup, H., Zhao, D. Deriving critical loads for Asia. **Water, Air and Soil Pollution** 85:2565-2570. 1996
- 1359 Hettelingh, J.P., Sverdrup, H., Zhao, D. Assessment of environmental effects of acidic deposition in Asia. **Water, Air, and Soil**
1360 **Pollution** 85:1-24. 1996.
- 1361 Hilley, G.E., Chamberlain, C.P., Moon, S., Porder, S., Willet, S.D., Competition between erosion and reaction kinetics in controlling
1362 silicate-weathering rates. **Earth and Planetary Science Letters** 293: 191-199. 2010.
- 1363 Holmqvist, J., Ögaard, A., Öborn, I., Edwards, T., Mattson, L., Sverdrup, H. Estimating potassium release from weathering in Northern
1364 European agricultural systems using PROFILE and long term experiments **European Journal of Agronomy** 20:149-163.
1365 2003
- 1366 Holmqvist, J., Thelin, G., Rosengren U., Stjernquist, I., Svensson, M., Wallman, P., Sverdrup, H. Assessing sustainability in the Asa
1367 research park In: Developing principles for sustainable forestry Results from a research program in southern Sweden. Sverdrup,
1368 H., and Stjernquist, I., (Eds.) **Managing Forest Ecosystems** 5:381-426. Kluwer Academic Publishers, Amsterdam. 2002
- 1369 Holmqvist, J. and Sverdrup, H. Vittringskartor ger uthålligare skogsbruk. **Skog och Forskning** 4/2001;25-27. 2001
- 1370 Holmqvist, J., Sverdrup, H., Petersson, P., Örlander G. Vittringens betydelse för uthållig produktion. In: Olsson, K. (Ed.). *Sustainable*
1371 *Forestry in Southern Sweden*, Årsrapport 1999; Tema Skogsmarkens långsiktiga produktionsförmåga 18-21. 1999
- 1372 Hodson, M.E. Does reactive surface area depend on grain size? Results from pH 3, 25 °C far-from-equilibrium flow-through
1373 experiments on anorthite and biotite. **Geochimica et Cosmochimica Acta** 70, 1655–1667. 2006a
- 1374 Hodson M. Searching for the perfect surface area normalizing term – a comparison of BET surface area-, geometric surface area-and
1375 mass-normalized dissolution rates of anorthite and biotite. **J. Geochem. Explor.** 88, 288–291. 2006b
- 1376 Hodson M.E. The influence of Fe-rich coatings on the dissolution of anorthite at pH 2.6. **Geochimica et Cosmochimica Acta** 67,
1377 3355–3363. 2003
- 1378 Hodson, M. and Langan, S.J. Considerations of uncertainty in setting critical loads of acidity of soils: the role of weathering rate
1379 determination. **Environmental Pollution** 106: 73–81. 1999b
- 1380 Hodson, M.E., Langan, S.J., Wilson, M.J.A sensitivity analysis of the PROFILE model in relation to the calculation of soil weathering
1381 rates. **Applied Geochemistry** 11: 835–844. 1996.
- 1382 Hodson, M.E., Langan, S.J. and Wilson, M.J.A critical evaluation of the use of the PROFILE model in calculating mineral weathering
1383 rates. **Water Air and Soil Pollution** 98: 79–104. 1997
- 1384 Houle, D., Lamoureux, P., Belanger, N., Bouchard, M., Gagnon, C., Couture, S., Bouffard, A., Soil weathering rates in 21 catchments
1385 of the Canadian Shield. **Hydrol. Earth Syst. Sci.**, 16, 685-697. 2012.
- 1386 Hänchen, M., Prigobbe V., Storti G., Seward T.M., Mazzotti M. Dissolution kinetics of forsteritic olivine at 90–150°C. **Geochimica**
1387 **et Cosmochimica Acta** 70, 4403–4416. 2006
- 1388 Huertas., F.J., Caballero, E., de Cisneros, C.J., Huertas, F., Linares, J. Kinetics of montmorillonite dissolution in granitic solutions.
1389 **Applied Geochemistry** 16, 397-407. 2001
- 1390 Huertas, F.J., Chou, L., Wollast, R. Mechanism of kaolinite dissolution at room temperature and pressure. Part II: kinetic study.
1391 **Geochimica et Cosmochimica Acta** 63, 3261–3275. 1999
- 1392 Hultberg, H., Hultengren, S., Grennfelt, P., Oskarsson, H., Kalén, C., Pleijel, H.: Air pollution, environment and future. 30 years of
1393 research on forest, soils and water. Gårdsjöstiftelsen and Naturcentrum AB. 60pp. 2007.
- 1394 Jin, L., Andrews, D.M., Holmes, G.H., Lin, H., Brantley, S.L. Opening the "black box": water chemistry reveals hydrological controls
1395 on weathering in the Susquehanna Shale Hills Critical Zone Observatory. **Vadose Zone Journal** 10:928-942. 2011
- 1396 Johnson, N.C., Thomas, B., Maher, K., Rosenbauer, R.J., Bird, D., Brown, J., Olivine dissolution and carbonation under conditions
1397 relevant for in situ carbon storage. **Chemical Geology** 373, 93–105. 2014.
- 1398 Johnsson, P.A., Blum, A.E., Hochella, M.F.Jr., Parks, G.A., Sposito, G. Direct observation of muscovite basal-plane dis-
1399 solution and secondary-phase formation: An XPS, LEED, and SFM study. In *Water–Rock International VII* (eds. G. Arehardt and R.
1400 Hulston), 159–162. Balkema. 1992
- 1401 Jönsson, C., Warfvinge, P., Sverdrup, H. Uncertainty in prediction of weathering rate and environmental stress factors with the
1402 PROFILE model. **Water, Air and Soil Pollution**, 81:1–23. 1995
- 1403 Jönsson, C., Warfvinge, P., Sverdrup, H. The SAFE model applied to the Solling data set. **Ecological Modelling**, 83:85–96, 1995
- 1404 Jonckbloedt, R.C.L., Olivine dissolution in sulphuric acid at elevated temperatures-implications for the olivine process, an alternative
1405 waste acid neutralizing process. **Journal of Geochemical Exploration** 62, 337–346. 1998.
- 1406 Kalinowski, B.E., Dissolution Kinetics and Alteration Products of Micas and Epidote in Acidic Solutions at Room Temperature, PhD
1407 Thesis. Stockholm University, Stockholm, 1997
- 1408 Kalinowski, B., Faith-Ell, C., Schweda, P. Dissolution kinetics and alteration of epidote in acidic solutions at 25°C. **Chemical**
1409 **Geology**. 151, 181–197. 1998
- 1410 Kalinowski, B.E. and Schweda, P. Kinetics of muscovite, phlogopite, and biotite dissolution and alteration at pH 1-4, room
1411 temperature. **Geochimica et Cosmochimica Acta**, 60, 367-385. 1995
- 1412 Kegan, R., Laskow-Lahey, L., The real reason people won't change. **Harvard Business Review** – OnPoint 103-111. Originally
1413 published in Harvard Business review November 2001. 2014.
- 1414 Kim, D.H., Toolbox: Guidelines for Drawing Causal Loop Diagrams, *The Systems Thinker*, 3; 5–6. 1992.
- 1415 Knauss, K. G., Nguyen S. N., Weed H. C. Diopside dissolution kinetics as a function of pH, CO₂, temperature, and time. **Geochimica**
1416 **et Cosmochimica Acta** 57, 285–294. 1993
- 1417 Knutson, G., Bergström, S., Danielsson, L., Jacks, G., Lundin, L., Maxe, L., Sanden, P., Sverdrup, H., Warfvinge, P. Acidification of
1418 groundwater in forested till areas. **Ecological Bulletins**, 44:271–300. 1995
- 1419 Kolka, R.K.; Grigal, D.F.; Nater, E.A. Forest soil mineral weathering rates: use of multiple approaches. **Geoderma** 73: 1-21. 1996
- 1420 Köhler, S.J., Bosbach, D., Oelkers E.H. Do clay mineral dissolution rates reach steady state? **Geochimica et Cosmochimica Acta** 69,
1421 1997–2006. 2005



- 1422 Köhler, S.J., Dufaud, F., Oelkers E.H. An experimental study of illite dissolution kinetics as a function of pH from 1.4 to 12.2 and
1423 temperature from 5 to 50°C. **Geochimica et Cosmochimica Acta** 67: 3583–3594. 2003
- 1424 Kurz, D., Rihm, B., Sverdrup, H., Warfvinge, P. Critical loads of acidity for forest soils: Regionalized PROFILE model.
1425 *Environmental documentation* no. 88. 1-117, Swiss Agency for the Environment, Forest and Landscape, Swiss Government,
1426 Bern. 1998a
- 1427 Kurz, D., Alveteg, M., Sverdrup, H. Acidification of Swiss forest soils; Development of a regional dynamic assessment: Regionalized
1428 PROFILE model. *Environmental documentation* no. 89. 1-115 Swiss Agency for the Environment, Forest and Landscape,
1429 Swiss Government, Bern. 1998b
- 1430 Kurz, D., Rihm, B., Alveteg, M., Sverdrup, H. Steady-state and dynamic assessment of forest soil acidification in Switzerland. **Water,
1431 Air and Soil Pollution** 130: 1217-1222. 2001
- 1432 Kuwahara, Y., In situ observations of muscovite dissolution under alkaline conditions at 25–50°C by AFM with an air/fluid heater
1433 system **American Mineralogist**, 93: 1028–1033, 2008
- 1434 Kuwahara, Y., In-situ, real time AFM study of smectite dissolution under high pH conditions at 25–50°C. **Clay science**, 12,
1435 supplement 2, 57–62. 2006a
- 1436 Kuwahara, Y., In-situ AFM study of smectite dissolution under alkaline conditions at room temperature. **American Mineralogist**, 91,
1437 1142–1149. 2006b
- 1438 Labat, D. and Viville, D. Modelling weathering processes at the catchment scale: the WITCH numerical model. **Geochimica et
1439 Cosmochimica Acta** 70, 1128–1147. 2006
- 1440 Lagache, M. Contribution à l'étude de l'altération des feldspaths, dans l'eau, entre 100 et 200°C, sous diverses pressions de CO₂, et
1441 application à la synthèse des minéraux argileux. **Bull. Soc. franç. Minér. Crist.** 88: 223- 253. 1965
- 1442 Lagache, M.: New data on the kinetics of the dissolution of the alkali feldspar at 200°C in CO₂ charged water, **Geochimica et
1443 Cosmochimica Acta** 40, 157-161. 1976,
- 1444 Lammers, K., Smith, M.M., Carrol, S.A., Muscovite dissolution kinetics as a function of pH at elevated temperature. **Chemical
1445 Geology** 466: 149-158. 2017.
- 1446 Langan, S.L., Reynolds, B., Bain, D.C. The calculation of base cation release from mineral weathering in soils derived from Palaeozoic
1447 greywackes and shales in upland UK. **Geoderma** 69, 275-285. 1996a.
- 1448 Langan, S.L., Sverdrup, H., Cull, M. Calculation of base cation release from the chemical weathering of Scottish soils using the
1449 PROFILE model. **Water, Air and Soil Pollution** 85:2487-2502. 1996b.
- 1450 Lartigue, J.E. Contribution à l'étude de l'altération des silicates. Approche expérimentale en milieu ouvert de la cinétique de
1451 dissolution à 25°C d'un pyroxène (Ca–Mg–Fe) en fonction du pH. These. Université de droit, d'économie et des sciences
1452 d'Aix-Marseille. 1994
- 1453 Lasaga, A.C. Fundamental approaches in describing mineral dissolution and precipitation rates. In: White, A.F., Brantley, S.L. (Eds.),
1454 Chemical Weathering Rates of Silicate Minerals, 31. Mineralogical Society of America, Washington, D.C., USA. **Reviews in
1455 Mineralogy** 31: 23–86. 1995
- 1456 Lasaga, A.C. Kinetic Theory in the Earth Sciences. Princeton University Press, Princeton, USA, 811pp. 1998
- 1457 Lazaro, A, Benac-Vegas, Brouwers, H.J.H., Geus, J.W., Bastida, J. The kinetics of the olivine dissolution under the extreme conditions
1458 of nano-silica production. **Applied Geochemistry** 52:1-15. 2015
- 1459 Laudon, H., Taberman, I., Ågren, A., Futter, M., Ottosson-Löfvenius M., Bishop, K. The Krycklan Catchment Study-A flagship
1460 infrastructure for hydrology, biogeochemistry, and climate research in the boreal landscape. **Water Resources Research** 49,
1461 7154-7158. 2013
- 1462 Leith, F.I., Dinsmore, K.J., Wallin, M.B., Billett, M.F., Heal, K.V., Laudon, H., Öquist, M.G., Bishop, K. Carbon dioxide transport
1463 across the hillslope-riparian-stream continuum in a boreal headwater catchment. **Biogeosciences** 12, 1881-1892. 2015.
- 1464 Lowson, R.T., Comarmond M.C.J., Rajaratnam G., Brown P.L. The kinetics of the dissolution of chlorite as a function of pH and at
1465 25°C. **Geochimica et Cosmochimica Acta** 69, 1687–1699. 2005
- 1466 Lowson, R.T, Brown, P.L., Comamond, M.C.J, Rajataratnam, G. The kinetics of chlorite dissolution. **Geochimica et Cosmochimica
1467 Acta** 71: 1431–1447. 2007
- 1468 Lu, P., Fu, Q., Seyfried, W.E. Jr, Hedges, S.W., Soong, Y., Jones, K., Zhu, C. Coupled alkali feldspar dissolution and secondary
1469 mineral precipitation in batch systems: 2. New experiments with supercritical CO₂ and implications for carbon sequestration.
1470 **Applied Geochemistry** 30:75–90 2013
- 1471 Lu, P., Konishi, H., Oelkers, E., Zhu, C. Coupled alkali feldspar dissolution and secondary mineral precipitation in batch systems: 5.
1472 Results of K-feldspar hydrolysis experiments **Chinese Journal of Geochemistry** 34:1–12. 2015
- 1473 Ludwig, C., Casey, W.H., Rock, P.A., Prediction of ligand-promoted dissolution rates from the reactivities of aqueous complexes.
1474 **Nature** 375, 44–46. 1995.
- 1475 Lüttge, A., Bolton, E.W., Lasaga, A.C. An interferometric study of the dissolution kinetics of anorthite: the role of reactive surface
1476 area. **American Journal of Science** 299, 652–678. 1999
- 1477 Lång, L.O. Mineral Weathering Rates and Primary Mineral Depletion in Forest Soils, SW Sweden. In: Effects of Acid Deposition
1478 and Tropospheric Ozone on Forest Ecosystems in Sweden **Ecological Bulletins** 44: 100-113. 1995
- 1479 Maher, K. The dependence of chemical weathering rates on fluid residence time. **Earth and Planetary Science Letters**. 294:101-
1480 110. 2010
- 1481 Malek, S., Martinsson, L., Sverdrup, H. Modelling future soil chemistry at a highly polluted forest site at Istebna in Southern Poland,
1482 using the SAFE model. **Environmental Pollution** 137:568-573. 2005,
- 1483 Malek, S., Belyazid, S., Sverdrup, H. Modelling changes in forest soil chemistry in the oldest spruce stands in the Potok Dupnianski
1484 catchment in Southern Poland using the ForSAFE model. **Folia Forestalia Polonica**, Series A, 54:209-214. 2012
- 1485 Malmström, M. and Banwart, S. Biotite dissolution at 25°C: The pH dependence of dissolution rate and stoichiometry. **Geochimica
1486 et Cosmochimica Acta**, 61, 2779-2799, 1997
- 1487 Malmström, M., Banwart, S., Lewenhagen, J., Duro, L., Bruno, J. The dissolution of biotite and chlorite at 25°C in the near-neutral
1488 pH region. **Journal of Contaminant Hydrology** 21: 201-213. 1996
- 1489 Martinsson, L., Alveteg, M., Kronnäs, V., Sverdrup, H., Westling, O., Warfvinge, P. A regional perspective on present and future soil
1490 chemistry at 16 Swedish forest sites. **Water, Air, and Soil Pollution** 162: 89–105, 2005.
- 1491 Mast, M.A., and Drever, J.L., The effect of oxalate on the dissolution rates of oligoclase and tremolite: **Geochimica et Cosmochimica**



- 1492 **Acta**, 51, 2559-2568. 1987,
1493 Maurice, P.A., Mcknight, D.M., Leff, L., Fulghum, J.E., Michael Gooseff, M. Direct observations of aluminosilicate weathering in
1494 the hyporheic zone of an Antarctic Dry Valley stream. **Geochimica et Cosmochimica Acta**, 66, 1335–1347, 2002
1495 Mazer, J.J. and Walther, J.V. Dissolution kinetics of silica glass as a function of pH between 40 and 85°C. **Journal of Non-crystalline**
1496 **Solids** 170:32–45. 1994
1497 McCourt, G.H. and Hendershot, W.H. 1992. A new method for determining mineral weathering rates in soils. **Commun. Soil Sci.**
1498 **Plant Anal.** 23: 939–952.
1499 McDonnell T.C., Belyazid S., Sullivan, T.J., Bell, M., Clark, C., Blett, T., Evans, T., Cass, W., Hyduke, A. Sverdrup, H., Vegetation
1500 dynamics associated with changes in atmospheric nitrogen deposition and climate in hardwood forests of Shenandoah and
1501 Great Smoky Mountains National Parks, USA. **Environmental Pollution** 237: 662-674. 2018.
1502 McDonnell T.C., S. Belyazid, T.J. Sullivan, H. Sverdrup, W.D. Bowman, E.M. Porter. Modeled subalpine plant community response
1503 to climate change and atmospheric nitrogen deposition in Rocky Mountain National Park, USA. **Environmental Pollution**
1504 187:55-64. 2014
1505 Meadows, D.L., Meadows, D.H., Eds.; Business and Economics: Geneva, Switzerland. 1973
1506 Meadows, D.H., Meadows, D.L., Randers, J., Behrens, W. Limits to growth. Universe Books, New York 1972
1507 Meadows, D.L., Behrens III, W.W., Meadows, D.H., Naill, R.F., Randers, J., Zahn, E.K.O.. Dynamics of Growth in a Finite World.
1508 Massachusetts: Wright-Allen Press, Inc. 1974
1509 Meadows, D.H., Meadows, D.L., Randers, J. Beyond the limits: Confronting global collapse, envisioning a sustainable future. Chelsea
1510 Green Publishing Company: 1992
1511 Meadows, D. H., Randers, J., Meadows, D. Limits to growth. The 30 year update. Universe Press, New York. 2005
1512 Melegy, A., and Paces, T., Calculating Geochemical Weathering Rates Of Three Different Catchments In The Czech Republic.
1513 **International Journal of Innovations in Engineering and Technology (IJET)** ISSN: 2319-1058. 2017.
1514 Metz, V., Raanan, H., Pieper, H., Bosbach, D., Ganor, J. Towards the establishment of a reliable proxy for the reactive surface area
1515 of smectite. **Geochimica et Cosmochimica Acta** 69, 2581– 2591. 2005
1516 Meyer, N.A. An investigation into the dissolution of pyroxene: A precursor to mineral carbonation of PGM tailings in South Africa.
1517 A thesis submitted for the degree of MSc in Engineering in Chemical Engineering at the University of Cape Town, South
1518 Africa. 2014
1519 Modin-Edman, A.K., Öborn, I., Sverdrup, H. FARMFLOW—A Dynamic Model for Phosphorus Mass Flow, Simulating Conventional
1520 and Organic Management of a Swedish Dairy Farm Agricultural Systems. **Agricultural systems** 94:431-444. 2007
1521 Mongeon, A., Aherne, J., Watmough, S. Weathering rates and steady-state critical loads for forest soils in the Georgia Basin.
1522 Proceedings. 9 pages. http://depts.washington.edu/uwconf/2007psgb/2007proceedings/papers/11d_monge.pdf 2007
1523 Montagnac, P., Kohler, S.J., Dufaud, F., Oelkers, E.H., An experimental study of the, dissolution stoichiometry and rates of a natural
1524 monazite as a function of temperature from 5 to 50 degrees C and pH from 1 to 12.3. **Geochimica Et Cosmochimica Acta** 66
1525 (15A), A311-A311. 2002
1526 Mulders, J.J.P.A., Harrison, A.L., Christ, J., Oelkers, E.H. Non-stoichiometric dissolution of sepiolite, **Energy Procedia** 146, 74-80.
1527 2018
1528 Murakami, T., Kogure, T., Kadohara, H., Ohnuki, T. Formation of secondary minerals and its effect on anorthite dissolution.
1529 **American Mineralogist** 83, 1209–1219. 1998
1530 Murphy, W.M., Pabalan, R.T., Prikryl, J.D., Goulet C.J. Dissolution rate and solubility of analcime at 25°C. **Water–Rock Interact.**
1531 **Proceedings**, 7, 107–110. 1992
1532 Murphy, W.M., Pabalan, R.T., Prikryl, J.D., Goulet, C.J. Reaction kinetics and thermodynamics of aqueous dissolution and growth of
1533 analcime and Na-clinoptilolite at 25°C. **American Journal of Science** 296, 128-86. 1996
1534 Murphy, S.F., Brantley, S.L., Blum, A.E., White, A.F., Dong, H. Chemical weathering in a tropical watershed, Luquillo Mountains,
1535 Puerto Rico. II: Rate and mechanism of biotite weathering. **Geochimica et Cosmochimica Acta** 62, 227–243 1998
1536 Murphy, W.M. and Helgeson, H.C.: Thermodynamic and kinetic constraints on reaction rates among minerals and aqueous solutions.
1537 III. Activated complexes and the pH-dependence of the rates of feldspar, pyroxene, wollastonite and olivine hydrolysis,
1538 **Geochimica et Cosmochimica Acta** 51, 3117–3153. 1987,
1539 Murphy, W.M., Oelkers, E.H., Lichtner, P.C. Surface reaction versus diffusion control of mineral dissolution and growth rates in
1540 geochemical processes. **Chemical Geology** 78, 357-380. 1989
1541 Nagy, K.L. Dissolution and precipitation kinetics of sheet silicates. In: **Chemical Weathering Rates of Silicate Minerals** (Eds.. A. F.
1542 White and S. L. Brantley). Mineralogical Society of America, Washington, DC, **Reviews in Mineralogy** 31, 173–225. 1995
1543 Nagy, K.L. and Lasaga, A. C. Dissolution and precipitation kinetics of gibbsite at 80°C and pH 3: The dependence on solution
1544 saturation state. **Geochimica et Cosmochimica Acta** 56: 3093-3111. 1992
1545 Nagy, K.L., Blum, A.E., Lasaga, A.C. Dissolution and precipitation kinetics of kaolinite at 80°C and pH 3: the dependence on solution
1546 saturation state. **American Journal of Science**, 291, 649–686. 1991
1547 Navarre-Sitchler, A. and Thyne, G. Effects of carbon dioxide on mineral weathering rates at earth surface conditions. **Chemical**
1548 **Geology** 243: 53-63. 2007
1549 Nesbitt, H.W., Macrae N.D., Shotyck W. Congruent and incongruent dissolution of labradorite in dilute acidic salt solutions. **Journal**
1550 **of Geology** 99, 429–442. 1991
1551 Nordstrom, D.K., Plummer, L.N., Langmuir, D., Busenberg, E., May, H.M., Jones, B.F., Parkhurst, D.L., Revised chemical
1552 equilibrium data for major water-mineral reactions and their limitations. In: Melchior and Bassett, R.L. (Eds.), **Chemical**
1553 **Modeling of Aqueous Systems II**, Chap. 31. American Chemical Society, Washington, DC, 398–413, ACS Symposium Series
1554 416, 1991
1555 Nyström Claesson, A., and Andersson, K., PHROKIN, a program simulating dissolution and precipitation kinetics in groundwater
1556 solutions. **Computers and Geosciences** 22:559-567. 1996.
1557 Numan A-L., and Weaver, C.E. Kinetics of acid-dissolution of palygorskite (attapulgite) and sepiolite. **Clays and Clay Minerals**, 17,
1558 169 – 178. 1969.
1559 Oelkers E.H. An experimental study of forsterite dissolution rates as a function of temperature and aqueous Mg and Si concentrations.
1560 **Chemical Geology**. 175, 485 – 494. 2001a
1561 Oelkers, E.H., General kinetic description of multi-oxide silicate mineral and glass dissolution. **Geochimica et Cosmochimica Acta**



- 1562 65, 3703–3719. 2001b
1563 Oelkers, E.H., and Gislason, S.R. The mechanism, rates, and consequences of basaltic glass dissolution: I. An experimental study of
1564 the dissolution rates of basaltic glass as a function of aqueous Al, Si, and oxalic acid concentration at 25°C and pH = 3 and 11.
1565 **Geochimica et Cosmochimica Acta** 65, 3671–3681. 2001
1566 Oelkers, E.H., Schott, J., An experimental study of enstatite dissolution rates as a function of pH, temperature, and aqueous Mg and Si
1567 concentration, and the mechanism of pyroxene/pyroxenoid dissolution. **Geochimica et Cosmochimica Acta** 65, 1219–1231.
1568 2001.
1569 Oelkers, E.H. and Schott J. Dissolution and crystallization rates of silicate minerals as a function of chemical affinity. **Pure Appl.**
1570 **Chem.** 67, 903–910. 1995a
1571 Oelkers, E.H. and Schott J. Experimental study of anorthite dissolution and the relative mechanism of feldspar hydrolysis. **Geochimica**
1572 **et Cosmochimica Acta** 59, 5039 – 5053. 1995b
1573 Oelkers, E.H. and Schott J. Does organic acid adsorption affect alkali-feldspar dissolution rates? **Chemical Geology** 151, 235–245.
1574 1998
1575 Oelkers, E. H. and Schott J. Experimental study of kyanite dissolution rates as a function of chemical affinity and solution composition.
1576 **Geochimica et Cosmochimica Acta.** 63, 785–797. 1999
1577 Oelkers, E.H., Schott, J., Devidal, J.-L. The effect of aluminum, pH, and chemical affinity on the rates of aluminosilicate dissolution
1578 rates. **Geochimica et Cosmochimica Acta** 58, 2011–2024. 1994
1579 Oelkers, E. H., Schott, J., Gauthier, J.M., Herrero-Roncal, T. An experimental study of the dissolution mechanism and rates of
1580 muscovite. **Geochimica et Cosmochimica Acta** 72, 4948–4961. 2008
1581 Oelkers, E.H., and Pointrasson, F., An experimental study of the dissolution stoichiometry and rates of a natural monazite as a function
1582 of temperature from 50 to 230 C and pH from 1.5 to 10. **Chemical Geology** 191, 73–87. 2002
1583 Oelkers, E.H., Benning, L.G., Lutz, S., Mavromatis, V., Pearce, C.R., Plümper, O., The efficient long-term inhibition of forsterite
1584 dissolution by common soil bacteria and fungi at Earth surface conditions. **Geochimica et Cosmochimica Acta** 168, 222–235.
1585 2013
1586 Oelkers, E.H., Declercq, J., Saldi, G.D., Gislason, S.R., Schott, J., Olivine dissolution rates: A critical review. **Chemical Geology** 500,
1587 1–19. 2018
1588 Olsen, A.A.. Forsterite dissolution kinetics: Applications and implications for chemical weathering. Dissertation submitted to the
1589 faculty of the Virginia Polytechnic Institute and State University *In: Geosciences*. June 21, 2007 Blacksburg, Virginia. 2007
1590 Olsen, A.A., Rimstidt, D.J., Oxalate-promoted forsterite dissolution at low pH. **Geochimica et Cosmochimica Acta** 72, 1758–1766.
1591 2008.
1592 Olsson, M., Rosén, K., Melkerud, P.-A. Regional modelling of base cation losses from Swedish forest soils due to whole-tree
1593 harvesting. **Applied Geochemistry**, Suppl. Issue No.2, 189–194. 1993
1594 Opolot, E and Finke, P. Sensitivity of mineral dissolution rates to physical weathering: A modeling approach. **Geophysical Research**
1595 **Abstracts** Vol. 17, EGU2015-1807. 2015
1596 Oxburgh, R. The effect of pH, oxalate ion, and mineral composition on the dissolution rates of plagioclase feldspars. M.S. Thesis,
1597 University of Wyoming, Laramie, Wyo., 69 pp. 1991
1598 Oxburgh, R., Drever, J.I., Sun, T.-Y. Mechanism of plagioclase dissolution in acid solution at 25°C. **Geochimica et Cosmochimica**
1599 **Acta**, 58: 661–669. 1994
1600 Palandri, J.L. and Kharaka, Y.K. A compilation of rate parameters of water–mineral interaction kinetics for application to geochemical
1601 modeling, U.S.G.S Open file report 2004–1068, 64p. 2004
1602 Parkhurst, D.L., Thorstenson, D.C., Plummer, L.N., PHREEQE-A computerized program for geochemical calculations. **Water**
1603 **Resources Invest.** 80–96, U.S. Geol. Survey, 1980
1604 Phelan, J., Belyazid, S., Kurz, D., Guthrie, S., Cajka, J., Sverdrup, H., Waite, R. Estimation of soil base Cation weathering rates with
1605 the PROFILE model to determine critical loads of acidity for forested ecosystems in Pennsylvania, USA; Pilot application of
1606 a potential National methodology. **Water, Air and Soil Pollution**, 225: 2109–2128. 2014
1607 Phelan, J., Belyazid, S., Jones, P., Cajka, J., Buckley, J., Clark, C.: Assessing the Effects of Climate Change and Air Pollution on Soil
1608 Properties and Plant Diversity in Northeastern U.S. hardwood forests: Model simulations from 1900 - 2100. **Water, Air and**
1609 **Soil Pollution**, 227:84, 2016.
1610 Pokrovsky, O.S. and Schott, J. Kinetics and mechanism of forsterite dissolution at 25°C and pH from 1 to 12. **Geochimica et**
1611 **Cosmochimica Acta.** 64, 3313–3325. 2000a
1612 Pokrovsky, O.S., and Schott, J., Forsterite surface composition in aqueous solutions: a combined potentiometric, electrokinetic, and
1613 spectroscopic approach. **Geochimica et Cosmochimica Acta** 64, 3299–3312. 2000b.
1614 Pokrovsky, O.S. and Schott, J. Surface chemistry and dissolution kinetics of divalent metal carbonates. **Environ. Sci. Technol.** 36,
1615 426 – 432. 2002
1616 Pokrovsky, O.S., Golubev, S.V., Schott, J. Impact of dissolved organics on mineral dissolution kinetics: towards a predictive model
1617 for Ca- and Mg-bearing oxides, carbonates and silicates. Abstract 13th V.M. Goldschmidt Conference, Copenhagen, Denmark.
1618 June 5–11, 2004. **Geochimica et Cosmochimica Acta.** 68, A141. 2004
1619 Porter, E., Sverdrup, H., Sullivan, T. Estimating and mitigating the impacts of climate change and air pollution on alpine plant
1620 communities in National parks. **Park Science Journal.** 28:58–64. 2011.
1621 Posch M., and Kurz D. A2M – A program to compute all possible mineral modes from geochemical analyses. **Computers &**
1622 **Geosciences** 33: 563–572. 2007
1623 Posch, M., Kurz, D., Alveteg, M., Akselsson, C., Eggenberger, U., Holmqvist, J; **A2M**, a model to quantify mineralogy from
1624 geochemical analyses. Available from [36](http://wgc-
1625 <u>ce.org/Methods_Data/Computing_Mineralogy_from_Geochemical_Analysis</u>; doi:10.1016/j.cageo.2006.08.007. 2007
1626 Posch, M., Hettelingh, J.-P., de Vries, W., Sverdrup, H., Wright, R.F. Manual for dynamic modelling of soil response to atmospheric
1627 deposition. UN/ECE Convention on long-range transboundary air pollution. Working group on effects/ICP on modelling and
1628 mapping. Coordination center for effects (CCE). RIVM/MNV, Bilthoven, Netherlands. 2006
1629 Poulson S.R., Drever J.I., and Stillings L.L. Aqueous Si-oxalate complexing, oxalate adsorption onto quartz, and the effect of oxalate
1630 upon quartz dissolution rates. Chemical Geology 140, 1–7. 1997</p></div><div data-bbox=)



- 1631 Prajapati, P.R., Srinivasan, T.G., Chandramouli, V., Bhagwat, S.S. Dissolution kinetics of zirconium dioxide in nitric acid.
1632 **Desalination and Water Treatment** 2 490–497. 2014
- 1633 Price, J., and Velbel, M.A. Rates of Biotite Weathering, and Clay Mineral Transformation and Neoformation, Determined from
1634 Watershed Geochemical Mass-Balance Methods for the Coweeta Hydrologic Laboratory, Southern Blue Ridge Mountains,
1635 North Carolina, USA. **Aquatic Geochemistry**. 20. 10.1007/s10498-013-9190-y 2004
- 1636 Price, J.R., Velbel, M.A., Patino, L.A., Allanite and epidote weathering at the Coweeta Hydrologic Laboratory, western North Carolina,
1637 U.S.A **American Mineralogist** 90: 101-114. 2005.
- 1638 Price, J.R.; Bryan-Ricketts, D.S.; Anderson, D.; Velbel, M.A. Weathering of almandine garnet: influence of secondary minerals on
1639 the rate-determining step, and implications for regolith-scale Al mobilization. **Clays and Clay Minerals** 61:34-56. 2013.
- 1640 Prigiobbe V., Costa G., Baciocchi R., Hanchen M. and Mazzotti M. The effect of CO₂ and salinity on olivine dissolution kinetics at
1641 120°C. **Chemical Engineering Science** 64, 3510–3515. 2009
- 1642 Probst, A., Obeidy, C., Gaudio, N., Belyazid, S., Gégout, J.-C., Alard, D., Corket, E., Party, J-P., Gauquelin, T., Mansat, A., Nihlgård,
1643 B., Leguédou S., Sverdrup H.U. Evaluation of plant-responses to atmospheric nitrogen deposition in France using integrated
1644 soil-vegetation models. In: W. de Vries, J-P. Hettelingh, M. Posch (Eds.) *Critical Loads and Dynamic Risk Assessments:*
1645 *Nitrogen, Acidity and Metals in Terrestrial and Aquatic Ecosystems:* 359-379. Springer Verlag, 2015
- 1646 Ouimet, R. and Duchesne, L. Base cation mineral weathering and total release rates from soils in three calibrated forest watersheds on
1647 the Canadian Boreal Shield. **Canadian Journal of Soil Science** 85: 245–260. 2005
- 1648 Ragnarsdottir K.V. Dissolution kinetics of heulandite at pH 2–12 and 25°C. **Geochimica et Cosmochimica Acta** 57:2439–2449. 1993
- 1649 Ragnarsdottir, K.V., Graham, C.M., Allen, G.C. Surface chemistry of reacted heulandite determined by SIMS and XPS. **Chemical**
1650 **Geology** 131, 167–181. 1996
- 1651 Raschman, P., Fedorockova, A., Dissolution kinetics of periclase in dilute hydrochloric acid. **Chemical Engineering Science** 63, 576–
1652 586. 2008.
- 1653 Rietz, F. Modeling mineral weathering and soil chemistry during post-glacial period., Reports in Ecology and Environmental
1654 Engineering, 1;1995. Department of Chemical Engineering, Lund University ISRN LUTKDH/TKKT-3004-SE. 1995
- 1655 Rimstidt, J.D., Brantley, S.L., Olsen, A.A. Systematic review of forsterite dissolution rate data. **Geochimica et Cosmochimica Acta**
1656 99, 159-178. 2012.
- 1657 Rizzetto, S., Belyazid, S., Gégout, J.-C., Nicholas, M., Alard, D., Corcket, E., Gaudio, N., Sverdrup, H., Probst, A., Modelling the impact
1658 of climate change and atmospheric N deposition on French forests biodiversity. **Environmental Pollution** 213: 1016-1027.
1659 2016.
- 1660 Rizzetto, S.; Gégout, J.-C.; Belyazid, S.; Kuhn, E.; Sverdrup, H.; Probst, A., How to couple ecological database to geochemical dynamic
1661 model to predict the impact of atmospheric nitrogen deposition and climate change on French forest ecosystems at the national
1662 scale? International Congress on Environmental Modelling and Software. 75.
1663 <https://scholarsarchive.byu.edu/jemssconference/2016/Stream-D/75>. 2016.
- 1664 Roberts, N., Andersen, D.F., Deal, R.M., Shaffer, W.A. 1982, Introduction to Computer Simulation: A System Dynamics Approach
1665 Productivity Press, Chicago
- 1666 Ross, G.J., Acid dissolution of chlorites: release of magnesium, iron and aluminum and mode of acid attack. **Clays and Clay Minerals**,
1667 17, 347-354. 1969
- 1668 Rosso, J.J., and Rimstidt, J.D. A high resolution study of forsterite dissolution rates. **Geochimica et Cosmochimica Acta**, 64, 797–
1669 811. 1999
- 1670 Rozalen, M., Ramos, M.E., Gervilla, F., Kerestédjian, T., Fiore, S., Huertas, F.J. Dissolution study of tremolite and anthophyllite: pH
1671 effect on the reaction kinetics. **Applied Geochemistry** 49:46-56. 2014
- 1672 RTI International. 2013. Application of the base cation weathering (BCw) methodology and PROFILE model to calculate terrestrial
1673 critical acid loads in Pennsylvania—evaluation of USGS landscapes project database as source of soil mineralogy data. Final
1674 report. pp. 85. [Google Scholar](#). 2013
- 1675 Running, S.W. and Gower, S.T. FOREST-BGC, a general model of forest ecosystem processes for regional applications, II. Dynamic
1676 carbon allocation and nitrogen budgets. **Tree Physiology**, 9, 147-160. 1991
- 1677 Running, S.W. Testing FOREST-BGC ecosystem process simulations across a climatic gradient in Oregon. **Ecol. Appl.**, 4, 238-247.
1678 1994
- 1679 Saldi, G.D., Köhler, S.J., Marty, N., Oelkers, E.H., Dissolution rates of talc as a function of solution composition, pH and temperature.
1680 **Geochimica et Cosmochimica Acta** 71, 3446–3457. 2007
- 1681 Savage, D., Rochelle, C., Moore, Y., Milodowski, A., Bateman, K., Bailey, D., Mihara, M., Analcime reactions at 25-90°C in
1682 hyperalkaline fluids **Mineralogical Magazine**, 65, 571–587. 2001.
- 1683 Schnoor, J.L. Kinetics of chemical weathering: a comparison of laboratory and field weathering rates. In: *Aquatic Chemical Kinetics*
1684 (ed. W. Stumm). Wiley, New York, 475–504. 1990
- 1685 Schofield, R.E., Hausrath, E.M., and Gainey, S.R. Zeolite weathering in laboratory and natural settings, and implications for mars.
1686 46th Lunar and Planetary Science Conference 2160.pdf. 2015
- 1687 Schott, J., Oelkers, E.H., Dissolution and crystallization rates of silicate minerals as a function of chemical affinity. Pure and applied
1688 chemistry 67, 903-910. 1995
- 1689 Schott, J., Pokrovsky, O.S., Oelkers, E.H. The Link Between Mineral Dissolution/Precipitation Kinetics and Solution Chemistry.
1690 **Reviews in Mineralogy and Geochemistry** 70: 207-258. 2009
- 1691 Schott, J., Oelkers, E., Benezeth, P., Godderis, Y. Francois, L. Can accurate kinetic laws be created to describe chemical weathering?
1692 **Comptes Rendus Geoscience** 344, 568-585. 2012
- 1693 Semenov, M., Bashkin, V., Sverdrup, H., Application of biochemical model PROFILE for assessment of North Asian ecosystem
1694 sensitivity to acid deposition. **Asian Journal of Energy and Environment** 1:143-161. 2000
- 1695 Senge P. The Fifth Discipline. The Art and Practice of the Learning Organisation. Century Business, New York. 1990
- 1696 Smits, M.M., and Wallander, H. Role of Mycorrhizal Symbiosis in Mineral Weathering and Nutrient Mining from Soil Parent Material.
1697 in *Mycorrhizal Mediation of Soil: Fertility, Structure, and Carbon Storage*. Elsevier Inc., pp. 35-46. DOI: 10.1016/B978-0-12-
1698 804312-7.00003-6. 2016
- 1699 Smits, M.M., Johansson, L., Wallander, H. Soil fungi appear to have a retarding rather than a stimulating role on soil apatite weathering.
1700 **Plant and Soil** 385: 217-228. 2014.



- 1701 Smith, M.M., Wolery, T.J., Carroll, S.A., Kinetics of chlorite dissolution at elevated temperatures and CO₂ conditions. **Chemical**
1702 **Geology** 347, 1–8. 2013.
- 1703 Soler, J.M., Cama, J., Galí, S., Meléndez, W., Ramírez, A., Estanga, J. Composition and dissolution kinetics of garnierite from the
1704 Loma de Hierro Ni-laterite deposit, **Venezuela Journal of Chemical Geology** 249, 191–202. 2008
- 1705 Starr, M., Lindroos, A.J., Tarvainen, T., Tanskanen, H., Weathering rates in the Hietajärvi Integrated Monitoring catchment. **Boreal**
1706 **Environment Research** 3: 275–285. 1998.
- 1707 Stegman B., and Sverdrup, H. Skogsmarkens försurning i Värmland – En prognos för framtiden. Länsstyrelsen i Värmlands Län,
1708 *Miljöenheden Rapport* 1997:11A:1-40. 1997
- 1709 Stegman B., Sverdrup, H. Skogsmarkens försurningskänslighet, kritisk belastning och modelberäkning. Länsstyrelsen i Älvsborgs
1710 Län, *Miljöenheden Meddelande* 1996:8:1-40. 1996
- 1711 Stendahl, J., Akselsson, C., Melkerud, P.A., Belyazid, S. Pedon-scale silicate weathering: Comparison of the PROFILE model and the
1712 depletion method at 16 forest sites in Sweden. **Geoderma**. 211–212. 65-74. 2013.
- 1713 Stephens, J.C., and Hering, J.G. Factors affecting the dissolution kinetics of volcanic ash soils: dependencies on pH, CO₂, and oxalate.
1714 **Applied Geochemistry** 19: 1217–1232. 2003
- 1715 Stillings, L., Brantley, S. and Machesky, M., Proton adsorption at an adularia feldspar surface, **Geochimica et Cosmochimica Acta**
1716 59, 1473-1482. 1995
- 1717 Stillings L.L. and Brantley S.L. Feldspar dissolution at 25°C and pH 3: reaction stoichiometry and the effect of cations. **Geochimica**
1718 **et Cosmochimica Acta** 59, 1483–1496. 1995
- 1719 Stillings L.L., Drever J.I., Brantley S.L., Sun Y., Oxburgh R. Rates of feldspar dissolution at pH 3–7 with 0–8 mM oxalic acid.
1720 **Chemical Geology** 132, 79–89. 1996
- 1721 Stockmann G., Wolff-Boenisch D., Gislason S.R., Oelkers E.H. Dissolution of diopside and basaltic glass: the effect of carbonate
1722 coating. **Mineralogical Magazine** 72, 135–139. 2008
- 1723 Stockmann, G.J., Wolff-Boenisch, D., Gislason, S.R., Oelkers, E.H., Do carbonate precipitates affect dissolution kinetics?: 2: Diopside.
1724 *Chemical Geology* 337, 56-66. 2013
- 1725 Stumm, W. and Wieland, E., Dissolution of oxide and silicate minerals; rates depend on surface speciation. In: Stumm, W. Ed.,
1726 *Aquatic Chemical Kinetics*. Wiley-Interscience, New York. 1990
- 1727 Stumm, W. and Wollast, R., Coordination chemistry of weathering. **Rev. Geophys.** 28, 53–69. 1990
- 1728 Sverdrup, H. Calcite dissolution and acidification mitigation strategies, **Lake and Reservoir Management** 2:345-355. 1984
- 1729 Sverdrup, H.U., Calcite dissolution kinetics and lake neutralization. PhD Thesis, Chemical Engineering, Lund University.
1730 LUTTKDH/TKKT/1002/1-169/1985. 169pp. 1985.
- 1731 Sverdrup, H. *The kinetics of chemical weathering*. Lund University Press, Lund, Sweden and Chartwell-Bratt Ltd, London, ISBN 0-
1732 86238-247-5, 245pp. 1990
- 1733 Sverdrup, H. Methods for the estimation of base cation weathering rates. In: Annex IV; In: Bobbink, R., Draaijers, G., Erisman, J.,
1734 Gregor, H.D., Henriksen, A., Hornung, M., Iversen, T., Kucera, V., Posch, M., Rihm, B., Spranger, T., Sverdrup, H., de Vries,
1735 W., Werner, B. In: Gregor H. D. and Werner B. (Eds.): *Manual on methodologies and criteria for mapping critical levels/loads*
1736 *and geographical areas where they are exceeded. Umweltbundesamt Texte* 71:96, ISSN 0722-186X. 1996.
- 1737 Sverdrup, H. Geochemistry, the key to understanding environmental chemistry. **Science of the Total Environment** 183, 67-87. 1996
- 1738 Sverdrup, H. Experimental kinetics of hornblende and epidote and their importance in integrated soil modelling. In: Sulovsky P., and
1739 Zeman, J., (Eds), *Environmental aspects of weathering processes*. Masaryk University Faculty of Science; 208-216. 1998
- 1740 Sverdrup, H. What is left for researchers in soil and water acidification modelling? Reflections over past experiences and future
1741 possibilities. In: Guardans, R. *Data analysis for modelling and assessment of biogeochemical effects of air pollution in*
1742 *temperate ecosystems*. Pages 49-60. CIEMAT, Madrid, Spain 8-11 October 1997. 1998.
- 1743 Sverdrup, H. Calculating critical loads of acidity and nitrogen for terrestrial ecosystems and some reflections on the Alberta situation.
1744 In K. Foster (Ed.), *Proceedings of the NOx/SOx management working group science colloquium on acid deposition, Alberta*
1745 *Research Council Reports*; 9-14, Edmonton. 2000
- 1746 Sverdrup, H. Nutrient sustainability for Swedish forests In: Developing principles for sustainable forestry Results from a research
1747 program in southern Sweden. Sverdrup, H., and Stjernquist, I., (Eds.) **Managing Forest Ecosystems** 5:427-432 Kluwer
1748 Academic Publishers, Amsterdam. 2002
- 1749 Sverdrup, H. Chemical weathering of soil minerals and the role of biological processes. **Fungal Biology Reviews** 23:94-100. 2009.
- 1750 Sverdrup, H. and Alveteg, M. PROFILE – The integrated model for transferring laboratory weathering kinetics to field conditions. In:
1751 Sulovsky P., and Zeman, J., (Eds), *Environmental aspects of weathering processes*, Masaryk University Faculty of Science;
1752 218-224. 1998
- 1753 Sverdrup, H. and Bjerle, I. Dissolution of calcite and other related minerals in aqueous solutions in a pH-stat, **Vatten, Journal of**
1754 **Water Management and Research** 38:59-73. 1982
- 1755 Sverdrup, H., and Belyazid, S. The ForSAFE-VEG model system - Developing an approach for Sweden, Switzerland, United States
1756 and France for setting critical loads based on biodiversity in a time when management, pollution and climate change.
1757 **Ecological Modelling** 306: 35-45, Special Issue for the 2013 ISEM Conference at Toulouse. (Invited keynote lecture paper,
1758 [doi:10.1016/j.ecolmodel.2014.09.020](https://doi.org/10.1016/j.ecolmodel.2014.09.020)). 2014.
- 1759 Sverdrup, H., Holmqvist, J., A critical assessment of the use of kinetics, steady state or equilibrium in relation to reversibility or
1760 irreversibility in chemical weathering rate modelling (Unpublished note available as pdf from Sverdrup). 2019
- 1761 Sverdrup, H. and Rosén, K. Long-term base cation mass balances for Swedish forests and the concept of sustainability. **Forest Ecology**
1762 **and Management** 110, 221-236. 1998.
- 1763 Sverdrup, H. and Stjernquist, I. *Developing Principles and Models for Sustainable Forestry in Sweden*. Kluwer Academic Publishers,
1764 Dordrecht, 480 pp. 2002.
- 1765 Sverdrup, H. and Warfvinge, P. Chemical weathering of minerals in the Gårdsjön catchment in relation to a model based on laboratory
1766 rate coefficients. In: *Critical loads for sulphur and nitrogen*, Nilsson, J., (Ed) Nordic Council of Ministers and The United
1767 Nations Economic Commission for Europe (UN/ECE). Stockholm, Nordic Council of Ministers *Miljörapport* 1988:15:131-
1768 150. 1988a
- 1769 Sverdrup, H. and Warfvinge, P. Assessment of critical loads of acid deposition on forest soils, In: *Critical loads for sulphur and*
1770 *nitrogen*, Nilsson, J., (Ed) Nordic Council of Ministers and The United Nations Economic Commission for Europe (ECE),



- 1771 Stockholm Nordic Council of Ministers *Miljörapport* 1988:15:81-130. 1988b
1772 Sverdrup, H. and Warfvinge, P. Weathering of primary silicate minerals in the natural soil environment in relation to a chemical
1773 weathering model, **Water, Air and Soil Pollution** 38:387-408. 1988c
1774 Sverdrup, H. and Warfvinge, P., The role of weathering in determining the acidity of lakes in Sweden. **Water, Air and Soil Pollution**,
1775 52:71–78. 1990
1776 Sverdrup, H. and Warfvinge, P. On the geochemistry of chemical weathering. In: Rosen, K., (Ed.) *Chemical weathering under field*
1777 *conditions*: 79–118. Department of Forest Soils. Swedish Agricultural University. 1991
1778 Sverdrup, H. and Warfvinge, P. PROFILE-A mechanistic geochemical model for calculation of field weathering rates. In: Kharka, Y.
1779 and Maest, A. (Eds.), *Proceedings of the 7th International Symposium on water-rock interaction*, Utah, 13-19 July 1992, 44–
1780 48. Balkema Publishers. 1992a
1781 Sverdrup, H. and Warfvinge, P. PROFILE-A mechanistic geochemical model for calculation of field weathering rates. In: Y. Kharka
1782 and A. Maest (Eds.), *Proceedings of the 7th International Symposium on water-rock interaction*, Utah, 13-19 July 1992, 44–
1783 48. Balkema Publishers. 1992b
1784 Sverdrup, H. and Warfvinge, P. Critical loads. In Warfvinge, P. and Sandén, P. editors, *Modeling Acidification of Groundwater*.
1785 SMHI, Norrköping, 171-186. 1992c
1786 Sverdrup, H. and Warfvinge, P. Calculating field weathering rates using a mechanistic geochemical model–PROFILE. **Journal of**
1787 **Applied Geochemistry**, 8:273–283. 1993
1788 Sverdrup, H. and Warfvinge, P. Estimating field weathering rates using laboratory kinetics. In: White, A.F., Brantley, S.L., (Eds.),
1789 *Chemical weathering rates of silicate minerals*. Mineralogical Society of America, Washington DC. **Reviews in Mineralogy**,
1790 31:485–541. 1995
1791 Sverdrup, H., Alveteg, M., Langan, S., Paces, T. Biogeochemical modelling of small catchments using PROFILE and SAFE. In S.
1792 Trudgill, (Ed), *Solute Modelling in Catchment Systems*, 75–99. John Wiley Science, New York. 1995
1793 Sverdrup H., Belyazid S., Nihlgård B., Ericson L. Modelling change in ground vegetation response to acid and nitrogen pollution,
1794 climate change and forest management in Sweden 1500-2100 A.D. **Water Air and Soil Pollution: Focus** 7: 163-179. 2007
1795 Sverdrup, H., Belyazid, S., Kurz, D., Braun, S. A proposed method for estimating critical loads for nitrogen based on biodiversity
1796 using a fully integrated dynamic model, with testing in Switzerland and Sweden. In: Sverdrup, H., (Ed.) *Towards critical loads*
1797 *for nitrogen based on biodiversity*. Background document for the 18th CCE workshop on the assessment of nitrogen effects
1798 *under the ICP for Modelling and Mapping*, LRTAP Convention (UNECE), Bern, Switzerland, 21-25 April 2008. Pages 3-37.
1799 Swiss Federal Office of the Environment (FOEN), Bern, Switzerland.. 2008
1800 Sverdrup, H., Belyazid, S., Akselsson, C., Posch, M. Assessing critical loads for nitrogen under climate change based on chemical
1801 and biological indicators in a sub-Arctic country; the case of Sweden. In: Bashkin, V., (Ed.); *Ecological and biogeochemical*
1802 *cycling in impacted polar ecosystems*. Nova Science Publishing, Hauppauge, New York. ISBN 978-1-53612-081-3. 2017.
1803 Sverdrup, H., Hagen-Thorn, A., Holmqvist, J., Warfvinge, P., Walse, C., Alveteg, M. Biogeochemical processes and mechanisms. In:
1804 *Developing principles for sustainable forestry Results from a research program in southern Sweden*. Sverdrup, H., and
1805 Stjernquist, I. (Eds.) **Managing Forest Ecosystems** 5:91-196. Kluwer Academic Publishers, Amsterdam. 2002
1806 Sverdrup H. (Ed.), Haraldsson, H., Koca, D., Belyazid, S. 2011 *System Thinking, System Analysis and System Dynamics: Modelling*
1807 *Procedures for Communicating Insight and Understanding by Using Adaptive Learning in Engineering for Sustainability*. 1st
1808 *edition for Iceland*. Two volumes, 30 printed. Háskolaprent Reykjavík. 310pp. 2011
1809 Sverdrup, H., Holmqvist, J., Butz-Braun, R., Clay-PROFILE – A new concept for modelling clay weathering rates and alteration
1810 sequences. (Unpublished note, available as pdf). 2010
1811 Sverdrup, H., Hoyesky, H., Achermann B. Critical loads of acidity for high precipitation areas. Bundesministerium fuer Umwelt,
1812 Jugend und Familie, Wien. 60pp. 1993
1813 Sverdrup, H., Martinsson, L., Alveteg, M., Moldan, F., Kronnäs, V., Munthe, J. Modeling recovery of Swedish ecosystems from
1814 acidification, **Ambio** 34:25-31. 2005
1815 Sverdrup, H., McDonnell, T.C., Sullivan, T.J., Nihlgård, B., Belyazid, S., Rihm, B., Porter, E., Bowman, W.D., Geiser, L. Testing the
1816 feasibility of using the ForSAFE-VEG model to map the critical load of nitrogen to protect plant biodiversity in the Rocky
1817 Mountains region, USA. **Water, Air and Soil Pollution**, 223:371-387. 2012.
1818 Sverdrup, H., Nihlgård, B., Svensson, M., Örländer, G. Skogsmarkens långsiktiga produktionsförmåga. In: J. Elmberg (Ed.)
1819 *Sustainable Forestry in Southern Sweden*, Årsrapport 1998; Tema Skogshälsa 37-39. 1998
1820 Sverdrup H., de Vries W., Henriksen A. Mapping Critical Loads. Environmental Report 1990:14 (NORD 1990:98), Nordic Council of
1821 Ministers, Copenhagen, 124 pp. 1990
1822 Sverdrup, H., Warfvinge, P., Bjerle, I. Oppløsningskinetikken for K-kalk i forhold till andre basiske mineral benyttet for nøytralisasjon
1823 av surt vann, Swedish Environmental Protection Board (SNV), Solna, Sweden *SNV Report* 3020. 1985
1824 Sverdrup, H., Warfvinge, P., Bjerle, I. Experimental determination of the kinetic expression for K-slag, a tricalcium silicate, in acidic
1825 aqueous solution at 25°C and in equilibrium with air, using the results from pH-stat experiments. **Vatten, Journal of Water**
1826 **Management and Research**. 42:210-217. 1986
1827 Sverdrup, H., Warfvinge, P., von Brömssen, U. A mathematical model for podzolic soil profiles exposed to acidic deposition. In:
1828 *Acidification and water pathways*, N. Christophersen (Ed), 435-444, ISBN 82-554-0486-4. Norwegian National Committee
1829 for Hydrology 1987a
1830 Sverdrup, H., Warfvinge, P., von Brömssen, U. A mathematical model for acidification and neutralization of soil profiles exposed to
1831 acid deposition. In: *Air pollution and ecosystems*—Proceedings of an International symposium held in Grenoble, France, 18-
1832 22 May, 1987, Mathy, P. (Ed) 817-822, D. Reidel publishing company, Dordrecht. 1987b
1833 Sverdrup, H., Warfvinge, P., Blake, L., Goulding, K. Modeling recent and historic soil data from the Rothamsted Experimental Station
1834 UK, using SAFE. **Agriculture, Ecosystems and Environment**, 53:161–177. 1995
1835 Sverdrup, H., Warfvinge, P., Wickman, T. Estimating the weathering rate at Gårdsjön using different methods. In: Hultberg H. and
1836 Skeffington R. (Eds.) *Experimental reversal of acid rain effects; The Gårdsjön roof project*: 231-250. John Wiley Science.
1837 1998
1838 Sverdrup, H., Warfvinge, P., Frogner, T., Håöya, A.O., Johansson, M., Andersen, B. Critical loads for forest soils in the Nordic
1839 countries. **Ambio**, 21:348–355. 1992
1840 Sverdrup, H., Warfvinge, P., Moldan, F., Hultberg, H., Modelling acidification and recovery in the roofed catchment at Lake Gårdsjön



- 1841 using the SAFE model. **Water, Air and Soil Pollution** 85:1753-1758. 1996
- 1842 Sverdrup, H., Warfvinge, P., Janicki A., Morgan, R., Rabenhorst, M., Bowman, M. Mapping critical loads and steady state stream
1843 chemistry in the state of Maryland. **Environmental Pollution**, 77:195–203. 1992
- 1844 Sverdrup, H., Warfvinge, P., Rosen, K. Critical loads of acidity and nitrogen for Swedish forest ecosystems, and the relationship to
1845 soil weathering. In: H. Raitio and T. Kilponen, (Eds), Critical loads and critical limit values, *Metsäntutkimuslaitoksen*
1846 *tiedonantoja* 513:109–138, Vaasa, Finland 1994
- 1847 Sverdrup, H., Warfvinge, P., Britt, D. Assessing the potential for forest effects due to soil acidification in Maryland. **Water, Air and**
1848 **Soil Pollution** 87:245-265. 1996
- 1849 Sverdrup, H., Warfvinge, P., Hultberg, H., Andersson, B., Moldan, F. Modelling soil acidification and recovery in a roofed catchment;
1850 Application of the SAFE model. In: Hultberg H. and Skeffington R. (Eds.) *Experimental reversal of acid rain effects; The*
1851 *Gårdsjön roof project*: 363-382. John Wiley Science. 1998
- 1852 Sverdrup, H., Thelin, G., Robles, M., Stjernquist, I., Sörensen, J. Assessing sustainability of different tree species considering Ca, Mg,
1853 K, N and P at Björnstorps Estate. **Biogeochemistry** 81:219-238. 2006.
- 1854 Swoboda-Colberg N.G. and Drever J.I. Mineral dissolution rates in plot-scale field and laboratory experiments. **Chemical Geology**
1855 105, 51–69. 1993
- 1856 Taylor, A.S., Blum, J.D., Lasaga, A.C., MacInnis, I.N. Kinetics of dissolution and Sr release during biotite and phlogopite weathering.
1857 **Geochimica et Cosmochimica Acta**, 64: 1191–1208. 1999.
- 1858 Taylor, A.S., Blum, J.D., Lasaga, A.C. The dependence of labradorite dissolution and Sr isotope release rates on solution saturation
1859 state. **Geochimica et Cosmochimica Acta** 64, 2389–2400. 2000
- 1860 Taylor, A. and Blum, J.D. Relation between soil age and silicate weathering rates determined from the chemical evolution of a glacial
1861 chronosequence. **Geology** 23: 979–982. 1995.
- 1862 Taylor, L.L., Beerling, D.J., Quegan, S., Banwart, S.A. Simulating carbon capture by enhanced weathering with croplands: an
1863 overview of key processes highlighting areas of future model development. **Biol. Lett.** 13 : 20160868.
1864 <http://dx.doi.org/10.1098/rsbl.2016.0868>, 2017
- 1865 Techer, I, Avocat, T, Vernaz, E., Lancelot, J.R., Liotard, J.M. Toulouse Goldschmidt Conference. **Mineralogical Magazine**, 62a:
1866 1498-1499. 1998
- 1867 Teir, S., Revitzer, H., Eloneva, S., Fogelholm, C-J., Zevenhoven, R. Dissolution of natural serpentinite in mineral and organic acids.
1868 **Int. J. Miner. Process.** 83 36–46. 2007
- 1869 Terry, B., The acid decomposition of silicate minerals Part I. Reactivities and modes of dissolution of silicates. **Hydrometallurgy** 10,
1870 135–150. 1983a.
- 1871 Terry, B., The acid decomposition of silicate minerals Part II. Hydrometallurgical applications. **Hydrometallurgy** 10, 151–171.
1872 1983b.
- 1873 Terry, B., Specific chemical rate constants for the acid dissolution of oxides and silicates. **Hydrometallurgy** 11, 315–344. 1983c.
- 1874 Terry, B., Monhemius, A.J. Acid dissolution of willemite (Zn,Mn)₂SiO₄ and hemimorphite (Zn₄Si₂O₇(OH)₂H₂O). **Metall. Trans. B**
1875 14, 335–346. 1983.
- 1876 Thelin, G., Sverdrup, H., Holmqvist, J., Rosengren, U., Linden M. Sustainability in spruce and mixed forest stands. In: Developing
1877 principles for sustainable forestry Results from a research program in southern Sweden. Sverdrup, H., and Stjernquist, I.,
1878 (Eds.) **Managing Forest Ecosystems** 5:337-354, Kluwer Academic Publishers, Amsterdam. 2002
- 1879 Thom, J.G.M., Dipple, G.M., Power, I.M., Harrison, A.L. Chrysotile dissolution rates: implication for carbon sequestration. **Applied**
1880 **Geochemistry** 35, 244–254. 2013
- 1881 Tominaga, K., Aherne, J., Watmough, S.A., Alveteg, M., Cosby, B.J., Driscoll, C.T., Posch, M., Pourmokhtarian, A., Predicting
1882 Acidification Recovery at the Hubbard Brook Experimental Forest, New Hampshire: Evaluation of Four Models
1883 **Environmental Science & Technology**. 44, 9003-9009. 2010
- 1884 Traven, L., Fijan-Parlov, S., Galović, L., Sverdrup, H.: Prospects for a regional assessment of forest soil chemistry dynamics in
1885 Croatia: Application of the SAFE model to a forested site in the region of mount Medvednica. **Periodicum Biologorum**
1886 01/2005; 107:17-26. 2005
- 1887 Turpault, M.P., and Troignon, L. The dissolution of biotite single crystals in dilute HNO₃ at 24°C; evidence of an anisotropic corrosion
1888 process of micas in acidic solution. **Geochimica et Cosmochimica Acta** 58, 2761–2775. 1994
- 1889 Ullman, W.J., Kirchman, D.L., Welch, S.A., Vandevivere P. Laboratory evidence for microbially mediate silicate dissolution in nature.
1890 **Chemical Geology** 132, 11–17. 1996
- 1891 Valsami-Jones, E., Ragnarsdottir, K.V., Putnis, A., Bosbach, D., Kemp, A.J., Cressey, G. The dissolution of apatite in the presence of
1892 aqueous metal cations at pH 2–7. **Chemical Geology** 151:215–233. 1998
- 1893 Velbel, M.A., Bond strength and the relative weathering rates of simple orthosilicates. **American Journal of Science** 299, 679–696.
1894 1999
- 1895 Velbel M.A. Constancy of silicate-mineral weathering-rate ratios between natural and experimental weathering: Implications for
1896 hydrologic control of differences in absolute rates. **Chemical Geology** 104, 89–99. 1993
- 1897 de Vries W., Wamelink, W., Dobben, H., Kros, H., Reinds, G. J., Mol-Dijkstra, J., Smart, S., Evans, C., Rowe, E., Belyazid, S.,
1898 Sverdrup, H., Hindsberg, A., Posh, M., Hettelingh, J-P., Spanger, T., Bobbink, R. Use of dynamic soil-vegetation models to
1899 assess impacts of nitrogen deposition on plant species composition: an overview. **Ecological Applications** 20: 60-79; DOI:
1900 [10.1890/08-1019.1](https://doi.org/10.1890/08-1019.1) 2010.
- 1901 de Vries, W., Kros, H., Reinds, G. J., Wamelink, W., van Dobben, H., Bobbink, R., Smart, S., Evans, C., Schlütow, A., Kraft, P.,
1902 Belyazid, S., Sverdrup, H., van Hinsberg, A., Posch, M., Hettelingh J-P. Developments in modelling critical nitrogen loads
1903 for terrestrial ecosystems in Europe 230pp, *Developments in Deriving Critical Limits and Modeling Critical Loads of Nitrogen*
1904 *for Terrestrial Ecosystems in Europe*. Alterra, CCE Report critical N limits and loads CCE. 174 ISSN 1566-7197 ©2006
1905 Alterra, Box 47, 6700 AA Wageningen; The Netherlands; e-mail: info.alterra@wur.nl. 2006
- 1906 Voltini, M., Artioli, G., Moret, M. The dissolution of laumontite in acidic aqueous solutions: A controlled-temperature in situ atomic
1907 force microscopy study **American Mineralogist**, 97: 150–158, 2012.
- 1908 Wallman, P., Svensson, M.G.E., Sverdrup, H., Belyazid, S., ForSAFE - an integrated process-oriented forest model for long-term
1909 sustainability assessments, **Forest Ecology and Management**, 207:19-36. 2005.
- 1910 Wallman, P., Sverdrup, H. Developing the complex forest ecosystem model FORSAFE - motives, means and the learning loop. In:



- 1911 Björk, L. (Ed.) *Sustainable Forestry in Temperate Regions*. Proceedings of the SUFOR International Workshop, April 7-9,
1912 2002 in Lund, Sweden: page 154. 2002.
- 1913 Wang, F., Silicate Mineral Dissolution and Associated Carbonate Precipitation at Conditions Relevant to Geologic Carbon
1914 Sequestration. All Theses and Dissertations (ETDs). PhD thesis. 1161.
1915 <http://openscholarship.wustl.edu/etd/1161> 170pp. 2013
- 1916 Wang, F., Giammar, D.E. Forsterite dissolution in saline water at elevated temperature and high CO₂ pressure. **Environ. Sci. Technol.**
1917 47, 168–173. 2012
- 1918 Wang, H., Feng, Q., Rang, X., Zuo, K., Liu, K., Insights into alkali-acid leaching of sericite: Dissolution behaviour and mechanism.
1919 **Minerals** 7: 196-208. 2017.
- 1920 Warfvinge, P., and Sverdrup, H., Soil liming and runoff acidification mitigation. **Lake and Reservoir Management** 2:389-393. 1984
- 1921 Warfvinge P. and Sverdrup H. Calculating critical loads of acid deposition with PROFILE - A steady-state soil chemistry model.
1922 **Water, Air and Soil Pollution** 63: 119-143. 1992a
- 1923 Warfvinge, P. and Sverdrup, H. Hydrochemical modeling 79-118. In: Warfvinge, P. and Sandén, P., (Eds.), *Modeling Acidification of*
1924 *Groundwater*. SMHI, Norrköping. 1992b.
- 1925 Warfvinge, P. and Sverdrup, H. Scenarios for acidification of groundwater 147-156. In: Warfvinge, P. and Sandén, P. (Eds.), *Modeling*
1926 *Acidification of Groundwater*. SMHI, Norrköping. 1992c
- 1927 Warfvinge, P. and Sverdrup, H. Modeling regional mineralogy and weathering rates. In: Kharka, Y. and Maest, A. (Eds.), *Proceedings*
1928 *of the 7th International Symposium on water-rock interaction*, held in Utah, July 13-19, 1992, 49–53. Balkema Publishers.
1929 1992d
- 1930 Warfvinge P., and Sverdrup H. Critical loads of acidity to Swedish forest soils. Reports in Ecology and Environmental Engineering
1931 1993;5, Lund University, Lund, Sweden, 104 pp. 1993
- 1932 Warfvinge, P., Sverdrup, H., Modelling limestone dissolution in soils. **Soil Science Society of America Journal**, 53:44–51. 1989
- 1933 Warfvinge, P., Sverdrup, H., Critical loads of acidity to Swedish forest soils, *Reports in Environmental Engineering and Ecology*, 5:95,
1934 127pp, Chemical Engineering II, Box 124, Lund University. 221 00 Lund, Sweden. 1995
- 1935 Warfvinge, P., Falkengren-Grerup, U., Sverdrup, H., Andersen, B. Modeling long-term cation supply in acidified forest stands.
1936 **Environmental Pollution** 80:209–221. 1993.
- 1937 Warfvinge, P., Mörth, M., Moldan, F. What processes govern recovery? In: *Recovery from Acidification in the Natural Environment:*
1938 *Present Knowledge and Future Scenarios*. Warfvinge, P. and Bertills, U. (eds). Report 5034, Swedish Environmental
1939 Protection Agency, 23–36. 2000.
- 1940 Warfvinge, P., Sverdrup, H., Alveteg, M., Rietz, F. Modelling geochemistry and lake pH since glaciation at lake Gårdsjön. **Water,**
1941 **Air and Soil Pollution** 85:713-718. 1996
- 1942 Warfvinge, P., Sverdrup, H., Norrström, A.C., Jacks, G. A model for dissolution of limestone in soils and neutralization of soil systems.
1943 In: *Acidification and Water Pathways*, N. Christophersen (Ed), 137-146, ISBN 82-554-0486-4. Norwegian National
1944 Committee for Hydrology. Bolkesjø, Norway. 1987
- 1945 Warfvinge, P., Sverdrup, H., Ågren, G., Rosen, K. Effekter av luftföroreningar på framtida skogstillväxt. In: L. Svensson (Ed.)
1946 Skogspolitiken inför 2000-talet—1990 års skogspolitiska kommitte, Peer-reviewed in a public Parliamentary hearing in 1992.
1947 **Statens Offentliga Utredningar**: 1992 SOU: 76: 377–412. Reviewed at a public hearing in the Swedish Parliament by
1948 parliament members and Swedish scientists. 1992
- 1949 Warfvinge, P., Sverdrup, H., Rosen, K. Calculating critical loads for N to forest soils. In: Grennfelt P.I. and Lövblad G., (Eds) *Critical*
1950 *Loads and Levels for Nitrogen*, 403–417. Nordic Council of Ministers. Nord 1992:41. 1992
- 1951 Warfvinge, P., Sverdrup, H., Alveteg, M. and Rietz, F.: Modelling geochemistry and lake pH since glaciation at lake Gårdsjön, In:
1952 P.I. Grennfelt and J. Wisniewski (eds), Proceedings of the Acid Reign 95? Conference, Water, Air and Soil Pollution Journal,
1953 Kluwer, Amsterdam, p. 6-12. 1996,
- 1954 Weissbart, E.J. and Rimstidt, J.D. Wollastonite: incongruent dissolution and leached layer formation. **Geochimica et Cosmochimica**
1955 **Acta** 64, 4007–4016. 2000
- 1956 Welch, S.A. and Ullman, W.J. The effect of organic acids on plagioclase dissolution rates and stoichiometry. **Geochimica et**
1957 **Cosmochimica Acta** 57, 2725–2736. 1993
- 1958 Welch, S. and Ullman, W. Feldspar dissolution in acidic and organic solutions: Compositional and pH dependence of dissolution rate.
1959 **Geochimica et Cosmochimica Acta** 60, 2939–2948. 1996
- 1960 Welch, S.A. and Ullman, W.J. The temperature dependence of bytownite feldspar dissolution in neutral aqueous solutions of inorganic
1961 and organic ligands at low temperature (5–35°C). **Chemical Geology** 167, 337–354. 2000
- 1962 Westrich, H.R., Cygan, R.T., Casey, W.H., Zemitis, C., Arbold, G.W. The dissolution kinetics of mixed-cation orthosilicate minerals.
1963 **American Journal of Science** 293, 869 – 893. 1993
- 1964 White A. and Brantley S.L. The effect of time on the weathering of silicate minerals: why do weathering rates differ in the laboratory
1965 and field? **Chemical Geology** 202, 479–506. 2003
- 1966 White, A.F., S.L. Brantley. Chemical Weathering Rates of Silicate Minerals: An Overview, in Chemical Weathering Rates of Silicate
1967 Minerals A.F. White and S.L. Brantley (eds.), Mineralogical Society of America Short Course, **Reviews in Mineralogy** 31,
1968 1-22. 1995.
- 1969 White, A.F. and Blum, A.E. Effects of climate on chemical weathering in watersheds. **Geochimica et Cosmochimica Acta** 59, 1729–
1970 1747. 1995
- 1971 White, A.F., Blum, A.E., Bullen, T.D., Vivit, D.V., Schulz, M., Fitzpatrick, J. The effect of temperature on experimental and natural
1972 chemical weathering rates of granitoid rocks. **Geochimica et Cosmochimica Acta** 63, 3277–3291. 1999
- 1973 Whitfield, C. J., Watmough, S. A., Aherne, J., and Dillon, P. J.: A comparison of weathering rates for acid-sensitive catchments in
1974 Nova Scotia, Canada and their impact on critical load calculations, **Geoderma**, 136, 899–911,
1975 doi:10.1016/j.geoderma.2006.06.004. 2006
- 1976 Whitfield, C.J., Phelan, J.N., Buckley, J., Clark, C.M., Guthrie, S., Lynch, J.A., Estimating Base Cation Weathering Rates in the
1977 USA: Challenges of Uncertain Soil Mineralogy and Specific Surface Area with Applications of the PROFILE Model. **Water,**
1978 **Air and Soil Pollution** 61 <https://doi.org/10.1007/s11270-018-3691-7>. 2018.
- 1979 Whitfield, C. J., and Watmough, S. A. (2012). A regional approach for mineral soil weathering estimation and critical load assessment
1980 in boreal Saskatchewan, Canada. **Science of the Total Environment**, 437, 165–172.



- 1981 Whitfield, C.J., Aherne, J., Watmough, S.A.. Modeling soil acidification in the Athabasca Oil Sands Region, Alberta, Canada.
1982 **Environ. Sci. Technol.** 43: 5844–5850. 2009.
- 1983 Whitfield, C.J., Aherne, J., Watmough, S.A., McDonald, M. Estimating the sensitivity of forest soils to acid deposition in the
1984 Athabasca Oil Sands Region, Alberta. **J. Limnol.** 69: 201–208. 2010.
- 1985 Wogelius, R.A. and Walther, J.V. Olivine dissolution at 25°C: effects of pH, CO₂, and organic acids. **Geochimica et Cosmochimica**
1986 **Acta** 55, 943–954. 1991
- 1987 Wogelius, R.A. and Walther, J.V. Olivine dissolution kinetics at near-surface conditions. **Chemical Geology** 97, 101 – 112. 1992
- 1988 Wolery, T.J. EQ3/6, a software package for geochemical modeling of aqueous systems. Lawrence Livermore National Laboratory
1989 Report UCRL MA-110662-PT-1. 1992.
- 1990 Wolff-Boenisch, D., Gislason, S.R., Oelkers, E.H. The effect of fluoride on the dissolution rates of natural glasses at pH 4 and 25°C.
1991 **Geochimica et Cosmochimica Acta** 68, 4571–4582. 2004a
- 1992 Wolff-Boenisch, D., Gislason, S.R., Oelkers, E.H., Putnis, C.V., The dissolution rates of natural glasses as a function of their
1993 composition at pH 4 and 10.6, and temperatures from 25 to 74°C. **Geochimica et Cosmochimica Acta** 68, 4843–4858. 2004b.
- 1994 Wolff-Boenisch, D., Wenau, S., Gislason, S.R., Oelkers, E.H. Dissolution of basalts and peridotite in seawater, in the presence of
1995 ligands, and CO₂: implications for mineral sequestration of carbon dioxide. **Geochimica et Cosmochimica Acta** 75, 5510–
1996 5525. 2011
- 1997 Wolff-Boenisch, D., Gislason, S.R., Oelkers, E.H., The effect of crystallinity on dissolution rates and CO₂ consumption capacity of
1998 silicates. **Geochimica et Cosmochimica Acta** 70, 858–870. 2006.
- 1999 Wood, A., Anovitz, L.M., Elam, J.M., Cole, D.R. Riciputi, Benzeth, P. The effect of fulvic acid on the extent and rate of dissolution
2000 of obsidian. Ninth Annual V. M. Goldschmidt Conference 1999.
- 2001 Xie, Z. and Walther, J.V. Dissolution stoichiometry and adsorption of alkali and alkaline earth elements to the acid-reacted
2002 wollastonite surface at 25°C. **Geochimica et Cosmochimica Acta** 58, 2587–2598. 1994
- 2003 Xiao, Y., and Lasaga, A. C., Ab initio quantum mechanical studies of the kinetics and mechanisms of silicate dissolution: H(H₃O⁺)
2004 catalysis: **Geochimica et Cosmochimica Acta**, 58, 5379–5400. 1994a,
- 2005 Xiao, Y., and Lasaga, A.C. Ab initio quantum mechanical studies of the kinetics and mechanisms of silicate dissolution: OH⁻ catalysis:
2006 **Geochimica et Cosmochimica Acta**, 60, 2283–2295. 1994b
- 2007 Yadaw, V.P, Sharma, T., Saxena, V.K., Dissolution kinetics of potassium from glauconitic sandstone in acid lixiviant. **International**
2008 **Journal of Mineral Processing** 60: 15–36. 2000
- 2009 Yadaw, S.K., and Chakrapani, G.J., Dissolution kinetics of rock–water interactions and its implications. **Current Science**, 90, 932–
2010 938. 2006
- 2011 Yang, L., and Steefel, C.I. Kaolinite dissolution and precipitation kinetics at 22°C and pH 4. **Geochimica et Cosmochimica Acta**, 72,
2012 99–116. 2008.
- 2013 Yoo, K., Kim, B-S., Kim, M-S., Lee, J., Jeong, J. Dissolution of Magnesium from Serpentine Mineral in Sulfuric Acid Solution.
2014 **Materials Transactions**, 50, 1225 – 1230. 2009
- 2015 Yu, L., Zanchi, G., Akselsson, C., Wallander, H., Belyazid, S. Modeling the forest phosphorus nutrition in a southwestern Swedish
2016 forest site. **Ecological Modelling** 369:88–100. 2017.
- 2017 Yu, L., Belyazid, S., Akselsson, C., van der Heijden, G., Zanchi, G. Storm disturbances in a Swedish forest—A case study comparing
2018 monitoring and modelling. **Ecological Modelling** 320, 102–113. 2016
- 2019 Zabowski, D., Skinner, M.F., Payn, T.W., Nutrient release by weathering: implications for sustainable harvesting of PINUS radiata in
2020 New Zealand soils. **New Zealand Journal of Forestry Science** 37: 336–354. 2007.
- 2021 Zanchi, G., Belyazid, S., Akselsson, C., Yu, L. Modelling the effects of management intensification on multiple forest services: a
2022 Swedish case study. **Ecological Modelling**, 284, 48–59. 2017
- 2023 Zanchi, G.: Modelling nutrient transport from forest ecosystems to surface waters: The model ForSAFE2D. Lund, Sweden: PhD
2024 Thesis. Lund University, Faculty of Science, Department of Physical Geography and Ecosystem Science. ISBN:
2025 9789185793686. 2016.
- 2026 Zanchi, G., Belyazid, S., Akselsson, C., Yu, L., Bishop, K., Köhler, S., Grip, H. A Hydrological Concept Including Lateral Water
2027 Flow Compatible with the Biogeochemical Model ForSAFE. **Hydrology**, 3, 11–28. doi:10.3390/hydrology3010011. 2016.
- 2028 Zassi, Å. Chlorite: Geochemical properties, Dissolution kinetics and Ni(II) sorption. Doctoral Thesis in Chemistry KTH Chemical
2029 Science and Engineering Stockholm, Sweden, 2009
- 2030 Zavodsky, D, Babiakova, G., Mitosinkova, M., Pukancikove, Roncak, P., Bodis, D., Rapant, S., Mondas, J., Skvarenina, J., Cambel,
2031 B., Rehak, S., Wathne, B., Henriksen, A., Sverdrup, H., Tørseth, K., Semb, A, Aamlid, D. Mapping critical loads/levels in the
2032 Slovak Republic. Acid Rain Research 37:1996. Niva, Oslo. 1995
- 2033 Zavodsky, D, Babiakova, G., Mitosinkova, M., Pukancikove, Roncak, P., Bodis, D., Rapant, S., Mondas, J., Skvarenina, J., Cambel,
2034 B., Rehak, S., Curlik, J., Wathne, B., Henriksen, A., Sverdrup, H., Tørseth, K., Semb, A, Aamlid, D., Mulder, J. Mapping
2035 critical loads/levels in the Slovak Republic. Final report. Acid Rain Research 43:1996. Niva, Oslo.1996
- 2036 Zhang, H.L., Bloom, P.R., Nater, E.A., Erich, M.S. Rates and stoichiometry of hornblende dissolution over 115 days of laboratory
2037 weathering at pH 3.6–4.0 and 25°C in 0.01M lithium acetate. **Geochimica et Cosmochimica Acta** 60, 941 – 950. 1996
- 2038 Zhang, H., Bloom, P. The pH dependence of hornblende dissolution **Soil Science**, 164:624–632. 1999
- 2039 Zhang, H., Bloom, P. Dissolution Kinetics of Hornblende in Organic Acid Solutions. **Soil Science Society of America Journal** 63:
2040 815–822. 1999
- 2041 Zhang, R., Zhang, X., Guy, B., Hu, S., de Ligny, D., Moutte, J. Experimental study of dissolution rates of hedenbergitic clinopyroxene
2042 at high temperatures: dissolution in water from 25°C to 374°C. **Eur. J. Mineral.** 25, 353–372. 2013
- 2043 Zhang, L. and Lüttge, A. Al-Si order in albite and its effect on albite dissolution processes: a Monte Carlo study. **American**
2044 **Mineralogist** 92, 1316–1324. 2007
- 2045 Zhang, L. and Lüttge, A. Theoretical approach to evaluating plagioclase dissolution mechanisms. **Geochimica et Cosmochimica**
2046 **Acta** 73, 2832–2849. 2009a
- 2047 Zhang, L. and Lüttge, A. Morphological evolution of dissolving feldspar pricles with anisotropic surface kinetics and implication for
2048 dissolution rate normalization and grain size deendence: A kinetic modelling study. **Geochimica et Cosmochimica Acta** 73,
2049 6757–6770. 2009b
- 2050 Zhu, C., and Lu, P., Alkali feldspar dissolution and secondary mineral precipitation in batch systems: 3. Saturation states of product



Table 4. Temperature dependencies, measured are in bold. Default values were computed and scaled with Madelung crystal lattice site energy from different minerals (See Sverdrup 1990 for a detailed explanation). Normal font means we have estimated it from the lattice energies and the properties of the mineral surface. Based on the modified Arrhenius equation (Sverdrup 1990, 1998, Sverdrup and Warfvinge 1988, 1992, 1995). The units are °K⁻¹ used in the Arrhenius equation as defined in Sverdrup (1990).

Mineral	Fundamental chemical reactions					Comments
	H ⁺	H ₂ O	CO ₂	Organic acids	OH ⁻	
1. Feldspars						
1.1-1.2 K-Feldspar I: Orthoclase, Sanidine	3500	1940	1700	1200	3200	Irreversible dissolution
1.3 K-Feldspar II: Microcline	3470	1820	1700	1200	3200	Irreversible dissolution
1.4 K-Feldspar III: Orthoclase	4090	2000	1700	1200	3500	Irreversible dissolution
1.5 Anorthoclase	3500	2000	1700	1200	3200	Irreversible dissolution
1.6 Plagioclase: Albite	3350	2500	1680	1200	3100	Irreversible dissolution
1.7 Plagioclase: Oligoclase	4200	2330	1700	1200	3600	Irreversible dissolution
1.8 Plagioclase: Labradorite	4200	2500	1700	2200	3500	Irreversible dissolution
1.9-1.10 Plagioclase: Bytownite and near anorthite	3500	2500	1700	1200	3100	Irreversible dissolution
1.11 All other feldspars	3685	2085	1690	1200	3100	Irreversible dissolution
1b. Zeolites						
1.12 Heulandite	3500	2550	1700	1200	3450	Irreversible dissolution
1.13 Analcime	3500	2500	1700	1200	3400	Reversible reaction
1.14 Clinoptilolite	3500	2550	1700	1200	3600	Irreversible dissolution
1.15 Stilbite	3500	2500	1700	1200	3400	Irreversible dissolution
2. Nesosilicates						
2.1 Monticellite	3480	4200	1700	1600	2200	Irreversible dissolution
2.2 Tephroite	2351	4400	1700	1534	1450	Irreversible dissolution
2.4 Anorthite (An)	1920	5670	1700	1800	1700	Irreversible dissolution
2.5 Forsterite (Fo)	3350	4510	1700	1800	2100	Irreversible dissolution
2.6 Olivine	2580	4510	1700	1800	2100	Irreversible dissolution
2.7 Fayalite	2550	4400	1700	1800	2200	Irreversible dissolution
2.13 Nepheline	3630	3130	1700	1800	2180	Irreversible dissolution
2.8-2.18 Garnet mixes, all garnets	2500	3500	1700	1800	2000	Irreversible dissolution
2.19 Staurolite	3100	3200	1700	1800	3100	Irreversible dissolution
2.20-2.21 Diethene, Kyanite	3918	2400	1700	1800	2200	Irreversible dissolution
2.22 All other nesosilicates	2676	4436	1700	1800	2180	Irreversible dissolution
4. Pyroxenes						
3.2 Wollastonite	3100	3600	1700	2000	2100	Irreversible dissolution
3.4 Diopside	2610	3400	1700	2000	2000	Irreversible dissolution
3.9 Hedenbergite	2311	3500	1700	2000	2000	Irreversible dissolution
3.7-3.8, 3.10 Augite	2700	4100	1700	2000	2000	Irreversible dissolution
3.11 Enstatite	2550	5950	1700	2000	2000	Irreversible dissolution
3.16 All other pyroxenes	2700	4100	1700	2000	2000	Irreversible dissolution
4. Amphiboles						
4.1 Glaucofane	4300	3800	1700	2000	3500	Irreversible dissolution
4.2 Hornblende I	4300	3800	1700	2000	3500	Irreversible dissolution
4.3 Hornblende II	4300	4000	1800	2200	3500	Irreversible dissolution
4.4 Tremolite	4500	3390	1700	2000	3600	Irreversible dissolution
4.5 Actinolite	3800	3300	1700	2200	4500	Irreversible dissolution
4.6 All other amphiboles	4300	3390	1700	2000	3500	Irreversible dissolution
5. Phyllosilicates						
5.1 Glauconite	4300	1950	1700	2000	3500	Irreversible dissolution
5.2 Serpentine, Chrysotile, Antigorite	4282	3600	1700	2000	3500	Irreversible dissolution
5.3 Talc	4200	3700	1700	2000	3500	Irreversible dissolution
5.4 Nontronite	4500	3500	1700	1200	3400	Irreversible dissolution
5.6 Biotite	4500	3840	1700	2000	3500	Irreversible dissolution
5.5 Phlogopite	4500	3840	1700	2000	3500	Irreversible dissolution
5.7 Vermiculite 1	4500	3840	1700	2000	3500	Alteration mineral, irreversible dissolution
5.8 Vermiculite 2	4500	3840	1700	2000	3500	Alteration mineral, irreversible dissolution
5.9 Vermiculite 3	4500	3840	1700	2000	3500	Irreversible dissolution
5.10 Fe-Chlorite	4500	3800	1700	2000	3500	Irreversible dissolution
5.14 Fe-Mg-Chlorite	4520	3500	1700	1800	3500	Irreversible dissolution
5.17 Mg-Chlorite	4500	1400	1700	1700	3500	Irreversible dissolution
5.19 Muscovite	3038	3800	1700	2000	4656	Irreversible dissolution
5.21 Illite 1	4500	3800	1700	2000	3500	Alteration mineral, irreversible dissolution
5.22 Illite 2	4500	3800	1700	2000	3500	Alteration mineral, irreversible dissolution
5.23 Illite 3	4500	3800	1700	2000	3500	Irreversible dissolution
5.24 Montmorillonite	4300	3840	1700	2000	3500	Alteration mineral, irreversible dissolution
5.27 All other phyllosilicates	4410	3770	1700	2000	3500	Irreversible dissolution
7. Cyclosilicates						
6.1 Tourmaline	3600	3100	1700	1800	2500	Irreversible dissolution
6.2 Cordierite	2600	5900	1700	2000	2000	Irreversible dissolution
6.3 All other cyclosilicates	3100	4500	1700	1900	2250	Irreversible dissolution
8. Sorosilicates						
7.1 Epidote	5330	3800	1700	2000	2300	Irreversible dissolution
7.2 Zoisite	4400	3900	1800	2200	3300	Irreversible dissolution
7.3 All other sorosilicates	4375	3850	1750	2100	3300	Irreversible dissolution
10. Oxides and simple aluminosilicates						
8.1 Kaolinite	5310	3580	1700	2000	4100	Irreversible dissolution, gibbsite possible outcome
8.2 Gibbsite	3400	3600	1700	2000	3170	Alteration mineral, irreversible dissolution
8.3 Quartz	3890	n.a.	2200	2000	3320	Reversible reactions, back reaction, dissolution is kinetically limited
11. Volcanic glasses						
9.1 Volcanic glass, base cation poor	3890	3010	2400	2800	2700	Irreversible dissolution
9.2 Volcanic glass, base cation rich	4500	3310	2500	2800	3400	Irreversible dissolution
9.3 All other volcanic glasses	4200	3110	2450	2800	3050	Irreversible dissolution
10 Carbonates						
10.1 Calcite and limestones	444	1180	2180	2200	-	Reversible reaction, Back reaction important
11 Phosphates						
10.2 Aragonite	530	1210	2200	2400	-	Reversible reaction, Back reaction important
10.3 Dolomite	1880	2700	1800	2200	-	Irreversible dissolution, Back reaction to calcite and magnesite
10.5 Siderite	3300	3500	1700	2000	2500	Irreversible dissolution
10.6 Rhodochrosite	3300	3500	1700	2000	2500	Irreversible dissolution
11.1 Apatite	3500	4900	1700	1200	2500	Irreversible dissolution, precipitates with oxalate and aluminium important
11.2 Fluorapatite	1110	4790	1700	1200	2500	Irreversible dissolution, precipitates with oxalate and aluminium important
11.3 Immobilized inorganic phosphorus, all other phosphorus	2350	4000	1700	1200	2200	Possibly reversible reaction

2068

2069

2070
2071



Table 5. Stoichiometry of the minerals applied in Tables 3 and 4.

1a. Feldspars	
Mineral	Formula
1.1 K-Feldspar	$KAlSi_3O_8 = Or$
1.2 K-Feldspar I; Orthoclase, K-Feldspar I; Sanidine, 100-90%	$Or_{99}An_1$
1.3 K-Feldspar II; 90%, Microcline	$Or_{99}Ab_1An_1$
1.4 K-Feldspar II; 80%, Orthoclase	$Or_{99}Ab_{20}$
1.5 Anorthoclase	$Or_{23}Ab_{53}An_{17}$
1.6 Albite	$NaAlSi_3O_8 = Ab$
1.7 Plagioclase; Oligoclase	$Ab_{95}An_{15}$
1.8 Plagioclase; Labradorite	$Ab_{65}An_{54}$
1.9 Plagioclase; Bytownite	$Ab_{22}An_{78}$
1.10 Plagioclase; feldsparic Anorthite	Ab_5An_{94}
1b. Zeolites with tectosilicate structure	
1.12 Helulandite	$(Ca, Na)_{0.45}Al_{0.85}Si_{3.1}O_8 \cdot 2.7 H_2O$
1.13 Analcime	$NaAlSi_3O_8 \cdot H_2O$
1.14 Clinoptilolite	$(Na, K, Ca)_2-3Al_2(Al, Si)_2Si_{12}O_{38} \cdot 12H_2O$
1.15 Stilbite	$Na_{0.98}Ca_{0.02}AlSi_3O_8 \cdot 3.1 H_2O$
2. Nesosilicates	
2.1 Monticellite	$CaMgSiO_4$
2.2 Tephroite	Mn_2SiO_4
2.3 Nepheline	$(Na_{0.75}K_{0.25})AlSiO_4$
2.4 Anorthite	$CaAl_2Si_2O_8 = An$
2.5 Forsterite	Mg_2SiO_4
2.6 San Carlos, Arizona Forsterite	$Mg_{1.81}Fe_{0.19}SiO_4$
Salem, Tamil Nadu Indian olivine	$Mg_{1.84}Fe_{0.16}SiO_4$
Norwegian Olivine (Fos ₉₅ Fas ₅)	$Mg_{1.8}Fe_{0.35}Al_{0.02}Si_{1.04}O_4$
2.7 Fayalite	Fe_2SiO_4
2.8-2.12 Generic garnet, continuous series	$Al_{14}Py_{14}Gr_{12}, Al_{16}Py_{25}, Ad_{30}Gr_{20}, Al_{50}Py_{40}Gr_{10}, Gr_{38}Py_6Ad_6$
2.13 Grossular	$Ca_3Al_2(SiO_4)_3$
2.14 Almandine =Al	$Fe_3Al_2(SiO_4)_3$
2.15 Spessartine = Sp	$Mn_3Al_2(SiO_4)_3$
2.16 Andradite = Ad	$Ca_3Fe_3(SiO_4)_3$
2.17 Uvarovite = Uv	$Ca_3Cr_3(SiO_4)_3$
2.18 Pyrope = Py	$Mg_3Al_2(SiO_4)_3$
2.19 Staurolite	$Mg_{12}Fe_{11}Al_{17}Si_{13}O_{22}(OH)_2$
2.20 Disthene	Al_2SiO_5
2.21 Kyanite	Al_2SiO_5
2.223. Pyroxenes (End members are diopside, hedenbergite, enstatite, ferrosillite)	
3.1 Ailite (T-slag, K-slag)	Ca_2SiO_5 or $(CaO)_2SiO_2$
3.2 Wollastonite ($Ca_2Si_2O_6$)	$Ca_{1.7}Mg_{0.11}Si_{2.2}O_6$
3.3 Spodumene ($LiAlSi_2O_6$)	$LiAl_{0.85}Fe_{0.3}Si_2O_6$
3.4 Diopside ($CaMgSi_2O_6$)	$Ca_{1.02}Mg_{1.0}Al_{0.02}Fe_{0.01}Si_{2.01}O_6, Ca_{0.9}Mg_{0.9}Fe_{0.2}Al_{0.2}Si_2O_6$
3.5 Jadeite ($NaAlSi_3O_6$)	$Na_{1.0}Ca_{0.2}Fe_{0.3}AlSi_3O_6$
3.6 Leucite ($KAlSi_3O_6$)	$Na_{0.05}K_{1.05}Al_{1.15}Si_3O_6$
3.7 Augite I	$He_{95}En_{15}$
3.8 Augite II	$En_{15}Wo_{38}He_{10}$
3.9 Hedenbergite ($CaFeSi_2O_6$)	$Ca_{0.4}Mg_{0.7}Fe_{0.05}Al_{0.15}Si_{1.85}O_6$
3.10 Augite III	$Ca_{0.88}Mg_{1.0}Fe_{0.02}Si_2O_6$
3.11 Enstatite ($Mg_2Si_2O_6$)	$Mg_{1.7}Fe_{0.3}Si_2O_6$
3.12 Hypersthene	$MgFeSi_2O_6$ (En ₉₀ Fs ₁₀)
3.13 Ferrosillite	$Fe_2Si_2O_6$
3.14 Bronzite (mixed)	$Mg_{1.54}Fe_{0.42}Ca_{0.2}Si_{1.9}O_6$ (En ₇₀ He ₁₀ Fs ₂₀)
3.15 Pidgeonite	$Mg_{50}Ca_{15}Fe_{35}Si_2O_6$
3.16 Mixed pyroxenes	$Ca_{0.8}Mg_{0.2}Fe_{0.3}Al_{0.04}Si_2O_6$ (Di _x En _y Fs _z He _w)
4. Amphiboles	
4.1 Glaucophane	$Na_2MgFe_2Al_2Si_8O_{22}(OH)_2$
4.2 Pargasite	$NaCa_2(Mg_4Al)(Si_6Al_2)O_{22}(OH)_2$
4.3 Hornblende I (Norwegian)	$Ca_2.1Mg_{4.5}Na_{0.08}Al_2.1Si_7O_{22}(OH)_2(PO_4)_{0.01}$
4.4 Hornblende II (Canadian)	$Ca_{2.3}Mg_{4.0}Na_{0.16}Al_{2.4}Si_{8.3}O_{22}(OH)_2$
4.5 Tremolite	$Ca_2Mg_5Si_8O_{22}(OH)_2$
4.6 Riebeckite	$Na_2Fe^{2+}Fe^{3+}Si_8O_{22}(OH)_2$
4.7 Anthophyllite	$Mg_5.7FeAl_1.3Si_7.9O_{22}(OH)_2$
4.8 Other amphiboles	Various compositions
5. Phyllosilicates	
5.1 Glauconite	$(K, Na)Fe^{2+}AlMg_2(Si, Al)_2O_{10}(OH)_2$
5.2 Serpentine, Antigorite, Chrysotile	$Mg_{2.1}Fe_{0.4}Al_{0.15}Si_{2.9}O_{10}(OH)_4, (Mg, Fe)_2Si_2O_5(OH)_4$
5.3 Talc	$Mg_3Si_4O_{10}(OH)_2$
5.4 Nontronite	$Ca_{0.5}Si_7Al_{1.8}Fe_{0.2}(Fe_3AlMg_1)O_{20}(OH)_4$
5.5 Phlogopite	$K_1.0Mg_3Al_1.5Si_3O_{10}(OH)_2$
5.6 Biotite	$K_0.9Mg_{1.9}Fe_{1.1}Al_{1.0}Na_{0.1}Si_3O_{10}(OH)_2$

2072

2073
 2074



5.7	Mg-Vermiculite I	$K_{0.9}Mg_{1.5}Fe_{1.1}Al_{1.7}Na_{0.05}Si_5O_{10}(OH)_2$
5.8	Mg-Vermiculite II	$K_{0.3}Mg_{1.5}Fe_{1.1}Al_{1.5}Si_5O_{10}(OH)_2$
5.9	Mg-Vermiculite III	$K_{0.1}Mg_{0.5}Fe_{1.1}Al_2Si_5O_{10}(OH)_2$
5.10	Fe-Vermiculite	$(Mg,Fe^{2+},Fe^{3+})_3(Al,Si)_4O_{10}(OH)_2 \cdot 4H_2O$
5.11	Illitic vermiculite	$K_{0.35}Mg_{0.11}Ca_{0.03}Al_2.19Fe_{0.32}Ti_{0.07}Si_{3.4}O_{10}(OH)_2$
5.12	Vermiculite Al-OH interlayer mineral	$(Mg,Al,Fe^{2+})_3(Si,Al)_4O_{10}(OH)_2 \cdot nH_2O$
5.13	Fe-Chlorite V, Chamosite	$Fe_3Al_2Si_3O_{10}(OH)_8$
5.14	Chlorite IV (mixed)	$Mg_2Fe_2Al_2Si_2O_{10}(OH)_8$
5.15	Chlorite III (mixed)	$Mg_2Fe_3Al_2Si_2O_{10}(OH)_8$
5.16	Chlorite II (mixed)	$Mg_2Fe_0.5Al_{1.5}Si_2O_{10}(OH)_8$
5.17	Mg-Chlorite I, Clinochlore	$Mg_3Al_2Si_3O_{10}(OH)_8$
5.18	Smectite	$Ca_{0.2}Mg_{1.0}Na_{0.13}Al_{1.0}Si_{4.0}O_{10}(OH)_2$
5.19	Muscovite	$KAl_3Si_3O_{10}OH_2$
5.20	Muscovite (mixed)	$K_{0.9}Na_{0.07}Mg_{0.3}Fe_{0.4}Al_{1.7}Si_{3.5}O_{10}(OH)_2$
5.21	Illite I	$K_0Mg_{0.28}Fe_{0.3}Al_{2.5}Si_{3.3}O_{10}(OH)_2$
5.22	Illite II	$K_{0.7}Mg_{0.26}Fe_{0.1}Al_{2.5}Si_{3.1}O_{10}(OH)_2$
5.23	Illite III	$K_{0.9}Mg_{0.25}Al_{2.5}Si_3O_{10}(OH)_2$
5.24	Montmorillonite	$Ca_{0.2}Mg_{1.0}Na_{0.13}Al_{1.0}Si_4O_{10}(OH)_2$
5.25	Bentonite	See illite
5.26	Sericite	$KAl_2Si_3O_{10}(OH)_2$
6. Cyclosilicates		
6.1	Tourmaline	$Ca_{1.0}Fe_{0.3}Mg_{0.5}Si_6O_{18}(BO_3)_3(OH)_4(PO_4)_{0.01}$
6.2	Cordierite	$Ca_2.5Fe_{0.07}K_{0.09}Al_3.5Si_{4.5}O_{18}$
7. Sorosilicates		
7.1	Epidote	$Ca_{1.5}K_{0.46}Fe_{0.74}Al_{1.5}Si_{3.4}O_{12}(OH)$
7.2	Zoisite (Clino-)	$Ca_{2.2}Fe_{0.13}Al_{1.5}Si_{3.2}O_{12}(OH)$
8. Clay minerals		
8.1	Kaolinite	$Al_2Si_2O_5(OH)_4$
8.2	Gibbsite	$Al(OH)_3$
8.3	Quartz	SiO_2
9. Glasses		
9.1	Volcanic glass, base cation poor	$Ca_{0.2}Mg_{0.2}K_{0.4}Na_{0.4}Al_{0.8}Si_3O_8$
9.2	Volcanic glass, base cation rich	$Ca_{0.62}Mg_{0.53}K_{0.27}Na_{0.27}Al_{0.66}Si_{2.68}O_8$
10. Carbonates		
10.1a	Calcite (Ca)	$(CaCO_3)_{99.9}(Ca_5(PO_4)_3(OH))_{0.1}$
10.1b	Köping limestone	$Ca_{97}Do_2Ma_1Ap_{0.1}$
10.1c	Red Öland limestone	$Ca_{97}Do_1Sd_2Ap_{0.1}$
10.1d	Ignaberqa limestone	$Ca_{95}Ar_{0.5}Do_1Sd_2Ap_{0.5}$
10.2	Aragonite (Ar)	$(CaCO_3)_{99.9}(Ca_5(PO_4)_3(OH))_{0.1}$
10.3	Dolomite (Do)	$(CaMg(CO_3)_2)_{99.9}(Ca_5(PO_4)_3(OH))_{0.1}$
10.4	Magnesite (Ma)	$MgCO_3$
10.6	Rhodochrosite	$MnCO_3$
10.5	Siderite (Sd)	$FeCO_3$
11. Phosphorus minerals		
11.1	Apatite (Ap)	$Ca_5(PO_4)_3(OH)$
11.2	Fluoroapatite	$Ca_5(PO_4)_3(OH_0.7F_{0.3})$
11.3	Immobilized inorganic phosphorus	Unknown, assume as semi-apatite $(Ca_2AlFe_{0.5})_5(PO_4)_3(F_{0.1}OH_{0.4}CO_3)_{0.5}$

2075

2076

2077

2078

2079

2080

2081

2082

2083

2084

2085

2086

2087

2088

2089

2090

2091

2092

2093

2094

2095

2096

2097

2098

2099

2100

2101

2102

2103

2104

2105

2106

2107

2108



2109 **Appendix. Overview of the PROFILE family of weathering rate modelling codes**

2110

2111 A large number of computational weathering models are based on PROFILE approach. To clarify these
2112 models and their interconnections the following list is provided

2113

2114 **1. Steady-state weathering rate models**

2115

2116 a. 1987-1995; Warfvinge P. and Sverdrup, H.; The single site version of the **PROFILE** model for
2117 the calculation and mapping of critical loads and rates of field chemical weathering was developed.
2118 It has been validated and used operationally in more than 50 countries worldwide. It uses
2119 laboratory generated kinetic models and coefficients to predict field weathering rates. The
2120 interface software for PROFILE became outdated, thus, this version is no longer available.

2121

2122 b. 1992-present; Sverdrup, H., Warfvinge, P., Alveteg, M., Walse, C., Kurz, P., Posch, M., Belyazid,
2123 S.; The code **RegionalPROFILE** was developed. This code is a regionalized version of
2124 PROFILE, used for creating weathering rate maps for soils and catchments across regions and
2125 countries, as well as to estimate critical loads for forest soils. Updated versions of the code are
2126 available upon request from Sverdrup, Akselsson or Belyazid.

2127

2128 c. 2000; Sverdrup, H. and Alveteg, M., The **CLAY-PROFILE** code was developed. This model was
2129 made for volcanic and clayey agricultural soils. This code is no longer operable. Archived, the
2130 code is available upon written request from Sverdrup or Belyazid.

2131

2132 **2. Dynamic weathering models**

2133

2134 a. 1987-2008; Warfvinge P., Sverdrup, H., Alveteg, M., Walse, C., Martinsson, L.: The **SAFE** model
2135 and its helper routine **MakeDep** were created. **SAFE** is a generally applicable dynamic soil
2136 chemistry and acidification model. This tool is used worldwide for acidification research, forest
2137 sustainability assessments and for mapping critical loads.

2138

2139 b. 1995-1996; Rietz, F., Sverdrup, H., Warfvinge, P.; The **SkogsSAFE** model was developed. This
2140 long-term dynamic model simulates soil genesis, mineralogy dynamics, soil chemistry and base
2141 cation release from chemical weathering in soils over time since the most recent glaciation (14,000
2142 years ago to present) (Rietz 1995, Warfvinge et al., 1996). This code is written in FORTRAN.
2143 This code and its databases are available upon written request from Sverdrup.

2144

2145 c. 1996-2004; Sverdrup, H., Wallman P., Belyazid, S., Alveteg, M., Walse, C., Martinsson, L.: These
2146 scientists developed **ForSAFE**, an integrated biogeochemical forest ecosystem model for growth,
2147 nitrogen and carbon cycling. This code is written in FORTRAN code, and the code is available
2148 upon written request from Sverdrup or Belyazid.

2149

2150 **3. Regional mineralogy estimation**

2151

2152 a. 1990; Sverdrup, H., Melkerud, P. A., Kurz, D.: The **UPPSALA** model was developed for the
2153 reconstruction of soil mineralogy from soil total analysis data. This model is run in a spreadsheet.
2154 It is available upon written request from Sverdrup.

2155

2156 b. 1998; Sverdrup, H. and Erdogan, B. The **Turkey** mineral depletion model (TMD) was developed.
2157 This model estimates soil mineralogy from bedrock geology and estimates of soil age. This code
2158 is written in STELLA[®]. It is archived and available upon written request from Sverdrup.

2159

2160 c. 2005-2010; Posch, M., Kurz, D., Alveteg, M., Akselsson, C., Eggenberger, U., Holmqvist, J; 2007
2161 **A2M**, a model to quantify mineralogy from geochemical analyses was developed. This code is
2162 available on-line from doi:10.1016/j.cageo.2006.08.007,
2163 https://dl.acm.org/citation.cfm?id=1231715 or from Kurz or Akselsson (Posch et al., 2006, 2007).

2164

2165 These models are not commercial products. They do not have ready-made handbooks (only the early single
2166 site PROFILE models had a good users interface and a user's manual). The models are available, but the best
2167 option to learn how to run these get training from the contact scientists in how to operate the models and how
2168 to set up the input data for a site or a region. The core code is written in FORTRAN